Resonance States of Positronium

Chris W Patterson

Abstract. *We solve both the two-body Dirac equation and the Bethe-Salpeter equation for positronium. The solutions give rise to both atomic and resonance states. We compare and contrast the properties of these states.*

Theoretical Division, Los Alamos National Laboratory, Los Alamos, NM 87545

E-mail: cwpatt2@gmail.com

Submitted to: *J. Phys. B*
on 6/13/2015

1. Introduction

We consider here the resonance solutions to both the two-body Dirac equation and the Bethe-Salpeter equation for positronium and we show the relationship between the atomic and resonance solutions. The resonance states considered here result from the free particle states of positronium with energy E for an electron with energy e_e and positron with energy e_p. From the two-body Dirac equation, this energy is given simply by,

$$E = e_e + e_p = \pm\sqrt{p_e^2c^2 + m^2c^4} \pm \sqrt{p_p^2c^2 + m^2c^4}. \tag{1}$$

Here, p_e and p_p are the magnitude of the momentum of the electron and positron, respectively. In the center of momentum frame, where the magnitudes of the electron and positron momentum are equal, we have

$$p_e = p_p \equiv \pi,$$

resulting in the energies

$$\begin{aligned} E_\pm &= \pm 2\sqrt{\pi^2c^2 + m^2c^4}, \\ E_0 &= 0. \end{aligned} \tag{2}$$

Note that for a given momentum π the $E_0 = 0$ states are doubly degenerate because either e_e or e_p is negative. We refer to the solutions for $E_0 = 0$ as the free particle 'resonance' states because such solutions are degenerate for all momenta π. The remaining two solutions for E_+ and E_- we refer to as the free particle 'atomic' states because they are the main contributors to the atomic positronium states in the presence of a potential. There are an infinite number of resonance states with $E_0 = 0$. These degenerate states will be strongly mixed by the electromagnetic potential between the particles and some of the resulting states have non-negative energies $E \geq 0$. It is the purpose of this paper to discuss these resonance states and their properties.

Numerous authors [1, 2, 3] have treated the two-body Dirac equations for quarks. Malenfant [4] and Scott, Shertzer, and Moore [5] specifically treated the two-body equations applicable to positronium which are used here. It appears that the resonance solutions themselves have not been considered previously in any detail because they are thought to be unimportant. Indeed, Salpeter [6] has shown a natural separation, to fourth order in the fine structure constant α, between the positronium atomic states and the resonance states resulting from the Bethe-Salpeter equation. This separation

is a common approximation in the no virtual-pair approximation used in multielectron many-body calculations of atoms [7, 8, 9] and is also important to eliminate continuum dissolution in such calculations [10, 11]. Thus, much effort has been expended to separate the atomic and resonance contributions to positronium and atomic energies but little effort to understand the properties of the resonances themselves. We emphasize that resonances play an important role in physics and that they should always be given serious consideration.

We treat the two-body Dirac equation for positronium in the first four sections. In order to develop the mathematics for understanding the resonance solutions to the two-body Dirac equation, we discuss in Section 2 the one-body Dirac equation for free particles in spherical coordinates. In Section 3, we consider the two-body Dirac equation in spherical coordinates relative to the electron and positron. This, of course, will be useful when considering any potential which depends only on the relative coordinates between these particles such as an electric or magnetic potential. However, the properties of the resonance structure in this coordinate system prove to be very interesting in themselves. First, we find the equations in the coordinate representation in agreement with previous authors [4, 5] and then show that these equations are reducible in the momentum representation and exhibit interesting symmetry relations for the resonance states. Furthermore, in the momentum representation the solutions clearly show the separability between atomic and resonance states and, indeed, the resonance states can have different charge conjugation symmetry than the atomic states. We also use the momentum representation to show the chirality properties of the resonance states in the case of zero rest mass.

In Section 4, we show that the resonance structure is preserved even when we consider a Coulomb potential between the electron and positron. The separability between the atomic and resonance states is maintained to fourth order in α. We repeat the finite element calculations of Scott, et al. [5] for atomic positronium and compare their results with the Pauli approximation found by methods shown by Bethe and Salpeter [12]. From these same calculations we can simultaneously determine the resonance energies and wavefunctions. For arbitrary total angular momentum J, we show numerically, using both the coordinate and momentum representation, that the resonance states are approximately delta functions. For an infinite basis set these delta functions are exact as shown analytically.

We treat the Bethe-Salpeter equation for positronium in Section 5. We derive the atomic and resonance state solutions to the Bethe-Salpeter equation with a Coulomb potential and show they are indeed separable to all orders in the momentum representation. To understand this separation it is important to distinguish between resonance states arising from the ladder approximation and virtual electron-positron pairs [7]. In Section 6 we also consider the magnetic potential and the resulting energy shifts for both the atomic and resonance states. In Section 7, we show that, unlike the case of atomic states, electron-positron annihilation is forbidden for the case of resonance states. We also show that the resonance states can neither absorb nor emit

light. Radiative transitions between resonance states and atomic states are forbidden. Finally, in the conclusion, we summarize the properties of the atomic and resonance states.

For the readers convenience, we give in Appendix A some important orthonormality properties of the spherical Bessel functions and in Appendix B some simple relations between the two-body resonance bases and their one-body constituents. This is equivalent to simplified addition theorems for spherical Bessel harmonics.

2. One-Body Dirac Equation - Free Particles

For a free particle we have the Dirac equation

$$\mathbf{h}_0\psi(\mathbf{r}) = (c\boldsymbol{\alpha}\cdot\mathbf{p} + mc^2\beta)\psi(\mathbf{r}) = e\psi(\mathbf{r}), \tag{3}$$

with Dirac Hamiltonian $\mathbf{h}_0$ and with Dirac alpha and beta matrices given by

$$\alpha_i = \begin{pmatrix} 0 & \sigma_i \\ \sigma_i & 0 \end{pmatrix}, \quad \beta = \begin{pmatrix} 1 & 0 \\ 0 & -1 \end{pmatrix}, \tag{4}$$

where σ_i are the Pauli spin matrices. The two-component wavefunction consists of positive and negative rest mass components ψ_1 and ψ_2, respectively,

$$\psi(\mathbf{r}) \equiv \begin{pmatrix} \psi_1(\mathbf{r}) \\ \psi_2(\mathbf{r}) \end{pmatrix} \equiv \psi_1(\mathbf{r})\mathbf{e}_1 + \psi_2(\mathbf{r})\mathbf{e}_2, \tag{5}$$

such that

$$\beta mc^2\psi = mc^2(\psi_1\mathbf{e}_1 - \psi_2\mathbf{e}_2).$$

Using spherical coordinates $\mathbf{r} \equiv (r\theta\varphi)$, we have the Dirac equations

$$\begin{aligned} mc^2\psi_1(r\theta\varphi) + c\boldsymbol{\sigma}\cdot\mathbf{p}\psi_2(r\theta\varphi) &= e\psi_1(r\theta\varphi), \\ -mc^2\psi_2(r\theta\varphi) + c\boldsymbol{\sigma}\cdot\mathbf{p}\psi_1(r\theta\varphi) &= e\psi_2(r\theta\varphi). \end{aligned} \tag{6}$$

For spherical symmetry we can couple the spherical harmonics $Y^l_m(\theta,\varphi)$ and spin functions $\chi^{\frac{1}{2}}_\sigma$ to find functions with total angular momentum $j = l \pm \frac{1}{2}$ and projection $j_z = n$

$$[Y^l, \chi^{\frac{1}{2}}]^j_n = \sum_{m,\sigma} C^l_{m\ \sigma\ n}^{\ \frac{1}{2}\ \ j} Y^l_m(\theta,\varphi)\chi^{\frac{1}{2}}_\sigma,$$

where the condition $m + \sigma = n$ on such sums is understood implicitly. We wish to evaluate $\boldsymbol{\sigma}\cdot\mathbf{p}$ in both the coordinate and momentum representation using these functions.

2.1. Coordinate representation

From the Dirac identity $(\boldsymbol{\sigma}\cdot\mathbf{a})(\boldsymbol{\sigma}\cdot\mathbf{b}) = \mathbf{a}\cdot\mathbf{b} + i\boldsymbol{\sigma}\cdot(\mathbf{a}\times\mathbf{b})$ and from the definition of the unit vector $\hat{\mathbf{r}} = \mathbf{r}/r$, it follows that

$$\begin{aligned} \boldsymbol{\sigma}\cdot\mathbf{p} &= [(\boldsymbol{\sigma}\cdot\hat{\mathbf{r}})(\boldsymbol{\sigma}\cdot\hat{\mathbf{r}})]\boldsymbol{\sigma}\cdot\mathbf{p}, \\ &= \frac{\boldsymbol{\sigma}\cdot\hat{\mathbf{r}}}{r}[\mathbf{r}\cdot\mathbf{p} + i\boldsymbol{\sigma}\cdot(\mathbf{r}\times\mathbf{p})], \\ &= -i\boldsymbol{\sigma}\cdot\hat{\mathbf{r}}[\hbar\frac{d}{dr} - \frac{\boldsymbol{\sigma}\cdot\mathbf{l}}{r}]. \end{aligned}$$

Using

$$\boldsymbol{\sigma}\cdot\hat{\mathbf{r}}[Y^{j-\frac{1}{2}},\chi^{\frac{1}{2}}]^j_n = -[Y^{j+\frac{1}{2}},\chi^{\frac{1}{2}}]^j_n,$$
$$\boldsymbol{\sigma}\cdot\hat{\mathbf{r}}[Y^{j+\frac{1}{2}},\chi^{\frac{1}{2}}]^j_n = -[Y^{j-\frac{1}{2}},\chi^{\frac{1}{2}}]^j_n,$$

and

$$\boldsymbol{\sigma}\cdot\mathbf{l}[Y^l,\chi^{\frac{1}{2}}]^j_n = \hbar[j(j+1)-l(l+1)-\frac{3}{4}][Y^l,\chi^{\frac{1}{2}}]^j_n,$$

we have in the coordinate representation the transformation between the two $l = j \pm \frac{1}{2}$ for the radial functions $y(r)$,

$$\boldsymbol{\sigma}\cdot\mathbf{p}\frac{y}{r}[Y^{j+\frac{1}{2}},\chi^{\frac{1}{2}}]^j_n = \frac{i\hbar}{r}[\frac{d}{dr}+\frac{1}{r}(j+\tfrac{1}{2})]y[Y^{j-\frac{1}{2}},\chi^{\frac{1}{2}}]^j_n, \tag{7}$$
$$\boldsymbol{\sigma}\cdot\mathbf{p}\frac{y}{r}[Y^{j-\frac{1}{2}},\chi^{\frac{1}{2}}]^j_n = \frac{i\hbar}{r}[\frac{d}{dr}-\frac{1}{r}(j+\tfrac{1}{2})]y[Y^{j+\frac{1}{2}},\chi^{\frac{1}{2}}]^j_n.$$

Equation (7) allows us to write coupled equations for the radial functions in the coordinate representation. We let the two-component Dirac wavefunctions be

$$\psi(r\theta\varphi) = \frac{1}{r}\begin{pmatrix} iy_1^-(r)[Y^{j-\frac{1}{2}},\chi^{\frac{1}{2}}]^j_n \\ y_2^+(r)[Y^{j+\frac{1}{2}},\chi^{\frac{1}{2}}]^j_n \end{pmatrix}, \tag{8}$$

where the $y_i(r)$ include the radial scale factor r such that they obey the boundary condition

$$y_i(0) = 0.$$

The coupled Dirac equations for the radial functions are then

$$mc^2y_1^- + c\hbar[\frac{d}{dr}+\frac{1}{r}(j+\tfrac{1}{2})]y_2^+ = ey_1^-, \tag{9}$$
$$-mc^2y_2^+ - c\hbar[\frac{d}{dr}-\frac{1}{r}(j+\tfrac{1}{2})]y_1^- = ey_2^+,$$

which is useful for finite element calculations.

2.2. Momentum representation

For the momentum representation we now use the spherical Bessel functions $j_l(kr)$ which are solutions of the Bessel equation in spherical coordinates for momentum $p = \hbar k$

$$\frac{1}{r^2}\frac{d}{dr}[r^2\frac{dj_l(kr)}{dr}] + [k^2 - \frac{l(l+1)}{r^2}]j_l(kr) = 0,$$

where $l = j \pm \frac{1}{2}$. The derivative relations for these Bessel functions are

$$[\frac{d}{dr}+\frac{1}{r}(j+\tfrac{1}{2})]rj_{j+\frac{1}{2}}(kr)=krj_{j-\frac{1}{2}}(kr), \tag{10}$$
$$[\frac{d}{dr}-\frac{1}{r}(j+\tfrac{1}{2})]rj_{j-\frac{1}{2}}(kr)=-krj_{j+\frac{1}{2}}(kr).$$

From (7) and the derivative relations (10) we have for the momentum representation,

$$\boldsymbol{\sigma}\cdot\mathbf{p}j_{j+\frac{1}{2}}(kr)[Y^{j+\frac{1}{2}},\chi^{\frac{1}{2}}]^j_n=i\hbar kj_{j-\frac{1}{2}}(kr)[Y^{j-\frac{1}{2}},\chi^{\frac{1}{2}}]^j_n, \tag{11}$$
$$\boldsymbol{\sigma}\cdot\mathbf{p}j_{j-\frac{1}{2}}(kr)[Y^{j-\frac{1}{2}},\chi^{\frac{1}{2}}]^j_n=-i\hbar kj_{j+\frac{1}{2}}(kr)[Y^{j+\frac{1}{2}},\chi^{\frac{1}{2}}]^j_n.$$

In (8) we let the orthonormal bases be $|k\ \ell\rangle$ for $\ell=j\pm\frac{1}{2}$ where

$$|k\ j-\frac{1}{2}\rangle=iN_{lk}rj_{j-\frac{1}{2}}(kr)[Y^{j-\frac{1}{2}},\chi^{\frac{1}{2}}]^j_n, \tag{12}$$
$$|k\ j+\frac{1}{2}\rangle=N_{lk}rj_{j+\frac{1}{2}}(kr)[Y^{j+\frac{1}{2}},\chi^{\frac{1}{2}}]^j_n.$$

It is shown in Appendix A that if the Bessel functions obey the boundary condition

$$j_l(k_nr_0)=0 \text{ for } n=1,2,...,$$

they form an orthonormal bases

$$N^2_{\ell k}\int_0^{r_0}r^2j_{l'}(k_mr)j_{l'}(k_nr)dr=\delta_{mn} \text{ for } l'=l-1,l,l+1.$$

The wavefunction equivalent to (8) then becomes for each k and j,

$$\psi=\frac{1}{r}\begin{pmatrix}c_1^-|k\ j-\frac{1}{2}\rangle\\ c_2^+|k\ j+\frac{1}{2}\rangle\end{pmatrix}. \tag{13}$$

In this momentum bases the equations in (9) become

$$mc^2c_1^-+c\hbar kc_2^+=ec_1^-, \tag{14}$$
$$-mc^2c_2^++c\hbar kc_1^-=ec_2^+,$$

with the two orthonormal solutions ψ_i for each k and j given by the columns below

$$\begin{array}{c|cc} & \psi_+ & \psi_- \\ c_1^- & \sqrt{\frac{e+mc^2}{2e}} & \sqrt{\frac{e-mc^2}{2e}} \\ c_2^+ & \sqrt{\frac{e-mc^2}{2e}} & -\sqrt{\frac{e+mc^2}{2e}} \end{array} \tag{15}$$

with corresponding energies e_i

$$\begin{aligned} e_\pm &= \pm\, e, \\ e &\equiv |e| = \sqrt{(c\hbar k)^2 + (mc^2)^2}. \end{aligned}$$

The relations for one-body operator $\boldsymbol{\sigma}\cdot\mathbf{p}$ in (7) or (11), corresponding to the coordinate or momentum representation, respectively, are used to determine the one-body Dirac equation. Fortunately, we can use the same relations for the one-body operators $\boldsymbol{\sigma}_e\cdot\mathbf{p}_e$ and $\boldsymbol{\sigma}_p\cdot\mathbf{p}_p$ of the electron and positron to determine the two-body Dirac equation in the two different representations as shown in the next section.

2.3. Spin

Note that the Dirac equations (9) or (14) are invariant with respect to the simultaneous exchange $m \leftrightarrow -m$ and $y_1 \leftrightarrow y_2$ so that the energies are doubly degenerate as expected for spin $\frac{1}{2}$ particles. That is, the exchange $m \leftrightarrow -m$ and $y_1 \leftrightarrow y_2$ is equivalent to replacing (8) in the coordinate representation with

$$\psi'(r\theta\varphi) = \frac{1}{r}\begin{pmatrix} y_1^+(r)[Y^{j+\frac{1}{2}}(\theta,\varphi),\chi^{\frac{1}{2}}]_n^j \\ iy_2^-(r)[Y^{j-\frac{1}{2}}(\theta,\varphi),\chi^{\frac{1}{2}}]_n^j \end{pmatrix}, \tag{16}$$

or replacing (13) in the momentum representation with

$$\psi' = \frac{1}{r}\begin{pmatrix} c_1^+|k\ j+\frac{1}{2}\rangle \\ c_2^-|k\ j-\frac{1}{2}\rangle \end{pmatrix}. \tag{17}$$

This results in solutions ψ'_i with the same coefficients as in (15) if we exchange $|k\ j-\frac{1}{2}\rangle \leftrightarrow |k\ j+\frac{1}{2}\rangle$. We find the two orthonormal solutions ψ'_i for each k and j in the columns below

$$\begin{array}{c|cc} & \psi'_+ & \psi'_- \\ c_1^+ & \sqrt{\frac{e+mc^2}{2e}} & \sqrt{\frac{e-mc^2}{2e}} \\ c_2^- & \sqrt{\frac{e-mc^2}{2e}} & -\sqrt{\frac{e+mc^2}{2e}} \end{array} \tag{18}$$

with the same corresponding energies e'_i

$$\begin{aligned} e'_\pm &= \pm\, e, \\ e &\equiv |e| = \sqrt{(c\hbar k)^2 + (mc^2)^2}, \end{aligned}$$

so that each energy is doubly degenerate with pairs of wavefunctions (ψ_+, ψ'_+) and (ψ_-, ψ'_-). We can show that this double degeneracy is the result of the spin degeneracy by looking at the effect of the helicity operator $\boldsymbol{\Sigma}\cdot\hat{\mathbf{p}}$ on the wavefunctions where

$$\mathbf{\Sigma}\cdot\hat{\mathbf{p}} = \begin{pmatrix} \boldsymbol{\sigma}\cdot\hat{\mathbf{p}} & 0 \\ 0 & \boldsymbol{\sigma}\cdot\hat{\mathbf{p}} \end{pmatrix},$$

with $\hat{\mathbf{p}} = \mathbf{p}/p$ and $p = \hbar k$. Using the properties in (11) we find

$$\mathbf{\Sigma}\cdot\hat{\mathbf{p}}\psi_{\pm} = \psi'_{\pm},$$

so that the degeneracy of the pair $(\psi_+,\ \psi'_+)$ with energy e and the pair $(\psi_-,\ \psi'_-)$ with energy $-e$ are a result of the two different spin components projected onto the momentum direction $\hat{\mathbf{p}}$. Namely, we have the projections

$$\begin{aligned}\mathbf{\Sigma}\cdot\hat{\mathbf{p}}(\psi_+ \pm \psi'_+) &= \pm(\psi_+ \pm \psi'_+),\\ \mathbf{\Sigma}\cdot\hat{\mathbf{p}}(\psi_- \pm \psi'_-) &= \pm(\psi_- \pm \psi'_-).\end{aligned}$$

For a given j we then have the total degeneracy $2(2j+1)$.

We can define the chirality operator $\mathbf{c}$ which exchanges the wavefunction components $\psi_1 \leftrightarrow \psi_2$ such that

$$\mathbf{c} = \begin{pmatrix} 0 & 1 \\ 1 & 0 \end{pmatrix}. \tag{19}$$

If we let $m = 0$ in (15) and (18), the coefficients are all $\sqrt{\frac{1}{2}}$ in magnitude and the chirality operator $\mathbf{c}$ is related to the helicity by

$$\mathbf{c}\psi^{\pm} = \pm\mathbf{\Sigma}\cdot\hat{\mathbf{p}}\psi_{\pm} = \pm\psi'_{\pm}. \tag{20}$$

The chirality operator can be expressed in terms of Dirac gamma matrices (using convention of Dirac, Pauli, and Sakurai) [13]

$$\mathbf{c} = -\gamma_1\gamma_2\gamma_3\gamma_4 = -\gamma_5, \tag{21}$$

where

$$\begin{aligned}\gamma_i &= -i\beta\alpha_i \text{ for } i = 1,2,3\\ \gamma_4 &= \beta.\end{aligned}$$

The chirality operator will be used for the two-body wavefunctions to determine important spin properties.

3. Two-Body Dirac Equation - Free Particles

We now consider the two-body Dirac equation for free particles in terms of their relative coordinates with respect to the center of momentum. Fortunately, for this purpose, we can use the one-particle equations derived above along with some simple recoupling coefficients for the angular momentum states. These equations are useful when we consider in the next section the effects of the simple Coulomb potential acting between the electron and positron. For a free electron and a free positron, the two-body Dirac Hamiltonian $\mathbf{H}_0$ is the sum of the individual Hamiltonians. The two-body Dirac equation becomes

$$\mathbf{H}_0\Psi = (\mathbf{h}_0^e + \mathbf{h}_0^p)\Psi = E\Psi, \tag{22}$$

or

$$(c\boldsymbol{\alpha}_e \cdot \mathbf{p}_e + mc^2\beta_e + c\boldsymbol{\alpha}_p \cdot \mathbf{p}_p + mc^2\beta_p)\Psi = E\Psi, \tag{23}$$

where the energy E is given by the sum

$$E = e_e + e_p = \pm\sqrt{p_e^2c^2 + m^2c^4} \pm \sqrt{p_p^2c^2 + m^2c^4}, \tag{24}$$

as in (1) and the wavefunction is the direct product

$$\Psi = \psi_e(\mathbf{r}_e)\psi_p(\mathbf{r}_p). \tag{25}$$

The four-component direct product wavefunction may be written in several ways:

$$\begin{aligned}\psi_e(\mathbf{r}_e)\psi_p(\mathbf{r}_p) &\equiv \begin{pmatrix}\psi_1(e)\psi_1(p)\\ \psi_1(e)\psi_2(p)\\ \psi_2(e)\psi_1(p)\\ \psi_2(e)\psi_2(p)\end{pmatrix} \equiv \begin{pmatrix}\Psi_{11}\\ \Psi_{12}\\ \Psi_{21}\\ \Psi_{22}\end{pmatrix},\\ &\equiv \Psi_{11}\mathbf{e}_{11} + \Psi_{12}\mathbf{e}_{12} + \Psi_{21}\mathbf{e}_{21} + \Psi_{22}\mathbf{e}_{22}.\end{aligned}$$

With this convention for Ψ_{ij}, the $i = 1, 2$ signifies the electron components with positive and negative rest mass, respectively, and the $j = 1, 2$ signifies the positron components with positive and negative rest mass, respectively, where

$$\begin{aligned}mc^2\beta_e\Psi &= mc^2(\Psi_{11}\mathbf{e}_{11} + \Psi_{12}\mathbf{e}_{12} - \Psi_{21}\mathbf{e}_{21} - \Psi_{22}\mathbf{e}_{22}),\\ mc^2\beta_p\Psi &= mc^2(\Psi_{11}\mathbf{e}_{11} - \Psi_{12}\mathbf{e}_{12} + \Psi_{21}\mathbf{e}_{21} - \Psi_{22}\mathbf{e}_{22}).\end{aligned}$$

We now transform to the relative coordinates given by

$$\begin{aligned}\boldsymbol{\rho} &= \mathbf{r}_e - \mathbf{r}_p,\\ \mathbf{R} &= \frac{1}{2}(\mathbf{r}_e + \mathbf{r}_p),\end{aligned} \tag{26}$$

with their conjugate momenta

$$\begin{aligned}\boldsymbol{\pi} &\equiv -i\hbar\boldsymbol{\nabla}_\rho = \frac{1}{2}(\mathbf{p}_e - \mathbf{p}_p),\\ \mathbf{P} &\equiv -i\hbar\boldsymbol{\nabla}_R = \mathbf{p}_e + \mathbf{p}_p.\end{aligned} \tag{27}$$

We let the total momentum be zero, $\mathbf{P} = \mathbf{0}$, corresponding to the center of momentum frame, so that

$$\begin{aligned}\mathbf{p}_e + \mathbf{p}_p &= \mathbf{0},\\ \mathbf{p}_e = -\mathbf{p}_p &= \boldsymbol{\pi},\end{aligned}$$

and the two-body Dirac equation becomes

$$(c\boldsymbol{\alpha}_e \cdot \boldsymbol{\pi} + mc^2\beta_e - c\boldsymbol{\alpha}_p \cdot \boldsymbol{\pi} + mc^2\beta_p)\Psi = E\Psi. \tag{28}$$

We have the energy solutions

$$\begin{aligned}E_\pm &= \pm 2\sqrt{\pi^2c^2 + m^2c^4},\\ E_0 &= 0,\end{aligned} \tag{29}$$

as in (2).

The individual spin functions couple to give us functions of total spin $S = 0$ and $S = 1$ where

$$\Omega^S_\Sigma \equiv [\chi^{\frac{1}{2}}_e, \chi^{\frac{1}{2}}_p]^S_\Sigma = \sum_{\sigma_e,\sigma_p} C^{\frac{1}{2}\ \frac{1}{2}\ S}_{\sigma_e\ \sigma_p\ \Sigma}\chi^{\frac{1}{2}}_{\sigma_e}\chi^{\frac{1}{2}}_{\sigma_p}, \tag{30}$$

or explicitly using the coupling coefficients for spin one-half particles,

$$\begin{aligned}\Omega^0_0 &\equiv [\chi^{\frac{1}{2}}_e, \chi^{\frac{1}{2}}_p]^0_0 = [\chi^{\frac{1}{2}}_{\frac{1}{2}}(e)\chi^{\frac{1}{2}}_{-\frac{1}{2}}(p) - \chi^{\frac{1}{2}}_{-\frac{1}{2}}(e)\chi^{\frac{1}{2}}_{\frac{1}{2}}(p)]/\sqrt{2},\\ \Omega^1_0 &\equiv [\chi^{\frac{1}{2}}_e, \chi^{\frac{1}{2}}_p]^1_0 = [\chi^{\frac{1}{2}}_{\frac{1}{2}}(e)\chi^{\frac{1}{2}}_{-\frac{1}{2}}(p) + \chi^{\frac{1}{2}}_{-\frac{1}{2}}(e)\chi^{\frac{1}{2}}_{\frac{1}{2}}(p)]/\sqrt{2},\\ \Omega^1_{-1} &\equiv [\chi^{\frac{1}{2}}_e, \chi^{\frac{1}{2}}_p]^1_{-1} = \chi^{\frac{1}{2}}_{-\frac{1}{2}}(e)\chi^{\frac{1}{2}}_{-\frac{1}{2}}(p),\\ \Omega^1_1 &\equiv [\chi^{\frac{1}{2}}_e, \chi^{\frac{1}{2}}_p]^1_1 = \chi^{\frac{1}{2}}_{\frac{1}{2}}(e)\chi^{\frac{1}{2}}_{\frac{1}{2}}(p).\end{aligned}$$

We will also make use of the exchange symmetry of the spin functions, namely

$$\begin{aligned}[\chi^{\frac{1}{2}}_e, \chi^{\frac{1}{2}}_p]^0_0 &= -[\chi^{\frac{1}{2}}_p, \chi^{\frac{1}{2}}_e]^0_0,\\ [\chi^{\frac{1}{2}}_e, \chi^{\frac{1}{2}}_p]^1_\Sigma &= [\chi^{\frac{1}{2}}_p, \chi^{\frac{1}{2}}_e]^1_\Sigma,\end{aligned} \tag{31}$$

so that the $S = 0$ spin functions are antisymmetric and the $S = 1$ spin functions are symmetric, respectively, under particle exchange.

Again, we use spherical coordinates where $\boldsymbol{\rho} \equiv (\rho, \theta, \varphi)$ and couple the spherical harmonics with the total spin functions

$$[Y^L(\theta,\varphi), \Omega^S]^J_N \equiv [Y^L(\theta,\varphi), [\chi^{\frac{1}{2}}_e, \chi^{\frac{1}{2}}_p]^S]^J_N = \sum_{M,\Sigma} C^{L\ \ S\ \ J}_{M\ \Sigma\ N} Y^L_M(\theta,\varphi)\Omega^S_\Sigma,$$

to obtain wavefunctions of total angular momentum J and projection $J_z = N$. There are four possible angular momentum states with a given J, N depending on the angular momentum L and spin S. These four are:

$$
\begin{aligned}
[Y^J,\Omega^0]^J_N &\equiv [Y^J,[\chi_e^{\frac{1}{2}},\chi_p^{\frac{1}{2}}]^0]^J_N \\
&= a[[Y^J,\chi_e^{\frac{1}{2}}]^{J+\frac{1}{2}},\chi_p^{\frac{1}{2}}]^J_N - b[[Y^J,\chi_e^{\frac{1}{2}}]^{J-\frac{1}{2}},\chi_p^{\frac{1}{2}}]^J_N, \\
[Y^J,\Omega^1]^J_N &\equiv [Y^J,[\chi_e^{\frac{1}{2}},\chi_p^{\frac{1}{2}}]^1]^J_N \\
&= b[[Y^J,\chi_e^{\frac{1}{2}}]^{J+\frac{1}{2}},\chi_p^{\frac{1}{2}}]^J_N + a[[Y^J,\chi_e^{\frac{1}{2}}]^{J-\frac{1}{2}},\chi_p^{\frac{1}{2}}]^J_N, \\
[Y^{J+1},\Omega^1]^J_N &\equiv [Y^{J+1},[\chi_e^{\frac{1}{2}},\chi_p^{\frac{1}{2}}]^1]^J_N = [[Y^{J+1},\chi_e^{\frac{1}{2}}]^{J+\frac{1}{2}},\chi_p^{\frac{1}{2}}]^J_N, \\
[Y^{J-1},\Omega^1]^J_N &\equiv [Y^{J-1},[\chi_e^{\frac{1}{2}},\chi_p^{\frac{1}{2}}]^1]^J_N = [[Y^{J-1},\chi_e^{\frac{1}{2}}]^{J-\frac{1}{2}},\chi_p^{\frac{1}{2}}]^J_N,
\end{aligned}
\tag{32}
$$

where

$$
a=\sqrt{\frac{J+1}{2J+1}},\ b=\sqrt{\frac{J}{2J+1}}, \tag{33}
$$

are the angular momentum recoupling coefficients for spin one-half particles.

3.1. Coordinate Representation

It is now a simple matter to derive the following three separate sets of two-body equations for free particles in the coordinate representation. From the one-particle equations (7), we find the useful equations for the radial functions $y(\rho)$,

$$
\begin{aligned}
\boldsymbol{\sigma}_e\cdot\boldsymbol{\pi}\frac{y}{\rho}[[Y^J,\chi_e^{\frac{1}{2}}]^{J+\frac{1}{2}},\chi_p^{\frac{1}{2}}]^J_N &= \frac{i\hbar}{\rho}(\frac{dy}{d\rho}-\frac{(J+1)y}{\rho})[Y^{J+1},\chi_e^{\frac{1}{2}}]^{J+\frac{1}{2}},\chi_p^{\frac{1}{2}}]^J_N, \\
\boldsymbol{\sigma}_e\cdot\boldsymbol{\pi}\frac{y}{\rho}[[Y^J,\chi_e^{\frac{1}{2}}]^{J-\frac{1}{2}},\chi_p^{\frac{1}{2}}]^J_N &= \frac{i\hbar}{\rho}(\frac{dy}{d\rho}+\frac{Jy}{\rho})[Y^{J-1},\chi_e^{\frac{1}{2}}]^{J-\frac{1}{2}},\chi_p^{\frac{1}{2}}]^J_N, \\
\boldsymbol{\sigma}_e\cdot\boldsymbol{\pi}\frac{y}{\rho}[[Y^{J+1},\chi_e^{\frac{1}{2}}]^{J+\frac{1}{2}},\chi_p^{\frac{1}{2}}]^J_N &= \frac{i\hbar}{\rho}(\frac{dy}{d\rho}+\frac{(J+1)y}{\rho})[Y^J,\chi_e^{\frac{1}{2}}]^{J+\frac{1}{2}},\chi_p^{\frac{1}{2}}]^J_N, \\
\boldsymbol{\sigma}_e\cdot\boldsymbol{\pi}\frac{y}{\rho}[[Y^{J-1},\chi_e^{\frac{1}{2}}]^{J-\frac{1}{2}},\chi_p^{\frac{1}{2}}]^J_N &= \frac{i\hbar}{\rho}(\frac{dy}{d\rho}-\frac{Jy}{\rho})[Y^J,\chi_e^{\frac{1}{2}}]^{J-\frac{1}{2}},\chi_p^{\frac{1}{2}}]^J_N.
\end{aligned}
\tag{34}
$$

where the latter two equations are just the Hermitian conjugate of the first two equations.

3.1.1. Case 1: $S=0$, $L=J$.

We first consider the bases

$$
\Psi=\frac{1}{\rho}\begin{pmatrix}
y^0_{11}(\rho)[Y^J,\Omega^0]^J_N \\
i\{y^+_{12}(\rho)[Y^{J+1},\Omega^1]^J_N+y^-_{12}(\rho)[Y^{J-1},\Omega^1]^J_N\} \\
i\{y^+_{21}(\rho)[Y^{J+1},\Omega^1]^J_N+y^-_{21}(\rho)[Y^{J-1},\Omega^1]^J_N\} \\
y^0_{22}(\rho)[Y^J,\Omega^0]^J_N
\end{pmatrix}, \tag{35}
$$

where, as in the one-body case, the radial functions $y_{ij}(\rho)$ include the radial scale factor ρ for which we have the boundary condition

$$
y_{ij}(0)=0.
$$

Note that it is the large-large component Ψ_{11} which defines the total spin $S = 0$ and angular momentum $L = J$ for the atomic states of this case.

We evaluate $\boldsymbol{\sigma}_e{\cdot}\mathbf{p}_e = \boldsymbol{\sigma}_e{\cdot}\boldsymbol{\pi}$ and $\boldsymbol{\sigma}_p{\cdot}\mathbf{p}_p = -\boldsymbol{\sigma}_p{\cdot}\boldsymbol{\pi}$ operating on the wavefunctions in (35) just as we did for single particles. We have using (34),

$$\begin{aligned}
\boldsymbol{\sigma}_e{\cdot}\boldsymbol{\pi}\frac{y}{\rho}[Y^J,\Omega^0]^J_N &= \boldsymbol{\sigma}_e{\cdot}\boldsymbol{\pi}\frac{y}{\rho}\{a[[Y^J,\chi_e^{\frac{1}{2}}]^{J+\frac{1}{2}},\chi_p^{\frac{1}{2}}]^J_N - b[[Y^J,\chi_e^{\frac{1}{2}}]^{J-\frac{1}{2}},\chi_p^{\frac{1}{2}}]^J_N\},\\
&= \frac{i\hbar}{\rho}\{a(\frac{dy}{d\rho}-\frac{(J+1)y}{\rho})[[Y^{J+1},\chi_e^{\frac{1}{2}}]^{J+\frac{1}{2}},\chi_p^{\frac{1}{2}}]^J_N\\
&- b(\frac{dy}{d\rho}+\frac{Jy}{\rho})[[Y^{J-1},\chi_e^{\frac{1}{2}}]^{J-\frac{1}{2}},\chi_p^{\frac{1}{2}}]^J_N\},\\
&= \frac{i\hbar}{\rho}\{a(\frac{dy}{d\rho}-\frac{(J+1)y}{\rho})[Y^{J+1}\Omega^1]^J_N - b(\frac{dy}{d\rho}+\frac{Jy}{\rho})[Y^{J-1}\Omega^1]^J_N\}.
\end{aligned}$$

We can also evaluate the operator $-\boldsymbol{\sigma}_p{\cdot}\boldsymbol{\pi}$,

$$\begin{aligned}
-\boldsymbol{\sigma}_p{\cdot}\boldsymbol{\pi}\frac{y}{\rho}[Y^J,\Omega^0]^J_N &= \boldsymbol{\sigma}_p{\cdot}\boldsymbol{\pi}\frac{y}{\rho}[Y^J,[\chi_p^{\frac{1}{2}},\chi_e^{\frac{1}{2}}]^0]^J_N,\\
&= \boldsymbol{\sigma}_p{\cdot}\boldsymbol{\pi}\frac{y}{\rho}\{a[[Y^J,\chi_p^{\frac{1}{2}}]^{J+\frac{1}{2}},\chi_e^{\frac{1}{2}}]^J_N - b[[Y^J,\chi_p^{\frac{1}{2}}]^{J-\frac{1}{2}},\chi_e^{\frac{1}{2}}]^J_N\},\\
&= \frac{i\hbar}{\rho}\{a(\frac{dy}{d\rho}-\frac{(J+1)y}{\rho})[Y^{J+1}\Omega^1]^J_N - b(\frac{dy}{d\rho}+\frac{Jy}{\rho})[Y^{J-1}\Omega^1]^J_N\},\\
&= \boldsymbol{\sigma}_e{\cdot}\boldsymbol{\pi}\frac{y}{\rho}[Y^J,\Omega^0]^J_N.
\end{aligned}$$

The latter result depends on the exchange symmetry (31) of the $S = 0$ and $S = 1$ states. Finally, using the fact that the operators $\boldsymbol{\sigma}_e{\cdot}\boldsymbol{\pi}$ and $-\boldsymbol{\sigma}_p{\cdot}\boldsymbol{\pi}$ are Hermitian, we find that the two-body Dirac equation for Case 1 ($S = 0$) gives us the six equations for the symmetrized radial functions (of which four are coupled),

$$2mc^2(y^0_{11}-y^0_{22}) - 2a\hbar c[\frac{d}{d\rho}+\frac{J+1}{\rho}](y^+_{12}+y^+_{21}) + 2b\hbar c[\frac{d}{d\rho}-\frac{J}{\rho}](y^-_{12}+y^-_{21}) = E(y^0_{11}+y^0_{22}), \tag{36}$$

$$\begin{aligned}
2mc^2(y^0_{11}+y^0_{22}) &= E(y^0_{11}-y^0_{22}),\\
2a\hbar c[\frac{d}{d\rho}-\frac{J+1}{\rho}](y^0_{11}+y^0_{22}) &= E(y^+_{12}+y^+_{21}),\\
-2b\hbar c[\frac{d}{d\rho}+\frac{J}{\rho}](y^0_{11}+y^0_{22}) &= E(y^-_{12}+y^-_{21}),\\
0 &= E(y^+_{12}-y^+_{21}),\\
0 &= E(y^-_{12}-y^-_{21}).
\end{aligned}$$

The last two equations are allowed but have the opposite charge conjugation parity from the four coupled equations as we discuss below. From the second equation above we have

$$(y^0_{11}-y^0_{22}) = \frac{2mc^2(y^0_{11}+y^0_{22})}{E}, \tag{37}$$

so that when $E = 0$ we must have $(y^0_{11}+y^0_{22}) = 0$ or else $(y^0_{11}-y^0_{22})$ would be singular.

3.1.2. Case 2: $S = 1$, $L = J$.

We now consider the bases

$$\Psi = \frac{1}{\rho}\begin{pmatrix} y^1_{11}(\rho)[Y^J,\Omega^1]^J_N \\ i\{y^+_{12}(\rho)[Y^{J+1},\Omega^1]^J_N + y^-_{12}(\rho)[Y^{J-1},\Omega^1]^J_N\} \\ i\{y^+_{21}(\rho)[Y^{J+1},\Omega^1]^J_N + y^-_{21}(\rho)[Y^{J-1},\Omega^1]^J_N\} \\ y^1_{22}(\rho)[Y^J,\Omega^1]^J_N \end{pmatrix}, \tag{38}$$

with the same boundary conditions as before, where the large-large component Ψ_{11} now corresponds to the spin $S = 1$ atomic state with $L = J$.

We evaluate $\boldsymbol{\sigma}_e{\cdot}\mathbf{p}_e = \boldsymbol{\sigma}_e{\cdot}\boldsymbol{\pi}$ and $\boldsymbol{\sigma}_p{\cdot}\mathbf{p}_p = -\boldsymbol{\sigma}_p{\cdot}\boldsymbol{\pi}$ operating on the wavefunctions as before. We have

$$\begin{aligned}
\boldsymbol{\sigma}_e{\cdot}\boldsymbol{\pi}\frac{y}{\rho}[Y^J,\Omega^1]^J_N &= \boldsymbol{\sigma}_e{\cdot}\boldsymbol{\pi}\frac{y}{\rho}\{b[[Y^J,\chi_e^{\frac12}]^{J+\frac12},\chi_p^{\frac12}]^J_N + a[[Y^J,\chi_e^{\frac12}]^{J-\frac12},\chi_p^{\frac12}]^J_N\},\\
&= \frac{i\hbar}{\rho}\{b(\frac{dy}{d\rho} - \frac{(J+1)y}{\rho})[[Y^{J+1},\chi_e^{\frac12}]^{J+\frac12},\chi_p^{\frac12}]^J_N\\
&+ a(\frac{dy}{d\rho} + \frac{Jy}{\rho})[[Y^{J-1},\chi_e^{\frac12}]^{J-\frac12},\chi_p^{\frac12}]^J_N\},\\
&= \frac{i\hbar}{\rho}\{b(\frac{dy}{d\rho} - \frac{(J+1)y}{\rho})[Y^{J+1}\Omega^1]^J_N + a(\frac{dy}{d\rho} + \frac{Jy}{\rho})[Y^{J-1}\Omega^1]^J_N\},
\end{aligned}$$

and

$$\begin{aligned}
-\boldsymbol{\sigma}_p{\cdot}\boldsymbol{\pi}\frac{y}{\rho}[Y^J,\Omega^1]^J_N &= -\boldsymbol{\sigma}_p{\cdot}\boldsymbol{\pi}(y/\rho)[Y^J,[\chi_p^{\frac12},\chi_e^{\frac12}]^1]^J_N,\\
&= -\boldsymbol{\sigma}_p{\cdot}\boldsymbol{\pi}(y/\rho)\{b[[Y^J,\chi_p^{\frac12}]^{J+\frac12},\chi_e^{\frac12}]^J_N + a[[Y^J,\chi_p^{\frac12}]^{J-\frac12},\chi_e^{\frac12}]^J_N\},\\
&= -\frac{i\hbar}{\rho}\{b(\frac{dy}{d\rho} - \frac{(J+1)y}{\rho})[Y^{J+1}\Omega^1]^J_N + a(\frac{dy}{d\rho} + \frac{Jy}{\rho})[Y^{J-1}\Omega^1]^J_N\},\\
&= -\boldsymbol{\sigma}_e{\cdot}\boldsymbol{\pi}\frac{y}{\rho}[Y^J,\Omega^1]^J_N.
\end{aligned}$$

Finally, using the fact that the operators $\boldsymbol{\sigma}_e{\cdot}\boldsymbol{\pi}$ and $-\boldsymbol{\sigma}_p{\cdot}\boldsymbol{\pi}$ are Hermitian, we find that the two-body Dirac equation for Case 2 ($S = 1$) gives us the six equations for the symmetrized radial functions (of which four are coupled),

$$\begin{aligned}
2mc^2(y^1_{11}+y^1_{22}) + 2b\hbar c[\frac{d}{d\rho} + \frac{J+1}{\rho}](y^+_{12}-y^+_{21}) + 2a\hbar c[\frac{d}{d\rho} - \frac{J}{\rho}](y^-_{12}-y^-_{21}) &= E(y^1_{11}-y^1_{22}), \qquad (39)\\
2mc^2(y^1_{11}-y^1_{22}) &= E(y^1_{11}+y^1_{22}),\\
-2b\hbar c[\frac{d}{d\rho} - \frac{J+1}{\rho}](y^1_{11}+y^1_{22}) &= E(y^+_{12}-y^+_{21}),\\
-2a\hbar c[\frac{d}{d\rho} + \frac{J}{\rho}](y^1_{11}+y^1_{22}) &= E(y^-_{12}-y^-_{21}),\\
0 &= E(y^+_{12}+y^+_{21}),\\
0 &= E(y^-_{12}+y^-_{21}).
\end{aligned}$$

Again, the last two equations are allowed but have the opposite charge conjugation parity from the four coupled equations as we discuss below. From the second equation above we have

$$(y^1_{11} + y^1_{22}) = \frac{2mc^2(y^1_{11} - y^1_{22})}{E}, \tag{40}$$

so that when $E = 0$ we must have $(y^1_{11} - y^1_{22}) = 0$ or else $(y^1_{11} + y^1_{22})$ would be singular.

3.1.3. Case 3: $S = 1$, $L \neq J$.

Case 3 can be obtained from Case 1 and Case 2 by a simple transformation. We use the wavefunction

$$\Psi = \frac{1}{\rho}\begin{pmatrix} i\{y^+_{11}(\rho)[Y^{J+1}, \Omega^1]^J_N + y^-_{11}(\rho)[Y^{J-1}, \Omega^1]^J_N\} \\ y^0_{12}(\rho)[Y^J, \Omega^0]^J_N + y^1_{12}(\rho)[Y^J, \Omega^1]^J_N \\ y^0_{21}(\rho)[Y^J, \Omega^0]^J_N + y^1_{21}(\rho)[Y^J, \Omega^1]^J_N \\ i\{y^+_{22}(\rho)[Y^{J+1}, \Omega^1]^J_N + y^-_{22}(\rho)[Y^{J-1}, \Omega^1]^J_N\} \end{pmatrix}. \tag{41}$$

Note that the large-large component Ψ_{11} can now correspond to the atomic state with either $L = J + 1$ or $L = J - 1$. The new equations can be found from Case 1 and Case 2 by the exchange $m_e \leftrightarrow -m_e$, $y_{11} \leftrightarrow y_{21}$, $y_{22} \leftrightarrow y_{12}$, or, equivalently, the exchange $m_p \leftrightarrow -m_p$, $y_{11} \leftrightarrow y_{12}$, $y_{22} \leftrightarrow y_{21}$. The two-body Dirac equation in this basis gives the eight equations for the radial functions (of which six are coupled),

$$\begin{aligned}
-2a\hbar c[\frac{d}{d\rho} + \frac{J+1}{\rho}](y^+_{11} + y^+_{22}) + 2b\hbar c[\frac{d}{d\rho} - \frac{J}{\rho}](y^-_{11} + y^-_{22}) &= E(y^0_{12} + y^0_{21}), \\
2mc^2(y^+_{11} - y^+_{22}) + 2a\hbar c[\frac{d}{d\rho} - \frac{J+1}{\rho}](y^0_{12} + y^0_{21}) &= E(y^+_{11} + y^+_{22}), \\
2mc^2(y^-_{11} - y^-_{22}) - 2b\hbar c[\frac{d}{d\rho} + \frac{J}{\rho}](y^0_{12} + y^0_{21}) &= E(y^-_{11} + y^-_{11}), \\
0 &= E(y^0_{12} - y^0_{21}), \\
2b\hbar c[\frac{d}{d\rho} + \frac{J+1}{\rho}](y^+_{11} - y^+_{22}) + 2a\hbar c[\frac{d}{d\rho} - \frac{J}{\rho}](y^-_{11} - y^-_{22}) &= E(y^1_{12} - y^1_{21}), \\
2mc^2(y^+_{11} + y^+_{22}) - 2b\hbar c[\frac{d}{d\rho} - \frac{J+1}{\rho}](y^1_{12} - y^1_{21}) &= E(y^+_{11} - y^+_{22}), \\
2mc^2(y^-_{11} + y^-_{22}) - 2a\hbar c[\frac{d}{d\rho} + \frac{J}{\rho}](y^1_{12} - y^1_{21}) &= E(y^-_{11} - y^-_{11}), \\
0 &= E(y^1_{12} + y^1_{21}).
\end{aligned} \tag{42}$$

With this transformation, the two separate sets of four coupled equations in the Case 1 and Case 2 bases now become six coupled equations in Case 3. The uncoupled equations are allowed but have opposite charge conjugation parity from the other equations as we discuss below.

3.2. Momentum Representation

Fortunately, there are analytic solutions to the above free-particle equations in terms of momentum functions. The structure of these equations and their solutions reveal some remarkable simplicity, symmetry, and reducibility as compared with their counterparts in the coordinate representation. As a result, this analysis is fundamental to our understanding of the resonance and atomic solutions.

The analytic solutions are found by 'Fourier' analyzing the radial equations in the coordinate representation with the spherical Bessel functions $j_L(k\rho)$ in momentum space $\hbar k$ for a given orbital angular momentum $L = J-1,\ J,\ J+1$. Consider $j_J(k_n\rho)$ where the k_n are determined by the boundary condition

$$j_J(k_n\rho_0) = 0, \text{ for } n = 1.2...., \tag{43}$$

with ρ_0 larger than the atomic radius $\rho_0 \gg 2na_0$ for positronium (where a_0 is the *Bohr* radius) and with the normalization N_{Jk} determined by

$$N_{Jk}^2 \int_0^{\rho_0} \rho^2 j_J^2(k_n\rho)d\rho = 1.$$

It is shown in Appendix A that the Bessel functions $j_L(k_n\rho)$ for $L = J-1, J, J+1$ all have the same normalization N_{Jk} given by (A.10)

$$N_{Jk} \equiv N_{Jn} = \sqrt{\frac{2}{\rho_0^3 j_{J\pm1}^2(k_n\rho_0)}} \sim k_n\sqrt{2/\rho_0},$$

where $j_{J+1}(k_n\rho_0) = -j_{J-1}(k_n\rho_0)$ and the approximation corresponds to high $n >> 1$ where (A.5)

$$k_n \sim (\frac{1}{2}J\pi + n\pi)/\rho_0.$$

Furthermore, it is shown in Appendix A that the functions $\rho j_L(k_n\rho)$ form an orthonormal set such that

$$N_{Jn}^2 \int_0^{\rho_0} \rho^2 j_L(k_n\rho) j_L(k_m\rho)d\rho = \delta_{nm} \text{ for } L = J-1,\ J,\ J+1,$$

where the k_n are, again, determined solely by (43) (where $L = J$).

As before, there are four possible angular momentum states with a given J, N and k depending on the orbital angular momentum L and spin S. The momentum bases $|L, S, k\rangle$ for these four states are (for a given J, N),

$$\begin{aligned}
|J, 0, k\rangle &= N_{Jk}\rho j_J(k\rho)[Y^J, \Omega^0]_N^J, \\
|J, 1, k\rangle &= N_{Jk}\rho j_J(k\rho)[Y^J, \Omega^1]_N^J, \\
|J+1, 1, k\rangle &= iN_{Jk}\rho j_{J+1}(k\rho)[Y^{J+1}, \Omega^1]_N^J, \\
|J-1, 1, k\rangle &= iN_{Jk}\rho j_{J-1}(k\rho)[Y^{J-1}, \Omega^1]_N^J.
\end{aligned} \tag{44}$$

Note that we choose to keep the scale factor ρ for spherical coordinates in our definition of the wavefunction as we did in the coordinate representation so that these wavefunctions are also zero at $\rho = 0$. Also note that we have one $S = 0$ state and three $S = 1$ states, as expected, corresponding to the four possible spin functions. It is very useful to define two orthogonal states which are linear combinations of $|J+1, 1, k\rangle$ and $|J-1, 1, k\rangle$, namely,

$$\begin{aligned} |J\alpha, 1, k\rangle &\equiv a|J+1, 1, k\rangle + b|J-1, 1, k\rangle, \\ |J\beta, 1, k\rangle &\equiv -b|J+1, 1, k\rangle + a|J-1, 1, k\rangle, \end{aligned} \tag{45}$$

where a and b are the recoupling coefficients given in (33). As we will see below, the solutions to the free-particle equations always appear in such combinations. These free particle wavefunctions may be expanded in terms of products of their single particle components $g^{\ell_e\, j_e}_{n_e}(kr_e, \theta_e, \varphi_e) g^{\ell_p\, j_p}_{n_p}(kr_p, \theta_p, \varphi_p)$ where

$$g^{\ell\, j}_n(kr, \theta, \varphi) \equiv j_\ell(kr)[Y^\ell(\theta, \varphi), \chi^{\frac{1}{2}}]^j_n,$$

as given by (B.10), (B.11), (B.18) and (B.19) in Appendix B.

Using the one-particle equations (11) for the spherical Bessel functions, we can find the equivalent to (34),

$$\begin{aligned} \boldsymbol{\sigma}_e{\cdot}\boldsymbol{\pi}\{j_{J+1}(k\rho)[[Y^{J+1}, \chi_e^{\frac{1}{2}}]^{J+\frac{1}{2}}, \chi_p^{\frac{1}{2}}]^J_N\} &= i\hbar k\{j_J(k\rho)[[Y^J, \chi_e^{\frac{1}{2}}]^{J+\frac{1}{2}}, \chi_p^{\frac{1}{2}}]^J_N\}, \\ \boldsymbol{\sigma}_e{\cdot}\boldsymbol{\pi}\{j_{J-1}(k\rho)[[Y^{J-1}, \chi_e^{\frac{1}{2}}]^{J-\frac{1}{2}}, \chi_p^{\frac{1}{2}}]^J_N\} &= -i\hbar k\{j_J(k\rho)[[Y^J, \chi_e^{\frac{1}{2}}]^{J-\frac{1}{2}}, \chi_p^{\frac{1}{2}}]^J_N\}, \\ \boldsymbol{\sigma}_e{\cdot}\boldsymbol{\pi}\{j_J(k\rho)[[Y^J, \chi_e^{\frac{1}{2}}]^{J+\frac{1}{2}}, \chi_p^{\frac{1}{2}}]^J_N\} &= -i\hbar k\{j_{J+1}(k\rho)[[Y^{J+1}, \chi_e^{\frac{1}{2}}]^{J+\frac{1}{2}}, \chi_p^{\frac{1}{2}}]^J_N\}, \\ \boldsymbol{\sigma}_e{\cdot}\boldsymbol{\pi}\{j_J(k\rho)[[Y^J, \chi_e^{\frac{1}{2}}]^{J-\frac{1}{2}}, \chi_p^{\frac{1}{2}}]^J_N\} &= i\hbar k\{j_{J-1}(k\rho)[[Y^{J-1}, \chi_e^{\frac{1}{2}}]^{J-\frac{1}{2}}, \chi_p^{\frac{1}{2}}]^J_N\}. \end{aligned} \tag{46}$$

where the latter two equations are just the Hermitian conjugate of the first two equations. Recoupling the angular wavefunctions as in (32) we can evaluate $\boldsymbol{\sigma}_e{\cdot}\mathbf{p}_e = \boldsymbol{\sigma}_e{\cdot}\boldsymbol{\pi}$ and $\boldsymbol{\sigma}_p{\cdot}\mathbf{p}_p = -\boldsymbol{\sigma}_p{\cdot}\boldsymbol{\pi}$ operating on the wavefunctions in (44) just as we did for single particles. We have

$$\begin{aligned} \boldsymbol{\sigma}_e{\cdot}\boldsymbol{\pi}\frac{c}{\rho}|J, 0, k\rangle &= \boldsymbol{\sigma}_e{\cdot}\boldsymbol{\pi} c N_{Jk} j_J(k\rho)\{a[[Y^J, \chi_e^{\frac{1}{2}}]^{J+\frac{1}{2}}, \chi_p^{\frac{1}{2}}]^J_N - b[[Y^J, \chi_e^{\frac{1}{2}}]^{J-\frac{1}{2}}, \chi_p^{\frac{1}{2}}]^J_N\}, \\ &= i\hbar k c N_{Jk}\{-a j_{J+1}(k\rho)[[Y^{J+1}, \chi_e^{\frac{1}{2}}]^{J+\frac{1}{2}}, \chi_p^{\frac{1}{2}}]^J_N \\ &\quad - b j_{J-1}(k\rho)[[Y^{J-1}, \chi_e^{\frac{1}{2}}]^{J-\frac{1}{2}}, \chi_p^{\frac{1}{2}}]^J_N\}, \\ &= -i\hbar k c N_{Jk}\{a j_{J+1}(k\rho)[Y^{J+1}\Omega^1]^J_N + b j_{J-1}(k\rho)[Y^{J-1}\Omega^1]^J_N\}, \\ &= -\hbar k \frac{c}{\rho}|J\alpha, 1, k\rangle, \end{aligned}$$

where c is a Bessel coefficient. Similarly, we find

$$-\boldsymbol{\sigma}_p{\cdot}\boldsymbol{\pi}\frac{c}{\rho}|J, 0, k\rangle = \boldsymbol{\sigma}_e{\cdot}\boldsymbol{\pi}\frac{c}{\rho}|J, 0, k\rangle.$$

We also have

$$\begin{aligned}
\boldsymbol{\sigma}_e{\cdot}\boldsymbol{\pi}\frac{c}{\rho}|J,1,k\rangle &= \boldsymbol{\sigma}_e{\cdot}\boldsymbol{\pi}cN_{Jk}.j_J(k\rho)\{b[[Y^J,\chi_e^{\frac{1}{2}}]^{J+\frac{1}{2}},\chi_p^{\frac{1}{2}}]_N^J + a[[Y^J,\chi_e^{\frac{1}{2}}]^{J-\frac{1}{2}},\chi_p^{\frac{1}{2}}]_N^J\},\\
&= i\hbar kcN_{Jk}.\{-bj_{J+1}(k\rho)[[Y^{J+1},\chi_e^{\frac{1}{2}}]^{J+\frac{1}{2}},\chi_p^{\frac{1}{2}}]_N^J\\
&+ aj_{J-1}(k\rho)[[Y^{J-1},\chi_e^{\frac{1}{2}}]^{J-\frac{1}{2}},\chi_p^{\frac{1}{2}}]_N^J\},\\
&= i\hbar kcN_{Jk}.\{-bj_{J+1}(k\rho)[Y^{J+1}\Omega^1]_N^J + aj_{J-1}(k\rho)[Y^{J-1}\Omega^1]_N^J\},\\
&= \hbar k\frac{c}{\rho}|J\beta,1,k\rangle,
\end{aligned}$$

and

$$-\boldsymbol{\sigma}_p{\cdot}\boldsymbol{\pi}\frac{c}{\rho}|J,1,k\rangle = -\boldsymbol{\sigma}_e{\cdot}\boldsymbol{\pi}\frac{c}{\rho}|J,1,k\rangle.$$

The three cases of equations in momentum space, equivalent to those in the coordinate representation, can now be given and readily solved analytically. In Section 5 we will show that, even in the presence of an electromagnetic potential between the electron and positron, we may use the momentum wavefunctions to separate the equations for atomic states and resonance states. We shall present the three cases first and then discuss them together rather than individually because it is important to show their relationships.

3.2.1. Case 1: $S = 0$, $L = J$.

We first consider the wavefunction Ψ in terms of the $|L,S,k\rangle$ states above for a given k, J which is equivalent to Case 1 in the coordinate representation,

$$\Psi = \frac{1}{\rho}\begin{pmatrix} c_{11}^0|J,0,k\rangle \\ c_{12}^\alpha|J\alpha,1,k\rangle \\ c_{21}^\alpha|J\alpha,1,k\rangle \\ c_{22}^0|J,0,k\rangle \end{pmatrix}. \tag{47}$$

Using the relations above, the two-body Dirac equation in momentum space gives us the coupled equations for the symmetrized Bessel coefficients for a given k, J,

$$\begin{aligned}
2mc^2(c_{11}^0 - c_{22}^0) - 2\hbar ck(c_{12}^\alpha + c_{21}^\alpha) &= E(c_{11}^0 + c_{22}^0),\\
2mc^2(c_{11}^0 + c_{22}^0) &= E(c_{11}^0 - c_{22}^0),\\
-2\hbar ck(c_{11}^0 + c_{22}^0) &= E(c_{12}^\alpha + c_{21}^\alpha),\\
0 &= E(c_{12}^\alpha - c_{21}^\alpha),
\end{aligned} \tag{48}$$

where we have used the Hermitian property of the operators. We have the four

orthonormal solutions Ψ_i, for each k, J given in the columns below

$$\begin{array}{c|cccc} & \sqrt{2}\Psi^0_+ & \sqrt{2}\Psi^0_- & \sqrt{2}\Psi^0_0 & \sqrt{2}\Psi^\alpha_0 \\ \hline (c^0_{11}+c^0_{22}) & 1 & 1 & . & . \\ (c^0_{11}-c^0_{22}) & \frac{mc^2}{e} & -\frac{mc^2}{e} & \frac{\sqrt{2}\hbar ck}{e} & . \\ (c^\alpha_{12}+c^\alpha_{21}) & -\frac{\hbar ck}{e} & \frac{\hbar ck}{e} & \frac{\sqrt{2}mc^2}{e} & . \\ (c^\alpha_{12}-c^\alpha_{21}) & . & . & . & \sqrt{2} \\ \hline C-parity & J & J & J & J+1 \end{array} \tag{49}$$

with corresponding energies E_i

$$\begin{aligned} E_\pm &= \pm 2e, \\ E_0 &= 0, \\ e &= \sqrt{(\hbar ck)^2+(mc^2)^2}. \end{aligned}$$

These, of course, are just the free particle energies discussed in the introduction for a given momentum $\pi = \hbar k$. Here, the $\Psi_\pm$ correspond to the atomic solutions with energies $E_\pm$ and the Ψ_0 correspond to the resonance solutions with energy E_0. We label the atomic states Ψ^λ_+ and Ψ^λ_- with superscript λ which corresponds to the state $c^\lambda_{ij} \neq 0$ after letting $k = 0$ and we label the resonance states Ψ^λ_0 with superscript λ which corresponds to the state $c^\lambda_{ij} \neq 0$ after letting $m = 0$. As we will show, this is the dominant component of Ψ for such states. Note that for the resonance state Ψ^0_0 we have $(c^0_{11}+c^0_{22}) = 0$ as in the coordinate representation (37) where $(y^0_{11}+y^0_{22}) = 0$.

3.2.2. Case 2: $S = 1$, $L = J$.

The wavefunction Ψ in terms of the $|L, S, k\rangle$ states above for a given J which is equivalent to Case 2 in the coordinate representation corresponds to

$$\Psi = \frac{1}{\rho}\begin{pmatrix} c^1_{11}|J,1,k\rangle \\ c^\beta_{12}|J\beta,1,k\rangle \\ c^\beta_{12}|J\beta,1,k\rangle \\ c^1_{22}|J,1,k\rangle \end{pmatrix}. \tag{50}$$

The two-body Dirac equation in momentum space gives us the coupled equations for the symmetrized Bessel coefficients for a given k, J,

$$\begin{aligned} 2mc^2(c^1_{11}+c^1_{22}) - 2\hbar ck(c^\beta_{12}-c^\beta_{21}) &= E(c^1_{11}-c^1_{22}), \\ 2mc^2(c^1_{11}-c^1_{22}) &= E(c^1_{11}+c^1_{22}), \\ -2\hbar ck(c^1_{11}-c^1_{22}) &= E(c^\beta_{12}-c^\beta_{21}), \\ 0 &= E(c^\beta_{12}+c^\beta_{21}), \end{aligned} \tag{51}$$

where we have used the Hermitian property of the operators. We have the four orthonormal solutions Ψ_i for each k, J in the columns below

$$\begin{array}{c|cccc} & \sqrt{2}\Psi^1_+ & \sqrt{2}\Psi^1_- & \sqrt{2}\Psi^1_0 & \sqrt{2}\Psi^\beta_0 \\ \hline (c^1_{11}-c^1_{22}) & 1 & 1 & . & . \\ (c^1_{11}+c^1_{22}) & \frac{mc^2}{e} & -\frac{mc^2}{e} & \frac{\sqrt{2}\hbar ck}{e} & . \\ (c^\beta_{12}-c^\beta_{21}) & -\frac{\hbar ck}{e} & \frac{\hbar ck}{e} & \frac{\sqrt{2}mc^2}{e} & . \\ (c^\beta_{12}+c^\beta_{21}) & . & . & . & \sqrt{2} \\ \hline C-parity & J+1 & J+1 & J+1 & J \end{array} \tag{52}$$

with corresponding energies E_i

$$\begin{aligned} E_\pm &= \pm 2e, \\ E_0 &= 0, \\ e &= \sqrt{(\hbar ck)^2+(mc^2)^2}. \end{aligned}$$

These, again, are just the free particle energies discussed in the introduction for a given momentum $\pi = \hbar k$. Here, the $\Psi_\pm$ again correspond to the atomic solutions with energies $E_\pm$ and the Ψ_0 correspond to the resonance solutions with energy E_0. Note that for the resonance state Ψ^1_0 we have $(c^1_{11}-c^1_{22})=0$ as in the coordinate representation (40) where $(y^1_{11}-y^1_{22})=0$. We can combine Case 1 and Case 2 and use the wavefunction

$$\Psi = \frac{1}{\rho}\begin{pmatrix} c^0_{11}|J,0,k\rangle \\ c^\alpha_{12}|J\alpha,1,k\rangle \\ c^\alpha_{21}|J\alpha,1,k\rangle \\ c^0_{22}|J,0,k\rangle \end{pmatrix} + \frac{1}{\rho}\begin{pmatrix} c^1_{11}|J,1,k\rangle \\ c^\beta_{12}|J\beta,1,k\rangle \\ c^\beta_{12}|J\beta,1,k\rangle \\ c^1_{22}|J,1,k\rangle \end{pmatrix} = \frac{1}{\rho}\begin{pmatrix} c^0_{11}|J,0,k\rangle + c^1_{11}|J,1,k\rangle \\ c^\alpha_{12}|J\alpha,1,k\rangle + c^\beta_{12}|J\beta,1,k\rangle \\ c^\alpha_{21}|J\alpha,1,k\rangle + c^\beta_{12}|J\beta,1,k\rangle \\ c^0_{22}|J,0,k\rangle + c^1_{22}|J,1,k\rangle \end{pmatrix},$$

to obtain the same eight equations and solutions as before.

3.2.3. Case 3: $S=1$, $L \neq J$.

The wavefunction Ψ in terms of the $|L,S,k\rangle$ states above for a given J which is equivalent to Case 3 in the coordinate representation corresponds to

$$\Psi = \frac{1}{\rho}\begin{pmatrix} c^\alpha_{11}|J\alpha,1,k\rangle + c^\beta_{11}|J\beta,1,k\rangle \\ c^0_{12}|J,0,k\rangle + c^1_{12}|J,1,k\rangle \\ c^0_{21}|J,0,k\rangle + c^1_{21}|J,1,k\rangle \\ c^\alpha_{22}|J\alpha,1,k\rangle + c^\beta_{22}|J\beta,1,k\rangle \end{pmatrix}. \tag{53}$$

As in the coordinate representation, the new equations can be found from Case1 and Case2 by the exchange $m_e \leftrightarrow -m_e$, $y_{11} \leftrightarrow y_{21}$, $y_{22} \leftrightarrow y_{12}$, or, equivalently, the exchange $m_p \leftrightarrow -m_p$, $y_{11} \leftrightarrow y_{12}$, $y_{22} \leftrightarrow y_{21}$. The two-body Dirac equation in momentum space gives us the coupled equations for the symmetrized Bessel coefficients for a given k, J,

$$
\begin{aligned}
2mc^2(c^{\alpha}_{11} - c^{\alpha}_{22}) - 2\hbar ck(c^{0}_{12} + c^{0}_{21}) &= E(c^{\alpha}_{11} + c^{\alpha}_{22}),\\
2mc^2(c^{+}_{11} - c^{+}_{22}) &= E(c^{\alpha}_{11} - c^{\alpha}_{22}),\\
-2\hbar ck(c^{\alpha}_{11} + c^{\alpha}_{22}) &= E(c^{0}_{12} + c^{0}_{21}),\\
2mc^2(c^{\beta}_{11} + c^{\beta}_{22}) - 2\hbar ck(c^{1}_{12} - c^{1}_{21}) &= E(c^{\beta}_{11} - c^{\beta}_{22}),\\
2mc^2(c^{\beta}_{11} - c^{\beta}_{22}) &= E(c^{\beta}_{11} + c^{\beta}_{22}),\\
-2\hbar ck(c^{\beta}_{11} - c^{\beta}_{22}) &= E(c^{1}_{12} - c^{1}_{21}),\\
0 &= E(c^{0}_{12} - c^{0}_{21}),\\
0 &= E(c^{1}_{12} + c^{1}_{21}),
\end{aligned}
\tag{54}
$$

where we have used the Hermitian property of the operators. We have the eight orthonormal solutions Ψ'_i for each k, J in the columns below

	$\sqrt{2}\Psi'^{\alpha}_{+}$	$\sqrt{2}\Psi'^{\alpha}_{-}$	$\sqrt{2}\Psi'^{\alpha}_{0}$	$\sqrt{2}\Psi'^{\beta}_{+}$	$\sqrt{2}\Psi'^{\beta}_{-}$	$\sqrt{2}\Psi'^{\beta}_{0}$	$\sqrt{2}\Psi'^{0}_{0}$	$\sqrt{2}\Psi'^{1}_{0}$
$(c^{\alpha}_{11} + c^{\alpha}_{22})$	1	1	$.$	$.$	$.$	$.$	$.$	$.$
$(c^{\alpha}_{11} - c^{\alpha}_{22})$	$\frac{mc^2}{e}$	$-\frac{mc^2}{e}$	$\frac{\sqrt{2}\hbar ck}{e}$	$.$	$.$	$.$	$.$	$.$
$(c^{0}_{12} + c^{0}_{21})$	$-\frac{\hbar ck}{e}$	$\frac{\hbar ck}{e}$	$\frac{\sqrt{2}mc^2}{e}$	$.$	$.$	$.$	$.$	$.$
$(c^{\beta}_{11} - c^{\beta}_{22})$	$.$	$.$	$.$	1	1	$.$	$.$	$.$
$(c^{\beta}_{11} + c^{\beta}_{22})$	$.$	$.$	$.$	$\frac{mc^2}{e}$	$-\frac{mc^2}{e}$	$\frac{\sqrt{2}\hbar ck}{e}$	$.$	$.$
$(c^{1}_{12} - c^{1}_{21})$	$.$	$.$	$.$	$-\frac{\hbar ck}{e}$	$\frac{\hbar ck}{e}$	$\frac{\sqrt{2}mc^2}{e}$	$.$	$.$
$(c^{0}_{12} - c^{0}_{21})$	$.$	$.$	$.$	$.$	$.$	$.$	$\sqrt{2}$	$.$
$(c^{1}_{12} + c^{1}_{21})$	$.$	$.$	$.$	$.$	$.$	$.$	$.$	$\sqrt{2}$
$C-parity$	J	J	J	J	J	J	$J+1$	$J+1$

(55)

with corresponding energies E'_i

$$
\begin{aligned}
E'_{\pm} &= \pm 2e,\\
E'_0 &= 0,\\
e &= \sqrt{(\hbar ck)^2 + (mc^2)^2}.
\end{aligned}
$$

These, again, are just the free particle energies discussed in the introduction for a given momentum $\pi = \hbar k$. Here, the $\Psi'_{\pm}$ correspond to the atomic solutions with energies $E'_{\pm}$ and the Ψ'_0 correspond to the resonance solutions with energy E'_0. Here we use the prime superscript to distinguish the Case 3 energies and wavefunctions from their Case 1 and Case 2 counterparts.

3.3. Reducibility

In the coordinate representation, Case 1 and Case 2 have one more coupled equation and one more uncoupled equation than for the momentum representation. This is because

there are actually redundant solutions for the resonance states Ψ_0^α and Ψ_0^β contained in the coordinate representation which have $E = 0$ solutions. This reducibility is maintained even in the presence of a Coulomb potential. In Case 3 both representations have the same number of coupled and uncoupled equations. However, we see that, in the momentum representation, Case 3 is indeed separable into two sets of three coupled equations, unlike in the coordinate representation. These two sets will be coupled by the Coulomb potential in the next section. Clearly, the momentum representation has enhanced symmetry and reducibility when compared to the coordinate representation. Using the momentum representation, we shall see in the Section 5 that we have the further advantage of being able to readily separate the atomic and resonance states by using their free particle bases even considering the Coulomb interaction between particles.

3.4. Chirality

The two-body Dirac equations are invariant with respect to the exchange $m_e \leftrightarrow -m_e$, $y_{11} \leftrightarrow y_{21}$, and $y_{22} \leftrightarrow y_{12}$ or the exchange $m_p \leftrightarrow -m_p$, $y_{11} \leftrightarrow y_{12}$, and $y_{22} \leftrightarrow y_{21}$. We now let $m = 0$ in (49), (52), and (55) to determine the Weyl spin or chirality properties as in the case above of single particle states. Considering the resonance solutions, the $S = 0$ states form doublets $(\Psi_0^0, \Psi_0'^0)$ comprised of $(\mathbf{e}_{11} - \mathbf{e}_{22})$ and $(\mathbf{e}_{12} - \mathbf{e}_{21})$ states, respectively, and the $S = 1$ states form doublets $(\Psi_0^\alpha, \Psi_0'^\alpha)$ comprised of $(\mathbf{e}_{12} - \mathbf{e}_{21})$ and $(\mathbf{e}_{11} - \mathbf{e}_{22})$ states, respectively. This is similar to what occurred for the single particle states with $m = 0$ shown in Section 2. Both of these doublets are comprised of states with different charge conjugation symmetry. The first state of the doublet is from Case 1 while the second state of the doublet is from Case 3 resulting from the exchange. From (19) it follows that the chirality operator for the electron $\mathbf{c}(e)$ corresponds to the exchange $\Psi_{11} \leftrightarrow \Psi_{21}$, and $\Psi_{22} \leftrightarrow \Psi_{12}$ whereas the chirality operator for the positron $\mathbf{c}(p)$ corresponds to the exchange $\Psi_{11} \leftrightarrow \Psi_{12}$, and $\Psi_{22} \leftrightarrow \Psi_{21}$. Operating with $\mathbf{c}(e)$ and $\mathbf{c}(p)$ on the $S = 0$ doublet $(\Psi_0^0, \Psi_0'^0)$ we find

$$\begin{aligned} \mathbf{c}(e)[\Psi_0^0 \pm \Psi_0'^0] &= \mp [\Psi_0^0 \pm \Psi_0'^0] \\ \mathbf{c}(p)[\Psi_0^0 \pm \Psi_0'^0] &= \pm [\Psi_0^0 \pm \Psi_0'^0] \end{aligned} \tag{56}$$

and on the $S = 1$ doublet $(\Psi_0^\alpha, \Psi_0'^\alpha)$ we find

$$\begin{aligned} \mathbf{c}(e)[\Psi_0^\alpha \pm \Psi_0'^\alpha] &= \mp [\Psi_0^\alpha \pm \Psi_0'^\alpha] \\ \mathbf{c}(p)[\Psi_0^\alpha \pm \Psi_0'^\alpha] &= \pm [\Psi_0^\alpha \pm \Psi_0'^\alpha] \end{aligned} \tag{57}$$

We conclude that for $m = 0$ both the resonance pairs $(\Psi_0^0, \Psi_0'^0)$ with $S = 0$ and $(\Psi_0^\alpha, \Psi_0'^\alpha)$ with $S = 1$ have definite chirality which can be either left or right handed.

A similar result occurs for the $S = 1$ resonance doublets $(\Psi_0^1, \Psi_0'^1)$ and $(\Psi_0^\beta, \Psi_0'^\beta)$. The doublets $(\Psi_0^1, \Psi_0'^1)$ are comprised of $(\mathbf{e}_{11} + \mathbf{e}_{22})$ and $(\mathbf{e}_{12} + \mathbf{e}_{21})$ states, respectively, and the other doublets $(\Psi_0^\beta, \Psi_0'^\beta)$ are comprised of $(\mathbf{e}_{12} + \mathbf{e}_{21})$ and $(\mathbf{e}_{11} + \mathbf{e}_{22})$ states,

respectively. The first state of the doublet is from Case 2 while the second state of the doublet is from Case 3 resulting from the exchange. Operating with $\mathbf{c}(e)$ and $\mathbf{c}(p)$ on the doublet $(\Psi_0^1, \Psi_0'^1)$ we find

$$\begin{aligned} \mathbf{c}(e)[\Psi_0^1 \pm \Psi_0'^1] &= \pm[\Psi_0^1 \pm \Psi_0'^1] \\ \mathbf{c}(p)[\Psi_0^1 \pm \Psi_0'^1] &= \pm[\Psi_0^1 \pm \Psi_0'^1] \end{aligned} \tag{58}$$

and on the doublet $(\Psi_0^\beta, \Psi_0'^\beta)$ we find

$$\begin{aligned} \mathbf{c}(e)[\Psi_0^\beta \pm \Psi_0'^\beta] &= \pm[\Psi_0^\beta \pm \Psi_0'^\beta] \\ \mathbf{c}(p)[\Psi_0^\beta \pm \Psi_0'^\beta] &= \pm[\Psi_0^\beta \pm \Psi_0'^\beta] \end{aligned} \tag{59}$$

Altogether, we have four resonance pairs or doublets when $m = 0$ with definite chirality. These degenerate pairs transform like massless Weyl spinors [13] and are therefore fermion. We show in the next Section 4 that letting $m = 0$ is justified when the degenerate resonance states are allowed to interact by means of a Coulomb potential and they still form such doublets. Furthermore, we show in Section 5 that there is still no mixing between the atomic and resonance states when the particles interact by means of a Coulomb potential.

3.5. Charge conjugation

We have labeled the solutions above with their charge conjugation $C - parity$. Note that the atomic solutions Ψ_+ and Ψ_- both have the same $C - parity$ for a given case and are always coupled. The uncoupled equations always correspond to the $E = 0$ resonance solutions as was the case in the coordinate representation as can be readily observed. Note that the electron and positron chirality operators can mix states with different charge conjugation symmetry.

The operation of charge conjugation $\mathbf{C}$ changes an electron state to the same positron state and visa versa. That is, it changes the sign of the charge on the electron or positron. The operations $\mathbf{CX}$ of charge conjugation and particle exchange must return the wavefunction Ψ back to its negative $-\Psi$,

$$\mathbf{CX}\Psi = (-1)^{C+X}\Psi = -\Psi. \tag{60}$$

This is a requirement for fermions as discussed by Wolfenstein and Ravenhall [14] for the case of atomic positronium. For atomic positronium, the charge conjugation symmetry $(-1)^C$ must be the negative of the exchange symmetry $(-1)^X$: that is, the charge conjugation parity C $(even, odd)$ must be opposite to the exchange parity X $(odd, even)$.

The exchange symmetry itself is made up of three factors. First, the exchange symmetry for orbital states $Y^L(\theta, \varphi)$ corresponding to $\boldsymbol{\rho} \rightarrow -\boldsymbol{\rho}$ is $(-1)^L$. Second, the exchange symmetry for spin states Ω^S is $(-1)^{S+1}$. The product of these two is $(-1)^{L+S+1}$. Finally, the exchange symmetry for symmetric states $(\mathbf{e}_{11} + \mathbf{e}_{22})$, $(\mathbf{e}_{11} - \mathbf{e}_{22})$,

and $(\mathbf{e}_{11}+\mathbf{e}_{22})$ is 1 and for antisymmetric state $(\mathbf{e}_{12}-\mathbf{e}_{21})$ is -1. Because the operation of charge conjugation $\mathbf{C}$ commutes with $\mathbf{H}_0$ in (23), states with different charge conjugation parity cannot interact and are separable as seen in the above equations. This is also true for interacting particles which we treat in the next section: states with different $C-parity$ cannot be coupled by the Coulomb potential or magnetic potential.

We list the case and $C-parity$ of the resonance pairs

$$\begin{array}{ccc} Resonance & Case & C-parity \\ (\Psi_0^0, \Psi_0'^0) & (1,3) & (J,\ J+1) \\ (\Psi_0^\alpha, \Psi_0'^\alpha) & (1,3) & (J+1,\ J) \\ (\Psi_0^1, \Psi_0'^1) & (2,3) & (J+1,\ J+1) \\ (\Psi_0^\beta, \Psi_0'^\beta) & (2,3) & (J,\ J) \end{array} .$$

The resonance pairs always come from different cases. By considering resonance states with different charge conjugation symmetries, we can understand their special chirality properties.

4. Two-Body Dirac Equation - Coulomb Potential

We now solve the two-body Dirac equation with the electric or Coulomb potential

$$V_C(\rho) = -e^2/\rho, \tag{61}$$

so that the new Hamiltonian is

$$\mathbf{H} = \mathbf{H}_0 + \mathbf{V}_C. \tag{62}$$

In Section 6 we will consider the effects of the magnetic potential. Below, we consider atomic and resonance states in the coordinate representation, but only resonance states in the momentum representation. In both cases we give numerical and analytic solutions.

4.1. Coordinate Representation

The Coulomb potential only gives diagonal terms in the coordinate representation and, moreover, there are no other diagonal terms in our symmetrized bases. That is, we can replace E by $(E - V_C)$ on the right hand side of the two-body free particle equations for the three cases (36), (39) and (42) above in the coordinate representation. We solve these coupled equations numerically using the finite element method following the work of Scott, et al. [5]. We use $n_p = 5$ Lagrangian polynomial interpolation functions for each element instead of the Hermite polynomial interpolation used by Scott, et al., anticipating the discontinuities that occur for the resonance states. Despite this difference in interpolation, our numerical results agree with those of Scott, et al. to 16 significant figures in energy units of $2mc^2$ or about 10 kHz in energy corresponding to the long-double precision accuracy of our calculations. Unlike previous authors, we consider the solutions for both the atomic and resonance states.

4.1.1. Atomic States The atomic solutions to the fourth order are linear combinations of the free particle atomic states Ψ_+ alone [12]. As described by Scott, et al., accurate $L = 0$ energies and wavefunctions can only be achieved with a grid which has elements in the region of $\rho \sim 1$ $Fermi$. For accurate results, we use a grid to cover three regions in all our calculations: the 'Fermi' region, or Region 1, with 10 equal elements of 10^{-5} $Bohr$ in the interval (0, 0.0001), the 'Compton' region, or Region 2, with 9 equal elements of 0.002 $Bohr$ in the interval $(0.002, 0.02)$ and the 'Bohr' region, or Region 3, with 79 equal elements of 0.5 $Bohr$ in the interval $(0.5, 40.)$ for $n = 1$ states. The endpoint and element size of this last region varies proportionately with the atomic Bohr radius $a = 2na_0$ of the particular state of positronium. We also have two 'connecting' elements in the intervals $(0.0001, 0.002)$ and $(0.02, 0.5)$ which connect the different regions. With five point Lagrangian interpolations, the 100 finite elements correspond to 399 grid points. In atomic units, Region 1 is near the classical radius of the electron or positron $\rho = \alpha^2 \sim (1/137)^2$ $Bohr$. Region 2 is near the Compton wavelength $\rho = \alpha \sim (1/137)$ $Bohr$ and Region 3 is near the radius $\rho = 2n$ $Bohr$ of positronium.

We have solved the two-body Coulomb-Dirac equation for all the bound states of positronium up to $n = 3$ and determined their energies to 10 kHz accuracy using long-double precision. We have thereby verified the calculations of Scott, et al.. to this accuracy. Scott, et al., themselves, actually achieved 0.1 kHz accuracy in their numerical calculations using only double precision. Note that this numerical accuracy is much greater than either the theoretical accuracy of QED calculations, presently to order $mc^2\alpha^6$, or the experimental error in any positronium spectroscopy, both of which are typically of MHz accuracy.

As an example of our calculations, we show the $L = 0$ and $S = 0$ ground state in Figure 1. We show the square of the wavefunction components and use a log scale to investigate the wavefunction at very small ρ. The large dots in the figure correspond to the grid points used for the three different regions. For five point Lagrangian interpolation there are four grid points for every element. The analytic wavefunction y_a^2 for the positronium ground state derived from Schrodinger's equation with reduced mass $\frac{1}{2}m$ is simply $y_a^2 = \frac{1}{2}\rho^2 e^{-\rho}$. This analytic wavefunction should be very close to the large component y_{11} as shown in Figure 1. In Region 1 we find that y_{22} reaches its maximum value as shown previously by Scott, et al.. Note that y_{11}^2 deviates from y_a^2 as y_{22}^2 becomes comparable to y_{11}^2 in this region because of the normalization condition $y_a^2 \cong y_{11}^2 + y_{22}^2$. Region 2 is where y_{12}^2 becomes larger than y_{22}^2 and the two wavefunction components cross. Finally, in region 3 where $\rho \sim 1\ Bohr$, the wavefunctions y_{11}^2 and y_{12}^2 reach their peak values and y_{22} changes sign.

We wish to compare these finite element calculations of Scott, el to the analytic results of the Pauli approximation valid to order $mc^2\alpha^4$. We follow closely the development of Bethe and Salpeter [12] and use their notation for the energy terms. Whilst Bethe and Salpeter give the results for both the Coulomb and Breit interaction together (as derived previously by Ferrell [15]), one can readily extract only the Coulomb part from their results. We have the following formulas for the Pauli approximation to the Coulomb energies E_P for a given n, L, S, and J:

$$
\begin{aligned}
H_0 &= -\frac{mc^2\alpha^2}{4n^2}, \qquad (63)\\
H_1 &= \frac{3mc^2\alpha^4}{64n^4} - \frac{mc^2\alpha^4}{8n^3(2L+1)},\\
H_3^C &= \frac{mc^2\alpha^4}{8n^3L(L+1)(2L+1)} \begin{Bmatrix} L & J=L+1 \\ -1 & J=L \\ -(L+1) & J=L-1 \end{Bmatrix} (1-\delta_{L0})\delta_{S1},\\
H_4^C &= \frac{mc^2\alpha^4}{8n^3}\delta_{L0},
\end{aligned}
$$

where

$$E_P = 2mc^2 + H_0 + H_1 + H_3^C + H_4^C. \qquad (64)$$

The term H_0 is just the second order positronium energy from the Schrodinger equation

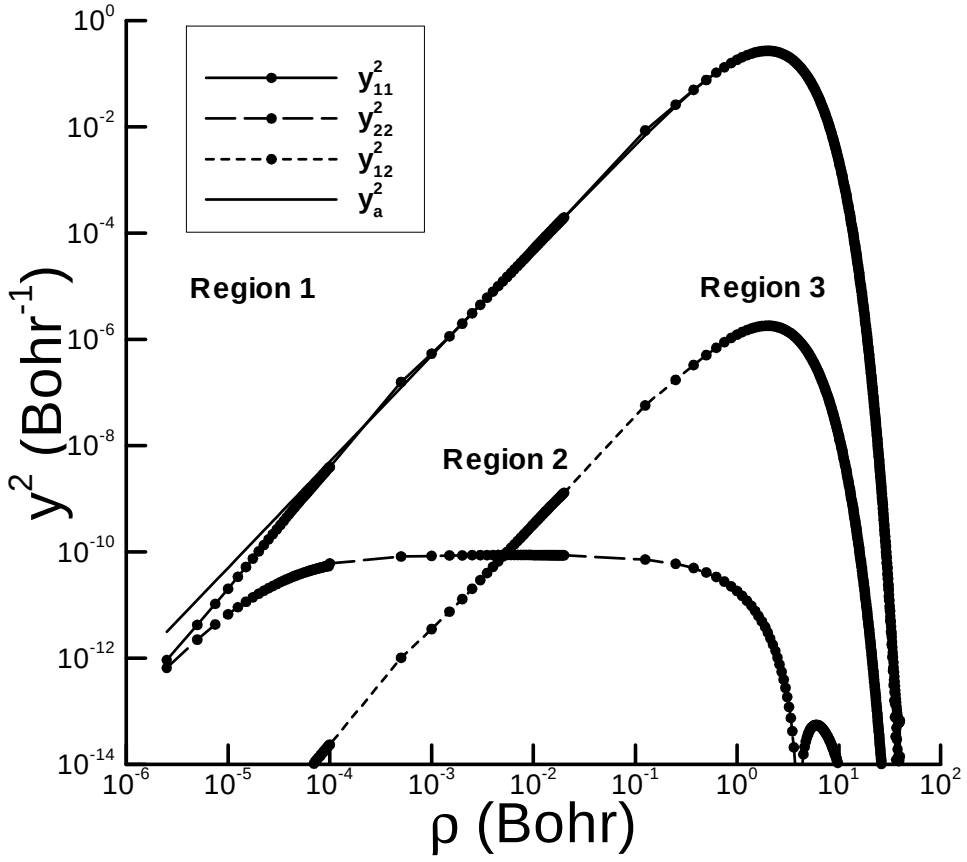

Figure 1. The square of the wavefunction components for the atomic positronium $S = 0$ ground state from finite element solutions of (36) with E replaced with $(E + e^2/\rho)$. The analytic wavefunction is $y_a^2 = \frac{1}{2}\rho^2 e^{-\rho}$. Large dots correspond to grid points used for the three regions.

and H_1 is the kinetic correction to the fourth order. The terms $H_3^C + H_4^C$ correspond to the fine structure corrections of positronium for a Coulomb potential to the fourth order. Note the Kronecker deltas are such that $H_3^C = 0$ if $L = 0$ or $S = 0$. Also, note that H_4^C cancels the second term of H_1 when $L = 0$. In Section 6 we consider the magnetic terms H_2^B, H_3^B, and H_5^B for the Breit potential which also contribute to the fourth order.

We compare the Dirac energies $E_D - 2mc^2$ of Scott, et al. with the Pauli energies $E_P - 2mc^2$ in Table I. We use the approximate value $\alpha = 1/137$ as do Scott, et al.. In Table I we show the energies in units of $Hartree = mc^2\alpha^2$ and the differences in energies $E_D - E_P$ in in units of Mhz where we use the conversion $Hartree = (mc^2\alpha^2/h)Hz = 6.579684 \times 10^9\ MHz$. It is interesting to note that E_D is lower than E_P for all $L = 0$ states. Also, for these $L = 0$ states, the energy E_D is always lower for the $S = 0$ state than for the $S = 1$ state, whereas the energies E_P are equal

$n\ L\ S\ J$	$Case$	$E_D - 2mc^2\ (Hartree)$	$E_P - 2mc^2\ (Hartree)$	$E_D - E_P\ (MHz)$
1 0 0 0	1	-0.249 997 504 147 52	-0.249 997 502 530 77	-10.6377
1 0 1 1	3	-0.249 997 503 636 33	-0.249 997 502 530 77	-7.2742
2 0 0 0	1	-0.062 499 844 110 14	-0.062 499 843 908 17	-1.3289
2 0 1 1	3	-0.062 499 844 044 37	-0.062 499 843 908 17	-0.8962
2 1 0 1	1	-0.062 500 121 403 76	-0.062 500 121 404 75	0.0066
2 1 1 0	3	-0.062 500 398 904 81	-0.062 500 398 901 33	-0.0229
2 1 1 1	2	-0.062 500 260 153 03	-0.062 500 260 153 04	0.0001
2 1 1 2	3	-0.062 499 982 656 70	-0.062 499 982 656 46	-0.0016
3 0 0 0	1	-0.027 777 747 004 71	-0.027 777 746 944 82	-0.3941
3 0 1 1	3	-0.027 777 746 985 12	-0.027 777 746 944 82	-0.2651
3 1 0 1	1	-0.027 777 829 165 71	-0.027 777 829 166 03	0.0021
3 1 1 0	3	-0.027 777 911 388 16	-0.027 777 911 387 24	-0.0060
3 1 1 1	2	-0.027 777 870 276 58	-0.027 777 870 276 64	0.0004
3 1 1 2	3	-0.027 777 788 055 52	-0.027 777 788 055 43	-0.0006
3 2 0 2	1	-0.027 777 796 277 54	-0.027 777 796 277 55	0.0001
3 2 1 1	3	-0.027 777 820 944 03	-0.027 777 820 943 91	-0.0007
3 2 1 2	2	-0.027 777 804 499 68	-0.027 777 804 499 67	-0.0001
3 2 1 3	3	-0.027 777 779 833 31	-0.027 777 779 833 31	-0.0000

Table 1. Comparison of Two-Body Dirac Energies of Scott, et al. and Pauli Energies for a Coulomb Potential

for such states. The agreement in Table 1 between E_D and E_P is surprising. It has been shown by Ishidzu [16, 17] that the energies for the atomic states for the two-body Dirac equation in a Coulomb potential can be expanded in a power series in α^2. Thus, energies $E_D - E_P$ in Table 1 should only be accurate to $mc^2\alpha^6 \sim MHz$ which is the agreement found for the $L = 0$ states. However, the $L = 1$ states have accuracies of $\sim 10\ kHz$ or less and the $L = 2$ states have accuracies of $\sim 1\ kHz$ or less.

We have seen that the solutions to the two-body Dirac equation for a Coulomb potential are separable into subspaces (Ψ_0, Ψ_0') and (Ψ_+, Ψ_-) to order $mc^2\alpha^4$ corresponding to resonance and atomic states, respectively, by using the Pauli approximation. In the next Section 5, we show that this separability between resonance states (Ψ_0, Ψ_0') and atomic states (Ψ_+, Ψ_-) is exact using the Bethe-Salpeter equation in the ladder approximation. It has been shown by Karplus and Klein [18] and also by Fulton and Martin [19] that the two-body Dirac equation for atomic energies actually has corrections of order $mc^2\alpha^5$ because of spurious mixing between the resonance and atomic states. Indeed, this mixing, due to the singularity at $-e^2/\rho'$, is responsible for the anomalous behavior of the y_{22}^2 wavefunction in Region 1 of Figure 1. In the next section we show the correct wavefunction without the mixing.

4.1.2. Resonance States We now solve the two-body Dirac equation with a Coulomb potential to find the energies and wavefunctions for the $L = 0$ and $S = 0$ resonance states. This corresponds to the exact same numerical calculation for which we obtained the energy and wavefunction of the atomic ground state above. The general case will be considered in the momentum representation below. Because of the degeneracy of the resonance states with $E = 0$ for any k, their free particle wavefunctions will be severely mixed by the Coulomb potential. From (36) we find the resonance solutions

$$(y^0_{11} - y^0_{22}) = \frac{2mc^2(y^0_{11} + y^0_{22})}{E + e^2/\rho}, \tag{65}$$

which should be compared to (37). Thus the radial function $(y^0_{11} - y^0_{22})$ is singular near $E \sim -e^2/\rho$ unless $(y^0_{11} + y^0_{22}) \sim 0$ in which case we have

$$\begin{aligned} E &\sim -\frac{e^2}{\rho'}, \\ (y^0_{11} - y^0_{22})/\sqrt{2} &\sim C\delta(\rho - \rho'), \end{aligned} \tag{66}$$

with C and ρ' to be determined. Clearly this solution for the $L = 0$ and $S = 0$ resonance states must correspond to linear combinations of the Ψ^0_0 in (49). Since this energy is negative such bound states are not allowed. However, we shall see in Section 6 that, in this case, the magnetic potential will shift these states to positive energy.

In Figure 2 we show the resonance energies E_D for the $L = 0$ and $S = 0$ state resulting from our finite element calculations with the corresponding normalized wavefunctions shown in Figure 3. Only the solutions in Region 1 are shown. Because the resonance states are delta functions which are discontinuous, it is convenient to choose Lagrangian interpolation functions for our finite element calculations instead of the Hermite interpolation functions used by Scott, et al. which assume the wavefunctions are continuous. The wavefunctions for these resonance solutions are necessarily orthogonal to those of the atomic ground state solutions above. We see that the solutions are just those in (66) where the $\rho' = \rho_i = i\Delta\rho$ are just the finite element grid points themselves. We use $n_p = 5$ Lagrangian interpolation functions of quartic degree with $n_p - 1$ nodes per element. The width is $\Delta\rho = 10^{-4}/40$ in Region 1 for the 10 elements and 39 forty grid points. The wavefunctions are linear combinations of Lagrangian interpolation functions themselves which are delta functions when $\Delta\rho \to 0$. Note that the delta functions at the element boundaries are not continuous and are narrower than the nodal wavefunctions. This is a result of using the Lagrangian interpolation functions which are only a poor approximation to the delta function solutions. For the same reason the delta functions are not quite equally spaced. We perform the same calculation in the momentum representation below using a better basis set.

We wish to find the normalization C of the delta functions $C\delta(\rho - \rho_i)$. For delta functions we have the property

$$\int \delta(\rho - \rho_i)\, d\rho = 1.$$

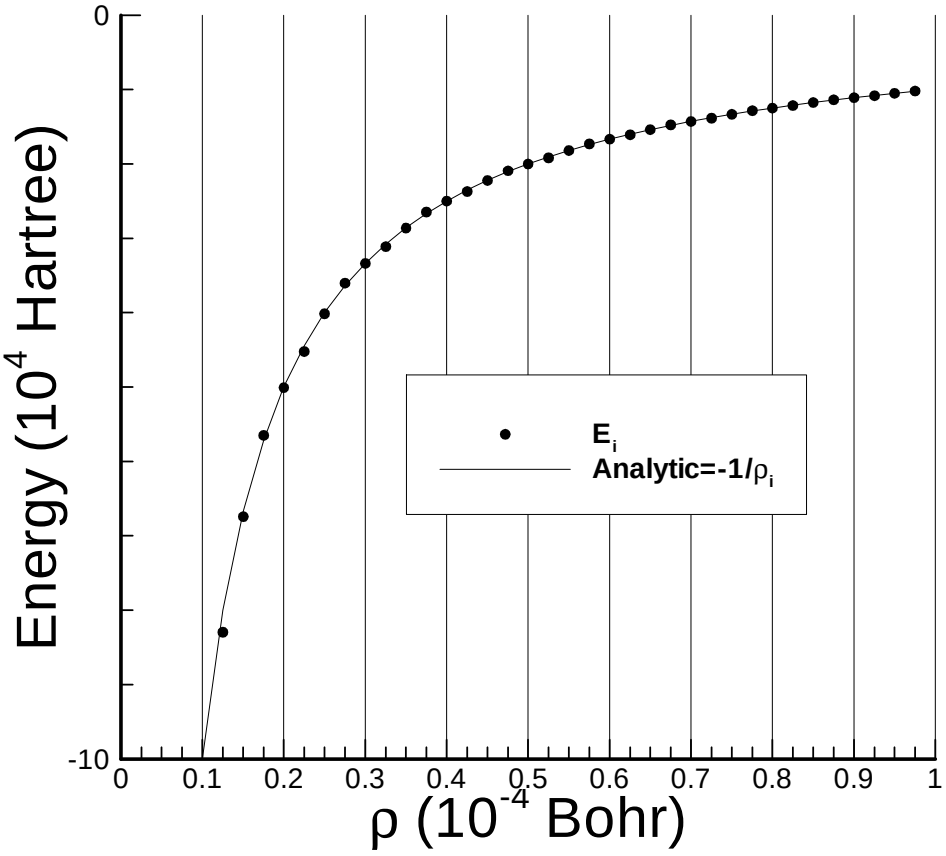

Figure 2. The lowest resonance $L = 0$, $S = 0$ energies E_i found by solving the same equations as in Figure 1. The finite element grid points ρ_i shown here are the same as in Region 1 of Figure 1. Energies are given analyticly by $-1/\rho_i$. Verticle lines are at the element boundaries.

But the delta functions $\delta(\rho - \rho_i)$ have a height $\delta(0)$ and a width $\Delta\rho$ so that the last equation becomes upon integration,

$$\int \delta(\rho - \rho_i)\ d\rho = \delta(0)\Delta\rho = 1,$$

or

$$\delta(0) = 1/\Delta\rho.$$

The normalization condition on the wavefunction $C\delta(\rho - \rho_i)$ then becomes

$$C^2 \int \delta(\rho - \rho_i)^2 d\rho = C^2\delta(0)^2\Delta\rho = 1,$$

so that

$$C = \sqrt{\Delta\rho}. \tag{67}$$

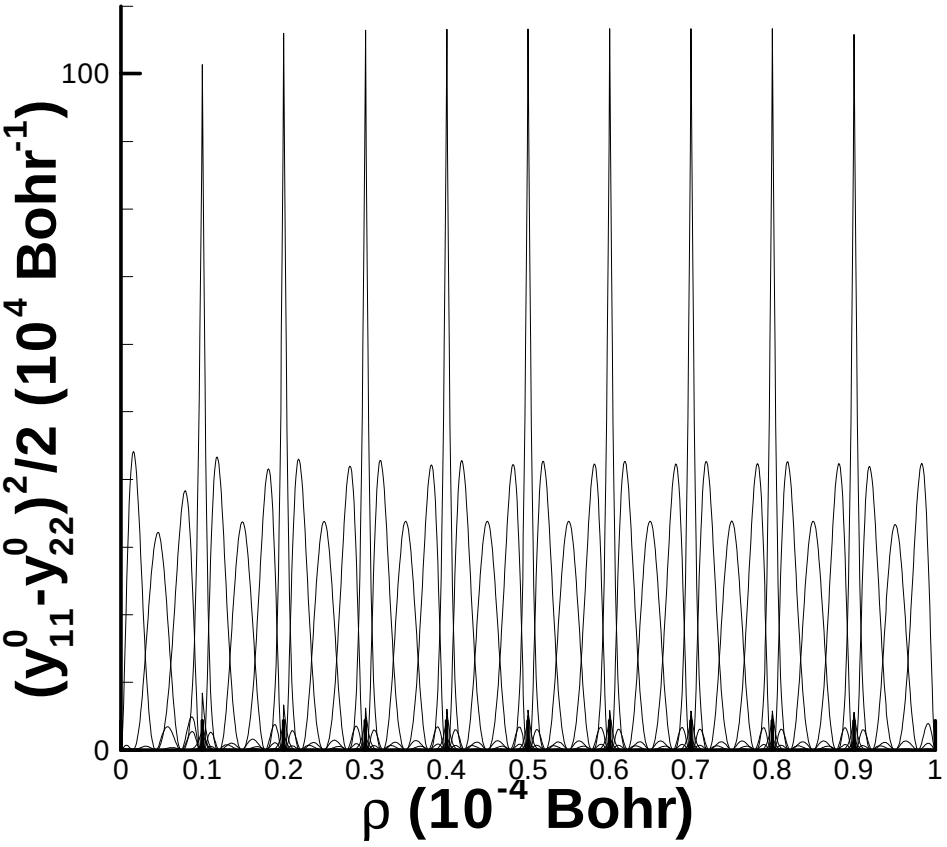

Figure 3. The resonance $S = 0$ wavefunctions in the coordinate representation for the energies in Figure 2. Note that $(y^+_{12} + y^+_{21}) \sim 0$ and cannot be seen on this scale. The wavefunctions are approximately evenly spaced delta functions with various widths.

Thus, in the coordinate representation we have the $L = 0$ and $S = 0$ resonance solutions given approximately by

$$E_i \sim -\frac{e^2}{\rho_i}, \tag{68}$$
$$(y^0_{11} - y^0_{22})_i/\sqrt{2} \sim \sqrt{\Delta\rho}\delta(\rho - \rho_i),$$

with $\rho_i = i\Delta\rho$.

Note that the resonance states of positronium are indeed bound at fixed ρ_i although they have negative energy $-e^2/\rho_i$. In Section 6 we shall look at the effects of the magnetic potential and show that the $S = 0$ states have positive energy $2e^2/\rho_i$ when this potential is included. Let us now return to the momentum representation to analyze the two-body Dirac equations in the presence of a potential.

4.2. Momentum representation

In the momentum representation we shall only consider the resonance states. Again, as in the coordinate representation for a Coulomb potential, we can replace E by $(E-V_C)$ on the right hand side of the two-body free particle equations for the three cases (48), (51), and (54) above. In the momentum representation we find that the Coulomb potential V_C in (61) now mixes states with different k. This mixing, which is diagonal in L and S, is determined by the potential matrices for the possible states $|L,S,k\rangle$ in (44) for a given J given by

$$
\begin{aligned}
V^0_{kk'} &= -\langle J,0,k|\frac{e^2}{\rho}|J,0,k'\rangle = -N_{Jk}N_{Jk'}e^2\int_0^{\rho_0} d\rho\ \rho j_J(k\rho)j_J(k'\rho), \qquad (69)\\
V^1_{kk'} &= -\langle J,1,k|\frac{e^2}{\rho}|J,1,k'\rangle = V^0_{kk'},\\
V^+_{kk'} &= -\langle J+1,1,k|\frac{e^2}{\rho}|J+1,1,k'\rangle = -N_{Jk}N_{Jk'}e^2\int_0^{\rho_0} d\rho\ \rho j_{J+1}(k\rho)j_{J+1}(k'\rho),\\
V^-_{kk'} &= -\langle J-1,1,k|\frac{e^2}{\rho}|J-1,1,k'\rangle = -N_{Jk}N_{Jk'}e^2\int_0^{\rho_0} d\rho\ \rho j_{J-1}(k\rho)j_{J-1}(k'\rho),
\end{aligned}
$$

where subscripts kk' denotes the possible discrete $k_nk'_m$ in the Bessel series expansions. Similarly, we find

$$
\begin{aligned}
V^\alpha_{kk'} &= aV^+_{kk'} + bV^-_{kk'}, \qquad (70)\\
V^\beta_{kk'} &= -bV^+_{kk'} + aV^-_{kk'}.
\end{aligned}
$$

For example, we find the equivalent equations to (48) for Case 1 (with k and k' now explicit) by replacing E with $E\delta_{kk'} - V^i_{kk'}$ on the right, using the appropriate potential $V^i_{kk'}$, and summing over k',

$$
\begin{aligned}
2mc^2[c^0_{11}(k) - c^0_{22}(k)] - 2\hbar ck[c^\alpha_{12}(k) + c^\alpha_{21}(k)] &= (E\delta_{kk'} - V^0_{kk'})[c^0_{11}(k') + c^0_{22}(k')], \quad (71a)\\
2mc^2[c^0_{11}(k) + c^0_{22}(k)] &= (E\delta_{kk'} - V^0_{kk'})[c^0_{11}(k') - c^0_{22}(k')], \quad (71b)\\
-2\hbar ck[c^0_{11}(k) + c^0_{22}(k)] &= (E\delta_{kk'} - V^\alpha_{kk'})[c^\alpha_{12}(k') + c^\alpha_{21}(k')], \quad (71c)\\
0 &= (E\delta_{kk'} - V^\alpha_{kk'})[c^\alpha_{12}(k') - c^\alpha_{21}(k')]. \quad (71d)
\end{aligned}
$$

We have similar equations for Case 2 and Case 3 in (51) and (54), respectively.

Continuing with our example for Case 1, we let $c^0_{11}(k) + c^0_{22}(k) = 0$ for all k and find from (71a) and (71b) above

$$
\begin{aligned}
mc^2[c^0_{11}(k) - c^0_{22}(k)] &= \hbar ck[c^\alpha_{12}(k) + c^\alpha_{21}(k)], \qquad (72a)\\
V^0_{kk'}[c^0_{11}(k') - c^0_{22}(k')] &= E\delta_{kk'}[c^0_{11}(k') - c^0_{22}(k')]. \qquad (72b)
\end{aligned}
$$

But (72a) is just the free particle conditions for the resonance states Ψ^0_0 given in (49). This shows that such solutions correspond to linear combinations of the $S=0$ free particle resonance states Ψ^0_0.

We solve the equations (71) numerically for $L = 0$ and $S = 0$ resonance states as we did in the case of the coordinate representation above. We are interested in Region 1 as shown in Figure 3 and use the boundary conditions

$$j_0(k_m\rho_0) = 0 \text{ for } \rho_0 = 10^{-4}\ Bohr,$$

so that

$$k_m = \frac{m\pi}{\rho_0}. \tag{73}$$

We solve (71) numerically using (69) by diagonalizing the potential matrix in this bases set for $m = 1, 2, ..., M$ where we use $M = 40$ as in the case of Region 1 in the coordinate representation. The wavefunctions are shown in Figure 4 and should be compared with Figure 3. We find that the radial wavefunctions for $\rho\Psi_0^0$ are approximately delta functions

$$(y_{11}^0 - y_{22}^0)_i/\sqrt{2} \sim C\delta(\rho - \rho_i), \tag{74}$$

with normalization C and with energies

$$E_i \sim -\frac{e^2}{\rho_i}, \tag{75}$$

with the ρ_i corresponding to M evenly spaced intervals $\Delta\rho = \rho_0/M$ between 0 and ρ_0,

$$\rho_i = i\Delta\rho \text{ for } i = 1, 2, ..., M-1, \tag{76}$$

just as in the case of the coordinate representation. The approximate delta functions are well behaved in our basis set unlike those in the coordinate representation above.

We can also find analytic wavefunctions which can be compared with the numerical calculations. The approximated delta functions for the ith eigenfunction are given simply by the completeness condition on the radial bases $N_m\rho j_0(k_m\rho) = \sqrt{2/\rho_0}\sin(k_m\rho)$ which is equivalent to the completeness condition on the sine series. We have the radial functions for $\rho\Psi_0^0$,

$$\begin{aligned}(y_{11}^0 - y_{22}^0)_i/\sqrt{2} &= C\frac{2}{\rho_0}\sum_{m=1}^{M-1}\sin(k_m\rho)\sin(k_m\rho_i), \\ &\sim C\delta(\rho - \rho_i),\end{aligned} \tag{77}$$

for $i = 1, 2, ..., M-1$. These analytic resonance wavefunctions for $M = 40$ are compared to those wavefunctions calculated numerically in the free particle basis in Figure 4. To find the exact wavefunctions in the limit $M \to \infty$, we can convert the sine series to the sine transform by converting the sum to an integral. Using $\Delta k_m = \pi/\rho_0$, we have the

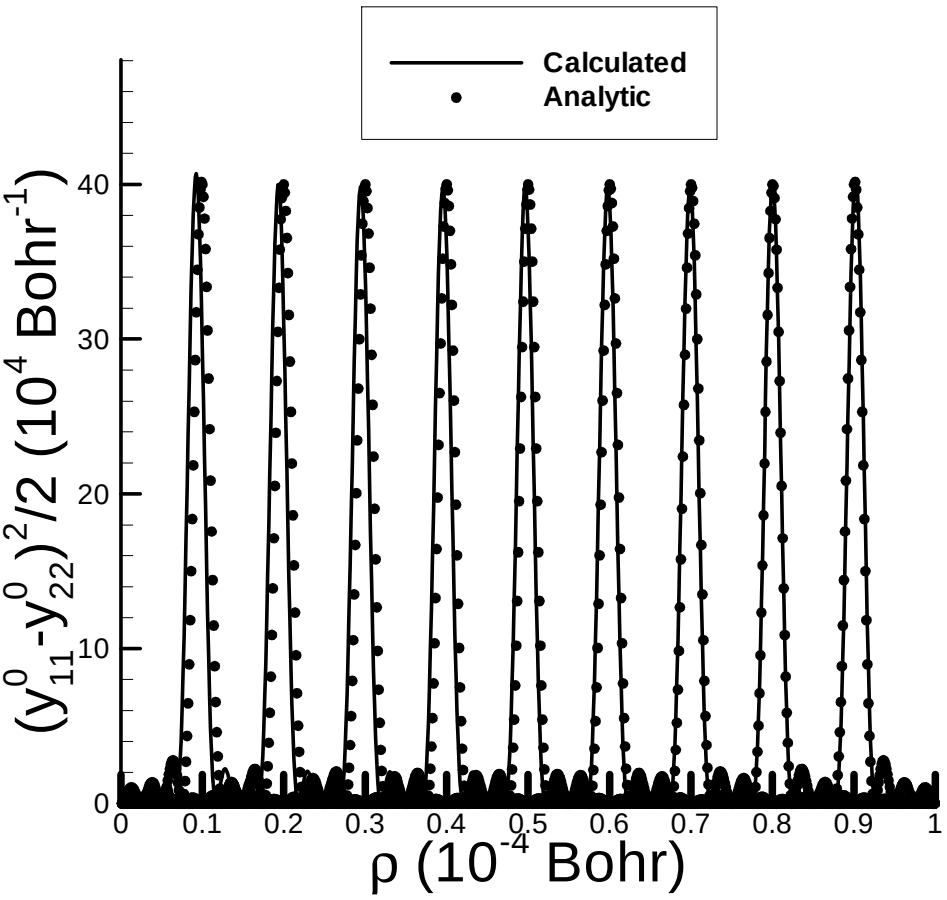

Figure 4. Resonance $S = 0$ wavefunctions calculated in the momentum representation. Analytic results from (77). Only 9 of the states are shown for clarity but the other states look the same. Again, $(y^+_{12} + y^+_{21}) \sim 0$ and cannot be seen on this scale.

equivalent completeness relations for the sine transform,

$$\lim_{\rho_0\to\infty} \frac{2}{\rho_0} \sum_{m=1}^{\infty} \sin(k_m\rho)\sin(k_m\rho_i) = \frac{2}{\pi} \sum_{m=0}^{\infty} \Delta k_m \sin(k_m\rho)\sin(k_m\rho_i), \tag{78}$$

$$= \frac{2}{\pi} \int_0^{\infty} dk \sin(k\rho)\sin(k\rho_i),$$

$$\delta(\rho - \rho_i), \tag{79}$$

where the delta functions $\delta(\rho - \rho_i)$ are now exact.

One can readily show that the different functions for $i = 1, 2, ..., M-1$ are orthonormal if we use the same normalization (67) as in the coordinate representation of the delta function,

$$C = \sqrt{\frac{\rho_0}{M}} = \sqrt{\Delta\rho}.$$

The orthonormality condition is then

$$I_{ij} = \frac{1}{2}\int_0^{\rho_0} d\rho (y^0_{11} - y^0_{22})_i (y^0_{11} - y^0_{22})_j, \tag{80}$$
$$= C^2 (\frac{2}{\rho_0})^2 \int_0^{\rho_0} d\rho \sum_{m=1}^{M-1}\sum_{m'=1}^{M-1} \sin(k_m\rho)\sin(k_m\rho_i)\sin(k_{m'}\rho)\sin(k_{m'}\rho_j),$$
$$= C^2 \frac{2}{\rho_0}\sum_{m=1}^{M-1} \sin(k_m\rho_i)\sin(k_m\rho_j),$$
$$= \delta_{ij}.$$

For the sine transform, the equivalent orthonormality condition is then

$$\lim_{\rho_0\to\infty} \frac{2}{\pi}\sum_{m=0}^{\infty} \Delta k_m \sin(k_m\rho_i)\sin(k_m\rho_j) = \frac{2}{\pi}\int_0^{\infty} dk \sin(k\rho_i)\sin(k\rho_j), \tag{81}$$
$$= \delta(\rho_i - \rho_j).$$

We have now obtained the same result as in the case of the coordinate representation for the $L = 0$ and $S = 0$ resonance states above. For $\rho_0 \to \infty$ the delta functions $\delta(\rho - \rho')$ are exact solutions for the resonance basis. That is, if we use the Bessel transform in momentum space, instead of the Bessel series, corresponding to an infinite basis with $\rho_0 \to \infty$, the delta function solutions become exact. The width $\Delta\rho$ of the delta functions then becomes zero so that the solutions are spatially continuous. Presumably in any physical process we can take a superposition of such delta functions with a finite width $\Delta\rho$ such that the normalization becomes $C = \sqrt{\Delta\rho}$. With the resonance solutions $\delta(\rho - \rho')$, we find in (72) that $[c^{\alpha}_{12}(k) + c^{\alpha}_{21}(k)] \to 0$ in the limit $M \to \infty$ and $\rho_0 \to 0$. These delta function solutions for the radial functions of the resonance states are then equivalent to letting the rest mass $m \to 0$ in (71).

In general, using delta function normalization, we can find radial functions using the Bessel transform

$$\lim_{\rho_0\to\infty} \frac{2}{\rho_0}\sum_{m=1}^{\infty} \rho^2 j_L(k_m\rho) j_L(k_m\rho_i) = \frac{2}{\pi}\int_0^{\infty} dk\rho^2 j_L(k\rho) j_L(k\rho_i),$$
$$= \delta(\rho - \rho_i) \text{ for } L = 0, 1, \ldots .$$

The resonance states then form the same degenerate pairs of Weyl spinors as given in Section 3,

$$\begin{aligned}\rho\Psi_0^0 &= \delta(\rho-\rho')[Y^J,\Omega^0]_N^J[e_{11}-e_{22}]/\sqrt{2}\ (Case\ 1), \\ \rho\Psi_0'^0 &= \delta(\rho-\rho')[Y^J,\Omega^0]_N^J[\mathbf{e}_{12}-\mathbf{e}_{21}]/\sqrt{2}\ (Case\ 3),\end{aligned} \tag{82a}$$

$$\begin{aligned}\rho\Psi_0^\alpha &= \delta(\rho-\rho')\{a[Y^{J+1},\Omega^1]_N^J \\ &\quad + b[Y^{J-1},\Omega^1]_N^J\}[\mathbf{e}_{12}-\mathbf{e}_{21}]/\sqrt{2}\ (Case\ 1), \\ \rho\Psi_0'^\alpha &= \delta(\rho-\rho')\{a[Y^{J+1},\Omega^1]_N^J \\ &\quad + b[Y^{J-1},\Omega^1]_N^J\}[\mathbf{e}_{11}-\mathbf{e}_{22}]/\sqrt{2}\ (Case\ 3),\end{aligned} \tag{82b}$$

$$\begin{aligned}\rho\Psi_0^1 &= \delta(\rho-\rho')[Y^J,\Omega^1]_N^J[\mathbf{e}_{11}+\mathbf{e}_{22}]/\sqrt{2}\ (Case\ 2), \\ \rho\Psi_0'^1 &= \delta(\rho-\rho')[Y^J,\Omega^1]_N^J[\mathbf{e}_{12}+\mathbf{e}_{21}]/\sqrt{2}\ (Case\ 3),\end{aligned} \tag{82c}$$

$$\begin{aligned}\rho\Psi_0^\beta &= \delta(\rho-\rho')\{-b[Y^{J+1},\Omega^1]_N^J \\ &\quad + a[Y^{J-1},\Omega^1]_N^J\}[\mathbf{e}_{12}+\mathbf{e}_{21}]/\sqrt{2}\ (Case\ 2), \\ \rho\Psi_0'^\beta &= \delta(\rho-\rho')\{-b[Y^{J+1},\Omega^1]_N^J \\ &\quad + a[Y^{J-1},\Omega^1]_N^J\}[\mathbf{e}_{11}+\mathbf{e}_{22}]/\sqrt{2}\ (Case\ 3),\end{aligned} \tag{82d}$$

with corresponding energy $E=-e^2/\rho'$.

4.3. Chirality

We have shown that the completeness condition with $\rho_0\to\infty$ such that the Bessel transform replaces the Bessel series leads to the delta function radial solutions $\delta(\rho-\rho')$ with energies $-e^2/\rho'$ for the resonance states. We have also shown that using the Bessel series with $M\to\infty$ or the Bessel transform with $\rho_0\to\infty$ give us $\Delta\rho\to 0$ and is entirely equivalent to the rest mass $m\to 0$. So our treatment of chirality in the case of free particles in Section 3 above where we let $m=0$ is now justified with a Coulomb potential acting between the particles. The degenerate pairs $(\Psi_0^0,\Psi_0'^0)$ with $S=0$ and $(\Psi_0^\alpha,\Psi_0'^\alpha)$, $(\Psi_0^1,\Psi_0'^1)$ and $(\Psi_0^\beta,\Psi_0'^\beta)$ with $S=1$ are Weyl spinors because of their chirality.

5. Bethe-Salpeter Equation: Separability of Atomic and Resonance States

The two-body Dirac equation for positronium is only an approximation to the Bethe-Salpeter equation [20] which is relativistically invariant and can include all the necessary QED (quantum electrodynamics) corrections. Ultimately, the justification for using the two-body Dirac equation comes from the Bethe-Salpeter equation. The Bethe-Salpeter equation itself has been related to S-matrix field theory by Gell-Mann and Low [21] and Sucher [22] to justify its application to bound states. Thus, the Bethe-Salpeter equation may be thought of as equivalent to bound state QED, whereas the original S-matrix field theory was applied to scattering QED. In this section only we shall use natural units where $c = 1$ and $\hbar = 1$ except for some obvious cases where clarity is helpful.

We can define the times τ and T as the fourth components of the relative coordinate four vectors $\rho \equiv (\boldsymbol{\rho}, i\tau)$ and $R \equiv (\mathbf{R}, iT)$, respectively. We can also define the energies ε and E as the fourth components of the conjugate momentum four vectors $\pi \equiv (\boldsymbol{\pi}, i\varepsilon)$ and $P \equiv (\mathbf{P}, iE)$, respectively. Note that we have also changed our notation in this section so that ρ, for example, is now a four-vector and is not equal to $|\boldsymbol{\rho}|$ which we shall now write out explicitly. From (26) we find the times

$$\begin{aligned} \tau &= t_e - t_p, \\ T &= \frac{1}{2}(t_e + t_p), \end{aligned} \tag{83}$$

and from (27) their conjugate energies

$$\begin{aligned} \varepsilon &= \frac{1}{2}(e_e - e_p), \\ E &= e_e + e_p, \end{aligned} \tag{84}$$

in terms of the one-body times and energies. The problem with the two-body Dirac equation is that its Hamiltonian formalism does not properly treat the relative time τ in the advanced or retarded potential nor the relative energy ε. Indeed, the two-body Dirac equation is only a function of the time T and energy E. Thus, it is implicit that $\tau = 0$ so that $t_e = t_p = T$ and $\varepsilon = 0$ so that $e_e = e_p = E/2$. It has already been mentioned that the resonance solutions to the two-body Dirac equation with a Coulomb potential are coupled to the atomic solutions to order $mc^2\alpha^5$. We now use the Bethe-Salpeter equation for a Coulomb potential, treating the relative time and energy τ and ε explicitly, to show that these resonance solutions of positronium are actually uncoupled from the atomic solutions to all orders in QED. To do so we must distinguish between the resonance solutions and virtual electron-positron pairs which also arise from the $E = 0$ free particle solutions. Such pairs can indeed couple to the atomic solutions.

The Feynman derivation of QED for positronium [23] is based on the one-body Green's function for the one-body Dirac equation. Similarly the Bethe-Salpeter equation is based on the two-body Green's function for the two-body Dirac equation. The two-body Dirac equation for positronium with a Coulomb potential is only accurate to order

$mc^2\alpha^4$ [6] as we have described above. Indeed Karplus and Klein [18] and Fulton and Martin [19] have given the corrections to order $mc^2\alpha^5$ for positronium using the Bethe-Salpeter equation. We now use the Bethe-Salpeter equation to derive the atomic and resonance solutions to positronium in a Coulomb potential which differ significantly from those of the two-body Dirac equation. For atomic states we shall follow the work of Salpeter and Bethe [6, 20] (using γ matrices consistent with Dirac, Pauli and Sakurai as defined above). In addition, we also derive the relevant equations and solutions for resonance states using the same formalism.

We start with the potential $G(k)$ in the momentum representation using the Feynman gauge

$$G(k) = -4\pi e^2 \frac{\gamma^e \cdot \gamma^p}{k \cdot k}, \tag{85}$$

where $k \equiv (\mathbf{k}, i\omega)$ is a four vector and the superscripts e and p on the γ matrices refer to operators acting on the electron or the positron, respectively. We have the Lorentz invariant scalar products $\gamma^e \cdot \gamma^p \equiv \gamma^e_u \gamma^p_u$ and

$$k \cdot k \equiv k_u k_u = \mathbf{k} \cdot \mathbf{k} - \omega^2,$$

so that $G(k)$ is a Lorentz invariant. Here, $\mathbf{k}$ is the change in the momentum and ω is the change in energy given by

$$\begin{aligned} \mathbf{k} &= \mathbf{p}' - \mathbf{p}, \\ \omega &= e' - e, \end{aligned}$$

or in terms of the four-vectors,

$$k = p' - p, \tag{86}$$

as a result of the potential scattering.

We can convert this potential from the Feynman gauge to the Coulomb gauge using the Dirac equation for p' and p,

$$\begin{aligned} i(\gamma \cdot p') + m &= 0, \\ i(\gamma \cdot p) + m &= 0, \end{aligned}$$

so that

$$\gamma \cdot (p' - p) = \gamma \cdot k = 0,$$

and

$$\boldsymbol{\gamma} \cdot \widehat{\mathbf{k}} = i\gamma_4 \frac{\omega}{|\mathbf{k}|}.$$

It follows that

$$\begin{aligned} \frac{\gamma^e_4 \gamma^p_4}{\mathbf{k} \cdot \mathbf{k}} &= \frac{\gamma^e_4 \gamma^p_4}{\mathbf{k} \cdot \mathbf{k} - \omega^2} + \frac{\boldsymbol{\gamma}^e \cdot \widehat{\mathbf{k}} \boldsymbol{\gamma}^p \cdot \widehat{\mathbf{k}}}{\mathbf{k} \cdot \mathbf{k} - \omega^2}, \\ &= \frac{\gamma^e_4 \gamma^p_4 + \boldsymbol{\gamma}^e \cdot \widehat{\mathbf{k}} \boldsymbol{\gamma}^p \cdot \widehat{\mathbf{k}}}{k \cdot k}. \end{aligned}$$

This equation shows that the exchange of Coulomb photons on the left is equivalent to the exchange of timelike and longitudinal covariant photons on the right. But we also have the relation for the two mutually orthogonal unit vectors $\widehat{\mathbf{k}}_1$ and $\widehat{\mathbf{k}}_2$ which are perpendicular to $\widehat{\mathbf{k}}_3 \equiv \widehat{\mathbf{k}}$,

$$\sum_{i=1,2} \frac{\boldsymbol{\gamma}^e \cdot \widehat{\mathbf{k}}_i \boldsymbol{\gamma}^p \cdot \widehat{\mathbf{k}}_i}{k \cdot k} = \frac{\boldsymbol{\gamma}^e \cdot \boldsymbol{\gamma}^p - \boldsymbol{\gamma}^e \cdot \widehat{\mathbf{k}} \boldsymbol{\gamma}^p \cdot \widehat{\mathbf{k}}}{k \cdot k}.$$

Adding the last two equations, we find the potential in the Coulomb gauge,

$$G(k) = -4\pi e^2 \frac{\gamma_4^e \gamma_4^p}{\mathbf{k} \cdot \mathbf{k}} - 4\pi e^2 \sum_{i=1,2} \frac{\boldsymbol{\gamma}^e \cdot \widehat{\mathbf{k}}_i \boldsymbol{\gamma}^p \cdot \widehat{\mathbf{k}}_i}{k \cdot k}. \tag{87}$$

(We note that our $G(k)$ corresponds to $(2\pi)^3 G(k)$ given by Salpeter [6]). The above equation demonstrates that the exchange of covariant photons in (85) is equivalent to the exchange of Coulomb photons and transverse photons in (87). The Coulomb gauge is useful when the momentum change is small $\hbar\,|\mathbf{k}| \ll mc$ as in the case of atomic bound states of positronium, whereas the Feynman gauge is useful when the momentum change is large $\hbar\,|\mathbf{k}| \gg mc$ as in the case of resonance bound states. We note that the Coulomb potential in the momentum representation is proportional to the first term in the Coulomb gauge above, where

$$V_C(\mathbf{k}) = -e^2 \int d^3\mathbf{r}\ \frac{e^{i\mathbf{k}\cdot\mathbf{r}}}{r} = -4\pi e^2 \frac{1}{\mathbf{k} \cdot \mathbf{k}}. \tag{88}$$

We shall use this potential $V_C(\mathbf{k})$ to relate the two-body Dirac equation to the Bethe-Salpeter equation.

We now let $K(r, r')$ be the Green's functions for the one-body Dirac equation

$$[i(\gamma \cdot p) + m]K(r, r') = \delta^4(r - r'), \tag{89}$$

for either the electron or the positron where $r = (\mathbf{r}, it)$, $p = (\mathbf{p}, ie)$ and $\delta^4(r - r')$ is the four-dimensional Dirac delta function,

$$\begin{aligned} \delta^4(r - r') &= \prod_{u=1}^{4} \delta(r - r'_u), \\ &= \frac{1}{(2\pi)^4} \int d^4p\ e^{ip\cdot(r-r')}. \end{aligned} \tag{90}$$

We let $K(p)$ be the Green's function in the momentum representation

$$K(r, r') = \frac{1}{(2\pi)^4} \int d^4p\ K(p)\ e^{ip\cdot(r-r')}, \tag{91}$$

Substituting the Fourier transforms above into (89), it follows that

$$K(p) = \frac{1}{[i(\gamma \cdot p) + m]}. \tag{92}$$

We can then find $K(r,r')$ from (91)

$$K(r,r') = \frac{1}{(2\pi)^4}\int d^4p\ \frac{e^{ip\cdot(r-r')}}{[i(\gamma\cdot p)+m]}, \tag{93}$$
$$= -\frac{1}{(2\pi)^4}\int d^3p\ e^{i\mathbf{p}\cdot(\mathbf{r}-\mathbf{r}')}\int_{-\infty}^{\infty}\frac{[-i(\gamma\cdot p)+m]e^{-ie(t-t')}}{[e+e_0][e-e_0]}de,$$

where

$$(\gamma\cdot p)(\gamma\cdot p) = p\cdot p = \mathbf{p}\cdot\mathbf{p} - e^2,$$

and

$$e_0 \equiv |e_0| = \sqrt{\mathbf{p}\cdot\mathbf{p}+m^2}.$$

The line integral over de has poles at $e = \pm e_0$. If we give the mass an infinitesimal imaginary amplitude $\delta > 0$ such that $m \to m - i\delta$, then we find the poles at $e = \pm e_0 \mp i\epsilon$ where $\epsilon = \delta/2$. We can take the residues of the integrand to find the line integral using Cauchy's theorem by closing the integral over de in the upper or lower half complex plane as long as the integrand converges at $e \to i\infty$ or at $e \to -i\infty$, respectively. However, the integrand can diverge depending on the sign of $(t-t')$ in $e^{-ie(t-t')}$. Note that the exponent $e^{-ie(t-t')}$ is only convergent for $e \to i\infty$ when $(t-t')$ is negative, so we can only use the pole $e = -e_0 + i\epsilon$ (which is in the upper half complex plane) when $t < t'$. This corresponds to negative energy states $e = -e_0$ propagating backward in time. Likewise, the exponent $e^{-ie(t-t')}$ is only convergent for $e \to -i\infty$ when $(t-t')$ is positive so we can only use the pole $e = e_0 - i\epsilon$ (which is in the lower half complex plane) when $t > t'$. This corresponds to positive energy states $e = e_0$ propagating forward in time. Using these boundary conditions we denote the Feynman Green's function by $K_F(r,r')$ which is related to the Feynman electron or positron propagator $S_F(r-r')$ by

$$S_F(r-r') = -K_F(r,r'). \tag{94}$$

If we let $m \to m + i\delta$ then the converse is true: negative energy states propagate forward in time and positive energy states propagate backward in time. Note that it is also possible to have mixed boundary conditions for the the poles of (93) such that positive energy states obey $m \to m - i\delta$ and negative energy states obey $m \to m + i\delta$ such that both positive and negative energy states propagate forward in time, or vice versa.

The correct boundary condition depends on physical consistency with the known temporal behavior of the particle undergoing scattering or annihilation. Obviously, positive energy electrons must propagate forward in time. Negative energy electrons must propagate backward in time for two important reasons [13, 23]. First, if negative energy electrons propagated forward in time, then positive energy electrons could scatter into negative energy electrons at a later time and be lost. This is not possible. Second, virtual negative energy electrons must propagate backward in time so that they can annihilate with virtual positive energy electrons which are moving forward in time. That is, virtual negative energy electrons moving backward in time are equivalent to

positrons moving forward in time. Such time behavior accounts for virtual electron-positron pairs. These boundary conditions strictly determine the location of the poles of e in the complex plane. Thus, for $K_F(r_e, r'_e)$ to correspond with electron propagation, we must chose $m_e \rightarrow m_e - i\delta$ for the proper boundary conditions. Likewise, for $K_F(r_p, r'_p)$ to correspond with positron propagation, we must also chose $m_p \rightarrow m_p - i\delta$ for similar reasons.

The two-body Green's function for the electron and positron is simply the product of the one-body Green's functions $K(r_e, r'_e)K(r_p, r'_p)$ and is a solution of the analogous two-body equation,

$$[i(\gamma^e \cdot p_e) + m_e][i(\gamma^p \cdot p_p) + m_p]K(r_e, r'_e)K(r_p, r'_p) = \delta^4(r_e - r'_e)\delta^4(r_p - r'_p), \tag{95}$$

without stipulating the boundary conditions. We wish to relate this Green's function to the solutions of the two-body Dirac equation by means of the Bethe-Salpeter equation which in the coordinate representation is

$$\psi(r_e, r_p) = i \int d^4r'_e d^4r'_p \int d^4r''_e d^4r''_p K(r_e, r''_e)K(r_p, r''_p)\overline{G}(r''_e, r''_p; r'_e, r'_p)\psi(r'_e, r'_p), \tag{96}$$

where $\overline{G}$ is the irreducible kernel corresponding to a sum of interaction terms $\overline{G}_i^n$ for each irreducible Feynman diagram of order α^{2n}

$$\overline{G} = \sum_{i,n} \overline{G}_i^n. \tag{97}$$

Multiplying both sides of (96) by $[i(\gamma^e \cdot p_e) + m_e][i(\gamma^p \cdot p_p) + m_p]$ we find

$$[i(\gamma^e \cdot p_e) + m_e][i(\gamma^p \cdot p_p) + m_p]\psi(r_e, r_p) = i \int d^4r'_e d^4r'_p \overline{G}(r_e, r_p; r'_e, r'_p)\psi(r'_e, r'_p). \tag{98}$$

Next, we transform this equation to relative coordinates, $\rho \equiv (\boldsymbol{\rho}, i\tau)$ and $R \equiv (\mathbf{R}, iT)$, and momenta, $\pi \equiv (\boldsymbol{\pi}, i\varepsilon)$ and $P \equiv (\mathbf{P}, iE)$, just like we did in the case of the two-body Dirac equation. We find, letting $\mathbf{P} = \mathbf{0}$, $\boldsymbol{\alpha} = i\beta\boldsymbol{\gamma}$, and multiplying by $\gamma_4^e\gamma_4^p = \beta_e\beta_p$,

$$[\frac{1}{2}E - \boldsymbol{\alpha}_e \cdot \boldsymbol{\pi} - \beta_e m + \varepsilon][\frac{1}{2}E + \boldsymbol{\alpha}_p \cdot \boldsymbol{\pi} - \beta_p m - \varepsilon]\psi(\rho, R) = i\beta_e\beta_p \int J \; d^4\rho' d^4R' \overline{G}(\rho, R; \rho', R')\psi(\rho', R'), \tag{99}$$

where $m_e = m_p = m$ and the Jacobian determinant is

$$J = \begin{vmatrix} \frac{\partial r'_e}{\partial \rho'} & \frac{\partial r'_e}{\partial \rho'} \\ \frac{\partial r'_p}{\partial R'} & \frac{\partial r'_p}{\partial R'} \end{vmatrix} = 1.$$

We now consider the irreducible interaction $\overline{G}(\rho, R; \rho', R')$ which corresponds to the exchange of a single photon in the Feynman or Coulomb gauge,

$$\overline{G}(\rho, R; \rho', R') = \overline{G}^1(\rho, R; \rho', R') \equiv G(\rho)\delta(\rho - \rho')\delta(R - R'),$$

where $G(\rho)$ is in the coordinate representation of the potential $G(k)$ in (85) or (87). We substitute this into (99) so that the Bethe-Salpeter equation becomes

$$F\psi(\rho) = i\beta_e\beta_p G(\rho)\psi(\rho), \tag{100}$$

where

$$\begin{aligned} F &= [\frac{1}{2}E - \boldsymbol{\alpha}_e{\cdot}\boldsymbol{\pi} - \beta_e m + \varepsilon][\frac{1}{2}E + \boldsymbol{\alpha}_p{\cdot}\boldsymbol{\pi} - \beta_p m - \varepsilon], \\ &= [\frac{1}{2}E - \mathbf{h}_0^e(\boldsymbol{\pi}) + \varepsilon][\frac{1}{2}E - \mathbf{h}_0^p(\boldsymbol{\pi}) - \varepsilon], \end{aligned} \tag{101}$$

in terms of the free-particle Hamiltonians $\mathbf{h}_0^e(\boldsymbol{\pi})$ of the electron and $\mathbf{h}_0^p(\boldsymbol{\pi})$ of the positron in (22) and (28). This is the so-called ladder approximation which generates all Feynman diagrams on the 'ladder' where the photon lines do not cross each other between vertices. The energy E is the total energy of the system with respect to the center of momentum where $\mathbf{P} = 0$ as in the case of the two-body Dirac equation.

We can readily transform this into the momentum representation using

$$\psi(\pi) = \int d^4\rho\ e^{-i\rho\cdot\pi}\psi(\rho).$$

On the right of (100) we have the transformation

$$\begin{aligned} \int d^4\rho\ e^{-i\rho\cdot\boldsymbol{\pi}}G(\rho)\psi(\rho) &= \int d^4\rho\ d^4\rho' e^{-i\rho\cdot\pi}\delta(\rho-\rho')G(\rho)\psi(\rho'), \\ &= \frac{1}{(2\pi)^4}\int d^4\rho\ d^4\rho' d^4\pi' e^{-i\rho\cdot\pi}e^{i(\rho-\rho')\cdot\pi'}G(\rho)\psi(\rho'), \\ &= \frac{1}{(2\pi)^4}\int d^4\rho\ d^4\rho' d^4\pi' e^{-i\rho\cdot(\pi-\pi')}e^{-i\rho\cdot\pi'}G(\rho)\psi(\rho'), \\ &= \frac{1}{(2\pi)^4}\int d^4\pi' G(\pi-\pi')\psi(\pi'), \end{aligned}$$

which is the convolution of the Fourier transforms $G(\pi)$ and $\psi(\pi)$ as expected. Using (86), where $k = \pi' - \pi$ and $d^4k = d^4\pi'$, (100) becomes

$$F\psi(\pi) = \frac{i\beta_e\beta_p}{(2\pi)^4}\int d^4k G(k)\psi(k+\pi), \tag{102}$$

where the interaction potential $G(-k) = G(k)$. This is the Bethe-Salpeter equation in the momentum representation for the ladder approximation. We now show that this equation separates the atomic and resonance states to all order of α for a Coulomb potential.

We ignore the exchange of transverse photons in (87) which gives rise to the magnetic potential for atomic states and consider only the instantaneous Coulomb potential so that $\beta_e\beta_p G(k) = V_C(\mathbf{k})$ in (88) and the equation above becomes

$$F\psi(\pi) = \frac{e^2}{(2\pi i)2\pi^2}\int d^4k\frac{1}{\mathbf{k}\cdot\mathbf{k}}\psi(k+\pi). \tag{103}$$

We can now integrate $\psi(k+\pi) \equiv \psi(\boldsymbol{\pi}', \varepsilon')$ over $dk_4 \equiv d\varepsilon'$ and define

$$\phi(\boldsymbol{\pi}') = \int d\varepsilon' \ \psi(\boldsymbol{\pi}', \varepsilon'),$$

so that

$$\psi(\pi) = F^{-1}\Gamma(\boldsymbol{\pi}), \tag{104}$$

where

$$\Gamma(\boldsymbol{\pi}) = \frac{e^2}{(2\pi i)2\pi^2} \int d^3k \frac{1}{\mathbf{k}\cdot\mathbf{k}} \phi(\mathbf{k}+\boldsymbol{\pi}).$$

The equation (104) is useful if we can integrate both sides by $d\pi_4 \equiv d\varepsilon$ where $\Gamma(\boldsymbol{\pi})$ is not dependent on ε. Using

$$\phi(\boldsymbol{\pi}) = \int d\varepsilon \ \psi(\boldsymbol{\pi}, \varepsilon),$$

we find

$$\phi(\boldsymbol{\pi}) = \int d\varepsilon \ F^{-1}\Gamma(\boldsymbol{\pi}). \tag{105}$$

On the right we need to decompose $\Gamma(\boldsymbol{\pi})$ into free particle states $\Psi(\rho)$ so that operator F^{-1} can be found from (101) where by definition,

$$\begin{aligned}
\mathbf{h}_0^i(\boldsymbol{\pi})\Psi(\rho) &= e_i(\boldsymbol{\pi})\Psi(\rho), \\
e_i(\boldsymbol{\pi}) \qquad &= \pm\, e_0, \\
e_0 \qquad &= \sqrt{\boldsymbol{\pi}\cdot\boldsymbol{\pi} + m^2},
\end{aligned}$$

for $i = e, p$ as in equations (22)-(29) and then integrated over $d\varepsilon$.

This decomposition can be accomplished by projecting out the free particle components using the single particle projection operators for the electron and the positron in the momentum representation. We can define the electron and positron projectors $\boldsymbol{\Lambda}_{\pm}^{e}(\boldsymbol{\pi})$ and $\boldsymbol{\Lambda}_{\pm}^{p}(\boldsymbol{\pi})$, respectively, by

$$\boldsymbol{\Lambda}_{\pm}^{i}(\boldsymbol{\pi}) = \frac{e_i(\boldsymbol{\pi}) \pm \mathbf{h}_0^i(\boldsymbol{\pi})}{2e_i(\boldsymbol{\pi})},$$

for $i = e, p$ such that

$$\mathbf{h}_0^i(\boldsymbol{\pi})\boldsymbol{\Lambda}_{\pm}^{i}(\boldsymbol{\pi}) = \boldsymbol{\Lambda}_{\pm}^{i}(\boldsymbol{\pi})\mathbf{h}_0^i(\boldsymbol{\pi}) = \pm e_0(\boldsymbol{\pi}). \tag{106}$$

These projectors have the orthonormality properties

$$\begin{aligned}
\boldsymbol{\Lambda}_{+}^{i}(\boldsymbol{\pi})\boldsymbol{\Lambda}_{+}^{i}(\boldsymbol{\pi}) &= \boldsymbol{\Lambda}_{+}^{i}(\boldsymbol{\pi}), \\
\boldsymbol{\Lambda}_{-}^{i}(\boldsymbol{\pi})\boldsymbol{\Lambda}_{-}^{i}(\boldsymbol{\pi}) &= \boldsymbol{\Lambda}_{-}^{i}(\boldsymbol{\pi}), \\
\boldsymbol{\Lambda}_{+}^{i}(\boldsymbol{\pi})\boldsymbol{\Lambda}_{-}^{i}(\boldsymbol{\pi}) &= 0, \\
\boldsymbol{\Lambda}_{-}^{i}(\boldsymbol{\pi})\boldsymbol{\Lambda}_{+}^{i}(\boldsymbol{\pi}) &= 0,
\end{aligned}$$

and completeness property

$$\boldsymbol{\Lambda}_{+}^{i}(\boldsymbol{\pi}) + \boldsymbol{\Lambda}_{-}^{i}(\boldsymbol{\pi}) = 1,$$

for $i = e, p$. Taking products of these projection operators we define

$$\begin{aligned}
\mathbf{\Lambda}_{\pm\pm}(\boldsymbol{\pi}) &= \mathbf{\Lambda}^e_{\pm}(\boldsymbol{\pi})\mathbf{\Lambda}^p_{\pm}(\boldsymbol{\pi}),\\
\phi_{\pm\pm}(\boldsymbol{\pi}) &= \mathbf{\Lambda}_{\pm\pm}(\boldsymbol{\pi})\phi(\boldsymbol{\pi}),\\
\Gamma_{\pm\pm}(\boldsymbol{\pi}) &= \mathbf{\Lambda}_{\pm\pm}(\boldsymbol{\pi})\Gamma(\boldsymbol{\pi}).
\end{aligned}$$

We apply $\mathbf{\Lambda}_{\pm\pm}(\boldsymbol{\pi})$ to (105) giving

$$\begin{aligned}
\phi_{\pm\pm}(\boldsymbol{\pi}) &= \int d\varepsilon\ \mathbf{\Lambda}_{\pm\pm}(\boldsymbol{\pi})F^{-1}\Gamma(\boldsymbol{\pi}), \qquad (107)\\
&= \int d\varepsilon\ F^{-1}\mathbf{\Lambda}_{\pm\pm}(\boldsymbol{\pi})\Gamma(\boldsymbol{\pi}),\\
&= \int d\varepsilon\ \frac{1}{[\frac{1}{2}E - \mathbf{h}^e_0(\boldsymbol{\pi}) + \varepsilon]}\frac{1}{[\frac{1}{2}E - \mathbf{h}^p_0(\boldsymbol{\pi}) - \varepsilon]}\mathbf{\Lambda}_{\pm\pm}(\boldsymbol{\pi})\Gamma(\boldsymbol{\pi}),\\
&= \int_{-\infty}^{\infty} d\varepsilon\ \frac{1}{[\frac{1}{2}E \mp e_0 + \varepsilon]}\frac{1}{[\frac{1}{2}E \mp e_0 - \varepsilon]}\Gamma_{\pm\pm}(\boldsymbol{\pi}),\\
&= -\int_{-\infty}^{\infty} d\varepsilon\ \frac{1}{[\varepsilon + \frac{1}{2}E \mp e_0]}\frac{1}{[\varepsilon - \frac{1}{2}E \pm e_0]}\Gamma_{\pm\pm}(\boldsymbol{\pi}),
\end{aligned}$$

where we have used (106) and (101). The latter integral can be readily performed using the Cauchy theorem of residues. The integrand has two poles at

$$\begin{aligned}
\varepsilon_e &= -\frac{1}{2}E \pm e_0,\\
\varepsilon_p &= \frac{1}{2}E \mp e_0,
\end{aligned}$$

corresponding to the first and second term in the integrand, respectively. Note we use a notation such that the signs of $\pm e_0$ in ε_e and $\mp e_0$ in ε_p correlate with the signs of $\mathbf{\Lambda}^e_{\pm}(\boldsymbol{\pi})$ and $\mathbf{\Lambda}^p_{\pm}(\boldsymbol{\pi})$, respectively, where $\mathbf{\Lambda}_{\pm\pm}(\boldsymbol{\pi}) = \mathbf{\Lambda}^e_{\pm}(\boldsymbol{\pi})\mathbf{\Lambda}^p_{\pm}(\boldsymbol{\pi})$ corresponding to the electron and positron terms.

5.1. Atomic States

As discussed above, for the proper boundary conditions for electron-positron pairs we must let $m \to m - i\delta$ which result in $e_0 \to e_0 - i\epsilon$ where $\epsilon = \delta/2$. Note that this means that positive energy states e_0 propagate forward in time τ whilst negative energy states $-e_0$ propagate backward in time τ, where the time is now conjugate to the energy ε. Consider first the case of $\phi_{++}(\boldsymbol{\pi})$ with poles at

$$\begin{aligned}
\varepsilon_e &= -\frac{1}{2}E + e_0 - i\epsilon,\\
\varepsilon_p &= \frac{1}{2}E - e_0 + i\epsilon.
\end{aligned}$$

We can complete the line integral in either the upper or lower half complex plane where the integrand is convergent with the same results

$$\begin{aligned}
\phi_{++}(\boldsymbol{\pi}) &= -\int_{-\infty}^{\infty} d\varepsilon\ \frac{1}{[\varepsilon - \varepsilon_e][\varepsilon - \varepsilon_p]}\Gamma_{++}(\boldsymbol{\pi}),\\
&= -\frac{2\pi i}{E - 2e_0}\Gamma_{++}(\boldsymbol{\pi}).
\end{aligned}$$

Similarly, for $\phi_{--}(\boldsymbol{\pi})$ with poles at

$$\varepsilon_e = -\frac{1}{2}E - e_0 + i\epsilon,$$
$$\varepsilon_p = \frac{1}{2}E + e_0 - i\epsilon,$$

the integral becomes

$$\phi_{--}(\boldsymbol{\pi}) = -\int_{-\infty}^{\infty} d\varepsilon \, \frac{1}{[\varepsilon - \varepsilon_e][\varepsilon - \varepsilon_p]}\Gamma_{--}(\boldsymbol{\pi}),$$
$$= \frac{2\pi i}{E + 2e_0}\Gamma_{--}(\boldsymbol{\pi}).$$

Finally, we find for the corresponding integrals for $\phi_{+-}(\boldsymbol{\pi})$ and $\phi_{-+}(\boldsymbol{\pi})$,

$$\phi_{+-}(\boldsymbol{\pi}) = 0,$$
$$\phi_{-+}(\boldsymbol{\pi}) = 0.$$

Combining these results and letting

$$\boldsymbol{\Lambda} = \boldsymbol{\Lambda}_{++}(\boldsymbol{\pi}) - \boldsymbol{\Lambda}_{--}(\boldsymbol{\pi}),$$

we have

$$(E - 2e_0)\phi_{++}(\boldsymbol{\pi}) + (E + 2e_0)\phi_{--}(\boldsymbol{\pi}) = -2\pi i\boldsymbol{\Lambda}\Gamma(\boldsymbol{\pi}),$$

or

$$[\mathbf{h}_0^e(\boldsymbol{\pi}) + \mathbf{h}_0^p(\boldsymbol{\pi})][\phi_{++}(\boldsymbol{\pi}) + \phi_{--}(\boldsymbol{\pi})] - \frac{e^2}{2\pi^2}\boldsymbol{\Lambda}\int d^3k \frac{1}{\mathbf{k}\cdot\mathbf{k}}\phi(\mathbf{k}+\boldsymbol{\pi}) = E[\phi_{++}(\boldsymbol{\pi}) + \phi_{--}(\boldsymbol{\pi})], \tag{108}$$

with $\phi_{+-}(\boldsymbol{\pi}) = \phi_{-+}(\boldsymbol{\pi}) = 0$ which is the Bethe-Salpeter equation for the atomic states for a Coulomb potential in the ladder approximation.

Because of the operator $\boldsymbol{\Lambda}$, the Coulomb potential is attractive for positive energy atomic states but is repulsive for negative energy atomic states. Only the free particle states $\phi_{++}(\boldsymbol{\pi})$ and $\phi_{--}(\boldsymbol{\pi})$ with energies $E = 2e_0$ and $E = -2e_0$, respectively, contribute to the atomic states for a Coulomb potential to all orders in the ladder approximation. In Figure 5 we perform the same calculation as in Figure 1 except we use only the free particles states $\phi_{++}(\boldsymbol{\pi})$ as our basis. Note that now,the wavefunction y_{22}^2 peaks in Region 2 instead of in Region 1. This is because because our basis is without the influence of the resonance states $\phi_{+-}(\boldsymbol{\pi})$ and $\phi_{-+}(\boldsymbol{\pi})$ which are responsible for the singularity at $-e^2/\rho'$. Below, we show that the resonance states arising from $\phi_{+-}(\boldsymbol{\pi})$ and $\phi_{-+}(\boldsymbol{\pi})$ are indeed solutions to the Bethe-Salpeter equation with different boundary conditions.

We can compare the above equation to the two body Dirac equation in the momentum representation

$$[\mathbf{h}_0^e(\boldsymbol{\pi}) + \mathbf{h}_0^p(\boldsymbol{\pi})]\Psi(\boldsymbol{\pi}) - \frac{e^2}{2\pi^2}\int d^3k \frac{1}{\mathbf{k}\cdot\mathbf{k}}\Psi(\mathbf{k}+\boldsymbol{\pi}) = E\Psi(\boldsymbol{\pi}). \tag{109}$$

which erroneously includes the resonances states $\phi_{+-}(\boldsymbol{\pi})$ and $\phi_{-+}(\boldsymbol{\pi})$.

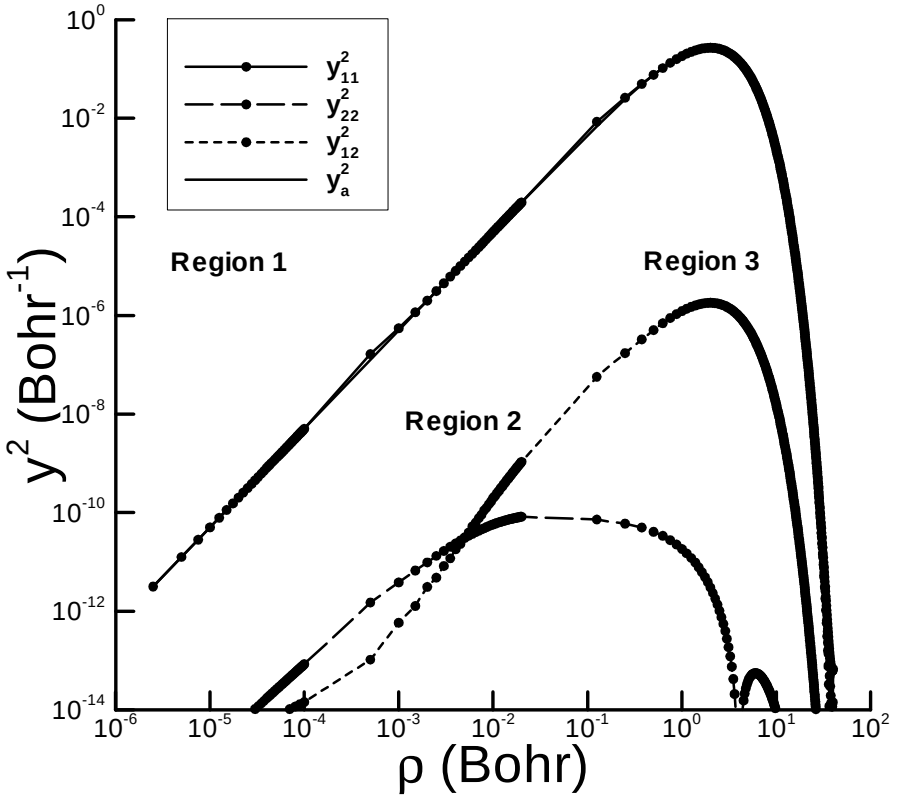

Figure 5. The square of the wavefunction components for the atomic positronium S=0 groud state. Same as Figure 1 except only the free particle states $\phi_{++}(\boldsymbol{\pi})$ are used for the basis. Note that y_{11}^2 and y_a^2 now completely overlap.

5.2. Resonance States

The resonance states $\phi_{+-}(\boldsymbol{\pi})$ and $\phi_{-+}(\boldsymbol{\pi})$ exist and are solutions of the Bethe-Salpeter equation if we change our boundary conditions. The appropriate boundary conditions for resonance states correspond to both positive and negative energy states propagating forward in time τ. This means that the negative energy states which comprise the resonance states cannot exist as separate free particles: negative states of free particles must propagate backward in time because they correspond to the antiparticle propagating forward in time. But this is not a problem for resonance states because they only exist as bound and not free states. Furthermore, as we show in Section 7 below, resonance states can neither annihilate into photons nor be created by photons. So, in the case of resonance bound states, the negative energy states do not propagate backward in time: they cannot comply with the boundary conditions of free particles or virtual electron-positron pairs to be physically consistent.

With this time behavior the poles of $\phi_{+-}(\boldsymbol{\pi})$ are

$$\begin{aligned}\varepsilon_e &= -\frac{1}{2}E + e_0 - i\epsilon,\\ \varepsilon_p &= \frac{1}{2}E + e_0 + i\epsilon.\end{aligned}$$

The integral for the Bethe-Salpeter equation becomes

$$\begin{aligned}\phi_{+-}(\boldsymbol{\pi}) &= -\int_{-\infty}^{\infty} d\varepsilon\ \frac{1}{[\varepsilon-\varepsilon_e][\varepsilon-\varepsilon_p]}\Gamma_{+-}(\boldsymbol{\pi}),\\ &= -\frac{2\pi i}{E}\Gamma_{+-}(\boldsymbol{\pi}),\end{aligned}$$

where we may close the line integral in either the upper- or lower-half complex plane. Similarly, the poles of $\phi_{-+}(\boldsymbol{\pi})$ are

$$\begin{aligned}\varepsilon_e &= -\frac{1}{2}E - e_0 - i\epsilon,\\ \varepsilon_p &= \frac{1}{2}E - e_0 + i\epsilon,\end{aligned}$$

and the integral becomes

$$\begin{aligned}\phi_{-+}(\boldsymbol{\pi}) &= -\int_{-\infty}^{\infty} d\varepsilon\ \frac{1}{[\varepsilon-\varepsilon_e][\varepsilon-\varepsilon_p]}\Gamma_{-+}(\boldsymbol{\pi}),\\ &= -\frac{2\pi i}{E}\Gamma_{-+}(\boldsymbol{\pi}).\end{aligned}$$

Combining these results, we have

$$-\frac{e^2}{2\pi^2}[\boldsymbol{\Lambda}_{+-}(\boldsymbol{\pi})+\boldsymbol{\Lambda}_{-+}(\boldsymbol{\pi})]\int d^3k\frac{1}{\mathbf{k}\cdot\mathbf{k}}\phi(\mathbf{k}+\boldsymbol{\pi}) = E[\phi_{+-}(\boldsymbol{\pi})+\phi_{-+}(\boldsymbol{\pi})], \tag{110}$$

with $\phi_{++}(\boldsymbol{\pi}) = \phi_{--}(\boldsymbol{\pi}) = 0$ which is the Bethe-Salpeter equation for the resonance states for a Coulomb potential in the ladder approximation.

As shown by Karplus and Kline [18], there will be mixing of atomics states $\phi_{++}(\boldsymbol{\pi})$ and $\phi_{--}(\boldsymbol{\pi})$ with $E = 0$ states $\phi_{+-}(\boldsymbol{\pi})$ and $\phi_{-+}(\boldsymbol{\pi})$ due to the Coulomb potential resulting from cross ladder terms of order $mc^2\alpha^5$ and above. Such terms correspond to virtual electron-positron pairs and are comprised of free particle solutions with $E = 0$ found by means of $\boldsymbol{\Lambda}_{+-}(\boldsymbol{\pi})$ and $\boldsymbol{\Lambda}_{-+}(\boldsymbol{\pi})$ projectors. These virtual electron-positron pairs are not resonance states because the negative energy states comprising the virtual pairs must propagate backward in time. Thus, we must distinguish between virtual electron-positron pairs and resonance states formed from $\phi_{+-}(\boldsymbol{\pi})$ and $\phi_{-+}(\boldsymbol{\pi})$ states due to their different time behavior. As a result, the resonance states formed from $\phi_{+-}(\boldsymbol{\pi})$ and $\phi_{-+}(\boldsymbol{\pi})$ only arise from the ladder terms of QED and never mix with atomic states. On the other hand the virtual electron-positron pairs formed from $\phi_{+-}(\boldsymbol{\pi})$ and $\phi_{-+}(\boldsymbol{\pi})$ can not arise from the ladder terms of QED and can mix with the atomic states.

In conclusion, we have shown that the resonance states are completely separable from the atomic states in the momentum representation even in the presence of a Coulomb potential if we use their free particle components. These free particle

components are found by means of projections operators $\mathbf{\Lambda}_{+-}(\boldsymbol{\pi})$ and $\mathbf{\Lambda}_{-+}(\boldsymbol{\pi})$ which are entirely equivalent to the $E = 0$ solutions found in Section 3 in (49), (52) and (55). Thus, the resonance solutions are only comprised of the free particle Weyl pairs $(\Psi_0^0, \Psi_0'^0)$ with $S = 0$ and $(\Psi_0^\alpha, \Psi_0'^\alpha)$, $(\Psi_0^1, \Psi_0'^1)$ and $(\Psi_0^\beta, \Psi_0'^\beta)$ with $S = 1$. Care must be taken to use the ladder approximation for the resonance states which excludes the virtual electron-positron pairs which can mix with the atomic states.

6. Magnetic Potential

We now solve the two-body Dirac equation with both the Coulomb potential $\mathbf{V}_C(\rho)$ and the magnetic potential $\mathbf{V}_M(\rho)$ so that the new Hamiltonian is

$$\mathbf{H} = \mathbf{H}_0 + \mathbf{V}_C + \mathbf{V}_M. \tag{111}$$

The form of $\mathbf{V}_M(\rho)$ is different for atomic and resonance states as discussed below.

6.1. Atomic States

To find the magnetic potential for atomic states we must use the Coulomb gauge. This is because $\hbar\,|\mathbf{k}| \ll mc$ for atomic states and $\boldsymbol{\alpha}_e$ and $\boldsymbol{\alpha}_p$ have expectation values $v/c \sim \alpha = e^2/\hbar c$. We can use the instantaneous limit of $\gamma_4^e\gamma_4^p G(k)$ in (87) by letting $\omega = 0$,

$$\begin{aligned}\gamma_4^e\gamma_4^p G(\mathbf{k},0) &= -4\pi e^2\frac{1}{\mathbf{k}\cdot\mathbf{k}} + 4\pi e^2\sum_{i=1,2}\frac{\boldsymbol{\alpha}_e\cdot\widehat{\mathbf{k}}_i\boldsymbol{\alpha}_p\cdot\widehat{\mathbf{k}}_i}{\mathbf{k}\cdot\mathbf{k}},\\ &= V_C(k) + 4\pi e^2\frac{\boldsymbol{\alpha}_e\cdot\boldsymbol{\alpha}_p - \boldsymbol{\alpha}_e\cdot\widehat{\mathbf{k}}\boldsymbol{\alpha}_p\cdot\widehat{\mathbf{k}}}{\mathbf{k}\cdot\mathbf{k}},\end{aligned}$$

where $\beta_e\beta_p = \gamma_4^e\gamma_4^p$ and $\boldsymbol{\alpha} = i\beta\boldsymbol{\gamma}$. Taking the inverse Fourier transform, we have

$$\mathbf{V}_C(\rho) + \mathbf{V}_M(\rho) = -\frac{e^2}{\rho} + \frac{e^2}{2\rho}[\boldsymbol{\alpha}_e\cdot\boldsymbol{\alpha}_p + (\boldsymbol{\alpha}_e\cdot\hat{\mathbf{r}}_e)(\boldsymbol{\alpha}_p\cdot\hat{\mathbf{r}}_p)],$$

and the Breit potential [24] is defined as

$$\mathbf{V}_M(\rho) = \mathbf{V}_B(\rho) = \frac{e^2}{2\rho}[\boldsymbol{\alpha}_e\cdot\boldsymbol{\alpha}_p + (\boldsymbol{\alpha}_e\cdot\hat{\mathbf{r}}_e)(\boldsymbol{\alpha}_p\cdot\hat{\mathbf{r}}_p)]. \tag{112}$$

The Breit energy is a result of second order perturbation theory corresponding to the exchange of a transverse photon in the Coulomb gauge and one must use expectation values of $\mathbf{V}_B$ for the states already determined by the Coulomb potential $\mathbf{V}_C$ previously [12].

For atomic states of positronium the Breit potential gives us fine structure corrections of order $mc^2\alpha^4$ which can be determined as in the case of the Coulomb potential above using expectation values in the Pauli approximation. We find [12], letting $H_5^B = H_5^B(1) + H_5^B(2)$,

$$
\begin{aligned}
H_2^B &= \frac{mc^2\alpha^4}{8n^4} - \frac{3mc^2\alpha^4}{8n^3(2L+1)} + \frac{mc^2\alpha^4}{8n^3}\delta_{L0}, \qquad (113)\\
H_3^B &= \frac{2mc^2\alpha^4}{8n^3L(L+1)(2L+1)} \left\{ \begin{array}{cc} L & J=L+1 \\ -1 & J=L \\ -(L+1) & J=L-1 \end{array} \right\} (1-\delta_{L0})\delta_{S1},\\
H_5^B(1) &= -\frac{mc^2\alpha^4}{4n^3}\delta_{S0}\delta_{L0} + \frac{mc^2\alpha^4}{12n^3}\delta_{S1}\delta_{L0},\\
H_5^B(2) &= -\frac{mc^2\alpha^4}{8n^3L(L+1)(2L+1)} \left\{ \begin{array}{cc} L/(2L+3) & J=L+1 \\ -1 & J=L \\ (L+1)/(2L-1) & J=L-1 \end{array} \right\} (1-\delta_{L0})\delta_{S1}.
\end{aligned}
$$

To this order there is a term missing due to the energy change resulting from positronium annihilation for $S=1$ states given by

$$H_{an} = \frac{mc^2\alpha^4}{4n^3}\delta_{S1}\delta_{L0}. \qquad (114)$$

The Pauli energies E'_p of $\mathbf{H}$ including H_{an} is then,

$$E'_P = 2mc^2 + H_0 + H_1 + H_3^C + H_4^C + H_2^B + H_3^B + H_5^B + H_{an}. \qquad (115)$$

Combining terms, we find to fourth order [15]

$$
\begin{aligned}
E'_P &= 2mc^2 - \frac{mc^2\alpha^2}{4n^2} + \frac{mc^2\alpha^4}{n^3}\{\frac{11}{64n} - \frac{1}{2(2L+1)} + \xi\delta_{S1}\}, \qquad (116)\\
\text{where } \xi &= \frac{7\delta_{L0}}{12} + \frac{1-\delta_{L0}}{4(2L+1)} \left\{ \begin{array}{cc} \frac{3L+4}{(L+1)(2L+3)} & J=L+1 \\ -\frac{1}{L(L+1)} & J=L \\ -\frac{3L-1}{L(2L-1)} & J=L-1 \end{array} \right\}.
\end{aligned}
$$

Note that $H_3 = H_3^C + H_3^B$ has both a Coulomb term and a Breit term .

In Table 2 we compare the Coulomb energy corrections, $E_C = H_3^C + H_4^C$, with Breit energy corrections, $E_B = H_2^B + H_3^B + H_5^B$, and give the total Pauli energies $E'_P - 2mc^2$ for $n \leq 3$ in $Hartree$. It is important to realize that the Breit energy correction is found from the expectation value of the Breit potential for the various states and not by a diagonalization as was the case for the Coulomb potential. This is a result of using the Coulomb gauge. This means that if we add the energy corrections for the Breit terms and H_{an} to both E_D and E_P in Table 1, the differences $E_D - E_P$ remain the same to order $mc^2\alpha^6$. Table 1 and Table 2 allow us to understand the two-body Dirac equation in the Coulomb gauge and the work of Scott, et al. in the context of positronium spectroscopy. We now apply our understanding to find the energy corrections for the resonance bound states due to the magnetic potential. We find that some of these resonance bound states no longer have negative energies as was the case for the Coulomb potential alone.

$n\ L\ S\ J$	$\mathbf{E}_C\ (10^{-9})$	$\mathbf{E}_B\ (10^{-9})$	$\mathbf{E}'_P - \mathbf{2mc}^2$
1 0 0 0	2 497. 469 23	-19 979. 753 85	-0.250 017 482 284 62
1 0 1 1	2 497. 469 23	-2 219. 972 65	-0.249 986 402 667 52
2 0 0 0	156. 091 83	-2 913. 714 10	-0.062 502 757 622 28
2 0 1 1	156. 091 83	-693. 741 45	-0.062 498 872 670 14
2 1 0 1	-121. 75 404	-416. 244 87	-0.062 500 537 649 62
2 1 1 0	-398. 901 34	-1248. 734 62	-0.062 501 647 635 95
2 1 1 1	-260. 153 45	-554. 993 16	-0.062 500 815 146 21
2 1 1 2	17. 343 54	-166. 497 95	-0.062 500 149 154 41
3 0 0 0	30. 832 95	-904. 433 30	-0.027 778 651 378 13
3 0 1 1	30. 832 95	-246. 663 63	-0.027 777 500 281 20
3 1 0 1	-51. 388 26	-164. 442 42	-0.027 777 993 608 45
3 1 1 0	-133. 609 47	-411. 106 05	-0.027 778 322 493 29
3 1 1 1	-92. 498 86	-205. 553 02	-0.027 778 075 829 66
3 1 1 2	-10. 277 65	-90. 443 33	-0.027 777 878 498 76
3 2 0 2	-18. 499 77	-65. 776 97	-0.027 777 862 054 52
3 2 1 1	-43. 166 13	-123. 331 81	-0.027 777 944 275 73
3 2 1 2	-26. 721 89	-73. 999 09	-0.027 777 878 498 76
3 2 1 3	-2. 055 53	-35. 237 66	-0.027 777 815 070 97

Table 2. Coulomb, Breit, and Total Pauli Energies in Hartree

6.2. Resonance States:

We can evaluate the magnetic part of the potential much more easily for the resonance states than for the atomic states. However, we can not use the Breit potential because it is not converging for the resonance states and is of the same order of magnitude as the Coulomb potential itself when operating on such states. This is due to the fact that the large-large and small-small components are equal in magnitude for the resonance states $(y_{11} \pm y_{22})$ and the small-large and large-small components are equal in magnitude for the resonance states $(y_{12} \pm y_{21})$. In other words, we are now dealing with states arising from very high momentum $\hbar\,|\mathbf{k}| \gg mc$ for which the Dirac operators $\boldsymbol{\alpha}_e$ and $\boldsymbol{\alpha}_p$ have expectation values of $v/c = 1$ and not $v/c \sim \alpha = e^2/\hbar c$ as in the case of atomic states. For such high momentum states, we must now use the covariant Feynman gauge instead of the Coulomb gauge.

We find the instantaneous limit of $\gamma_4^e \gamma_4^p G(k)$ in (85) is

$$\begin{aligned}\gamma_4^e \gamma_4^p G(\mathbf{k}, 0) = & -4\pi e^2 \frac{1}{\mathbf{k}\cdot\mathbf{k}} + 4\pi e^2 \frac{\boldsymbol{\alpha}_e \cdot \boldsymbol{\alpha}_p}{\mathbf{k}\cdot\mathbf{k}}, \\ & = V_C(k) + 4\pi e^2 \frac{\boldsymbol{\alpha}_e \cdot \boldsymbol{\alpha}_p}{\mathbf{k}\cdot\mathbf{k}}.\end{aligned}$$

Taking the inverse Fourier transform we have

$$\mathbf{V}_C(\rho) + \mathbf{V}_M(\rho) = -\frac{e^2}{\rho} + \frac{e^2}{\rho}\boldsymbol{\alpha}_e \cdot \boldsymbol{\alpha}_p,$$

and the Gaunt potential [24] is defined as

$$\mathbf{V}_M(\rho) = \mathbf{V}_G(\rho) = \frac{e^2}{\rho}\boldsymbol{\alpha}_e \cdot \boldsymbol{\alpha}_p, \tag{117}$$

or, equivalently,

$$\mathbf{V}_G(\rho) = \frac{e^2}{\rho}\begin{pmatrix} 0 & 0 & 0 & \boldsymbol{\sigma}_e{\cdot}\boldsymbol{\sigma}_p \\ 0 & 0 & \boldsymbol{\sigma}_e{\cdot}\boldsymbol{\sigma}_p & 0 \\ 0 & \boldsymbol{\sigma}_e{\cdot}\boldsymbol{\sigma}_p & 0 & 0 \\ \boldsymbol{\sigma}_e{\cdot}\boldsymbol{\sigma}_p & 0 & 0 & 0 \end{pmatrix}. \tag{118}$$

For the singlet ($S = 0$) and triplet ($S = 1$) spin functions Ω_0^0 and Ω_Σ^1, respectively, we find that

$$\begin{aligned} \boldsymbol{\sigma}_e{\cdot}\boldsymbol{\sigma}_p\Omega_0^0 &= -3\Omega_0^0, \\ \boldsymbol{\sigma}_e{\cdot}\boldsymbol{\sigma}_p\Omega_\Sigma^1 &= \Omega_\Sigma^1, \end{aligned} \tag{119}$$

and the resonance state's magnetic energies are a function of the total spin. Note that the energy eigenfunctions of the Coulomb potential in Section 3 for the resonance states are also eigenfunctions of $\mathbf{V}_G(\rho)$.

For the three cases in Section 3 we have the following possibilities:

$$\begin{aligned} \boldsymbol{\alpha}_e \cdot \boldsymbol{\alpha}_p\Omega_0^0[\mathbf{e}_{11} - \mathbf{e}_{22}] &= -3\Omega_\Sigma^1[\mathbf{e}_{22} - \mathbf{e}_{11}], \\ &= 3\Omega_0^0[\mathbf{e}_{11} - \mathbf{e}_{22}], \\ \boldsymbol{\alpha}_e \cdot \boldsymbol{\alpha}_p\Omega_0^0[\mathbf{e}_{12} - \mathbf{e}_{21}] &= -3\Omega_0^0[\mathbf{e}_{21} - \mathbf{e}_{12}], \\ &= 3\Omega_0^0[\mathbf{e}_{12} - \mathbf{e}_{21}], \end{aligned} \tag{120a}$$

$$\begin{aligned} \boldsymbol{\alpha}_e \cdot \boldsymbol{\alpha}_p\Omega_\Sigma^1[\mathbf{e}_{11} + \mathbf{e}_{22}] &= \Omega_\Sigma^1[\mathbf{e}_{22} + \mathbf{e}_{11}], \\ &= \Omega_\Sigma^1[\mathbf{e}_{11} + \mathbf{e}_{22}], \\ \boldsymbol{\alpha}_e \cdot \boldsymbol{\alpha}_p\Omega_\Sigma^1[\mathbf{e}_{12} + \mathbf{e}_{21}] &= \Omega_\Sigma^1[\mathbf{e}_{21} + \mathbf{e}_{12}], \\ &= \Omega_\Sigma^1[\mathbf{e}_{12} + \mathbf{e}_{21}], \end{aligned} \tag{120b}$$

$$\begin{aligned} \boldsymbol{\alpha}_e \cdot \boldsymbol{\alpha}_p\Omega_\Sigma^1[\mathbf{e}_{11} - \mathbf{e}_{22}] &= \Omega_\Sigma^1[\mathbf{e}_{22} - \mathbf{e}_{11}], \\ &= -\Omega_\Sigma^1[\mathbf{e}_{11} - \mathbf{e}_{22}], \\ \boldsymbol{\alpha}_e \cdot \boldsymbol{\alpha}_p\Omega_\Sigma^1[\mathbf{e}_{12} - \mathbf{e}_{21}] &= \Omega_\Sigma^1[\mathbf{e}_{21} - \mathbf{e}_{12}], \\ &= -\Omega_\Sigma^1[\mathbf{e}_{12} - \mathbf{e}_{21}]. \end{aligned} \tag{120c}$$

Referring to (82) we have the following energy $E = V_C + V_G$ for the resonance pairs

$(\Psi_0^0, \Psi_0'^0)$ with $S = 0$ and $(\Psi_0^\alpha, \Psi_0'^\alpha)$, $(\Psi_0^1, \Psi_0'^1)$ and $(\Psi_0^\beta, \Psi_0'^\beta)$ with $S = 1$

$$(\Psi_0^0, \Psi_0'^0) : E = \frac{-e^2}{\rho'} + \frac{3e^2}{\rho'} = \frac{2e^2}{\rho'}, \tag{121a}$$

$$(\Psi_0^\alpha, \Psi_0'^\alpha) : \ E = \frac{-e^2}{\rho'} - \frac{e^2}{\rho'} = -\frac{2e^2}{\rho'}, \tag{121b}$$

$$(\Psi_0^1, \Psi_0'^1) \ : \ E = \frac{-e^2}{\rho'} + \frac{e^2}{\rho'} = 0, \tag{121c}$$

$$(\Psi_0^\beta, \Psi_0'^\beta) : \ E = \frac{-e^2}{\rho'} + \frac{e^2}{\rho'} = 0.$$

We have shown that the radial wavefunctions $C\delta(\rho - \rho')$ and the energies for the resonance states in 82 are independent and angular momentum L of J. For a given J, the degeneracy of the resonance states is $2(2J + 1)$. Thus the $S = 0$ resonance pairs $(\Psi_0^0, \Psi_0'^0)$ form bound states (82a) with positive energy $E = 2e^2/\rho'$ and the $S = 1$ resonance pairs $(\Psi_0^\alpha, \Psi_0'^\alpha)$ form bound states (82b) with positive energy $E = 2e^2/\rho'$. Finally, the $S = 1$ resonance pairs $(\Psi_0^1, \Psi_0'^1)$ and $(\Psi_0^\beta, \Psi_0'^\beta)$ form bound states (82c) and (82d) with zero energy $E = 0$.

7. Annihilation and Radiative Transitions for Resonance States

Because the resonance states are Weyl spinors or fermions with half-integral Weyl spin, they cannot annihilate into photons which are bosons. Note that for such resonance states, either the electron or the positron must be in a negative energy state and also must propagate forward in time. This time behavior for negative energy states is inconsistent with annihilation.

Also, there can be no radiative transitions from atomic positronium which is a boson to resonance states which are fermions. However, in principle it is possible to have radiative transitions between resonance states. We wish to show that this is impossible and that resonance states can neither emit nor absorb light. Consider radiative transitions from $S = 0$ resonance states $(\Psi_0^0, \Psi_0'^0)$ in (82a) with positive energy $2e^2/\rho'$ to other such resonance states or to $S = 1$ resonance states $(\Psi_0^1, \Psi_0'^1)$ and $(\Psi_0^\beta, \Psi_0'^\beta)$ in (82c) and (82d) with zero energy $E = 0$. For a given polarization direction $\boldsymbol{\epsilon}_i$ we wish to find matrix elements of the Dirac transition operator $\mathbf{T}_i$ for transverse radiation

$$\mathbf{T}_i = -e\boldsymbol{\alpha}_i(e) + e\boldsymbol{\alpha}_i(p). \tag{122}$$

From (30) we define

$$\begin{aligned}
\Omega_x^1 &= \sqrt{\frac{1}{2}}(-\Omega_1^1 + \Omega_{-1}^1), \\
\Omega_y^1 &= i\sqrt{\frac{1}{2}}(\Omega_1^1 + \Omega_{-1}^1), \\
\Omega_z^1 &= \Omega_0^1,
\end{aligned}$$

so that

$$\boldsymbol{\sigma}_i(e)\Omega_0^0 = \Omega_i^1,$$

for $i = x, y,$ or z. Using the exchange symmetry of the $S = 0$ and $S = 1$ states in (31), we also find

$$\begin{aligned}
\boldsymbol{\sigma}_i(p)\Omega_0^0 &= \boldsymbol{\sigma}_i(p)[\chi^{\frac{1}{2}}, \chi^{\frac{1}{2}}]_0^0, \\
&= -\boldsymbol{\sigma}_i(p)[\chi^{\frac{1}{2}}, \chi^{\frac{1}{2}}]_0^0, \\
&= -[\chi^{\frac{1}{2}}, \chi^{\frac{1}{2}}]_i^1, \\
&= -\Omega_i^1.
\end{aligned}$$

The transition operator T_i acts only on the factor $\Omega_0^0[\mathbf{e}_{11} - \mathbf{e}_{22}]$ for Ψ_0^0 and $\Omega_0^0[\mathbf{e}_{12} - \mathbf{e}_{21}]$ for $\Psi_0'^0$ in (82a). We have

$$\begin{aligned}
-e\boldsymbol{\alpha}_i(e)[\mathbf{e}_{11} - \mathbf{e}_{22}]\Omega^0 &= -e[\mathbf{e}_{21} - \mathbf{e}_{12}]\boldsymbol{\sigma}_i(e)\Omega_0^0, \\
&= e[\mathbf{e}_{12} - \mathbf{e}_{21}]\Omega_i^1,
\end{aligned}$$

and

$$\begin{aligned} e\boldsymbol{\alpha}_i(p)[\mathbf{e}_{11}-\mathbf{e}_{22}]\Omega^0 &= e[\mathbf{e}_{12}-\mathbf{e}_{21}]\boldsymbol{\sigma}_i(p)\Omega_0^0, \\ &= -e[\mathbf{e}_{12}-\mathbf{e}_{21}]\Omega_i^1, \end{aligned}$$

so that

$$T_i\Psi_0^0 = 0, \tag{123}$$

and similarly,

$$T_i\Psi_0'^0 = 0. \tag{124}$$

for a given J. Because of the above equations and the fact that the transition operator T_i is Hermitian, the radiative transition matrix of T_i for $S = 0$ resonance states is zero. Such states cannot absorb or emit photons and are therefore dark. The lack of radiative transitions can also be expected because the delta functions in (82) cannot have any n-pole transition moments between different states. That is, for $\rho' \neq \rho''$ we have

$$\langle \delta(\rho-\rho')\,|\rho^n|\,\delta(\rho-\rho'')\rangle = 0.$$

8. Conclusions

We have shown that there are two types of solutions to the two-body Dirac equation for positronium: there are both the normal atomic solutions and the resonance solutions. We have also shown, using the Bethe-Salpeter equation, that these two solutions are entirely separable and noninteracting in a Coulomb and magnetic potential. This separability is a consequence of the different time behavior of the negative energy states for atomic and resonance states. A list of the properties of the atomic and resonance states is shown in Table 3.

The atomic and resonance solutions for positronium both result in bound states with completely different properties. The bound atomic solutions have electron-positron separations of *Bohr* or more whilst the resonance solutions can have separations of *Fermi* or less. The bound atomic states occur at low non-relativistic energies where the magnetic potential is small (hyperfine structure) and the binding is due to the electric potential. On the other hand, the resonance solutions occur at high relativistic energies for the individual particles where the magnetic potential is comparable to the electric potential and the binding is due to both potentials. We have shown that it is the presence of the resonance states which accounts for the singularities in the two-body Dirac wavefunctions. We therefore consider it to be both physically and mathematically compelling to include the resonance solutions.

We have derived the wavefunctions and energies of the resonance states by solving both the two-body Dirac equation and the Bethe-Salpeter with an electromagnetic potential. We have shown, both numerically and analytically, that the radial solutions are simply delta functions $C\delta(\rho-\rho')$ in the limit of an infinite basis set where $\Delta\rho \to 0$ and the Bessel series becomes a Bessel transform. The resonance states are highly localized radially resulting from a superposition of high momentum states $h/\Delta\rho \gg mc$ in accordance with the uncertainty principle. There are three types of resonance solutions corresponding to $S=0$ and $S=1$ resonances. The $S=0$ resonances have positive energies $E=2e^2/\rho'$ and the $S=1$ $(L=J-1,J+1)$ resonances have energies $E=0$. Finally, the $S=1$ $(L=J)$ resonances have energies $E=-2e^2/\rho'$. The energies are independent of the angular momentum L and J. It is interesting that for the $S=0$ resonances we obtain bound states for a repulsive potential where larger separations ρ' lead to lower energies. We assume that the $S=1$ $(L=J)$ resonances with negative energy $E=-2e^2/\rho'$ are not allowed but could correspond to an antiparticle with energy $2e^2/\rho'$.

We have shown the two-fold degeneracy of all the resonance states to be a result of their intrinsic Weyl spin one-half if our basis set is infinite $(\Delta\rho \to 0)$. This spin one-half is a result of the opposite chirality of Weyl spinors for the two degenerate resonance states corresponding to zero rest mass and is entirely a relativistic effect of the Lorentz group and not the spin angular momentum. Indeed the resonance states form $S=0$ and $S=1$ angular momentum spin states as expected. It is quite surprising that an electron and a positron can combine to form a fermion for the resonance states and a boson for

Property	**Atomic States**	**Resonance States**
Particle Type	Bosons	Fermions
Chirality	No	Yes
Charge Conjugation Symmetry	Yes	No
Spin Angular Momentum	$S = 0, 1$	$S = 0, 1$
Negative Energy States	Backward in Time	Forward in Time
Annihilation	Yes	No
Radiative Transitions	Yes	No
Bound States	Yes	Yes
Energy	$E = 2mc^2(1 - \alpha^2/8n^2)$	$E = 2e^2/\rho'$ for $S = 0$ $E = 0, -2e^2/\rho'$ for $S = 1$
Wavefunction Form	$\rho^x e^{-\rho/2na_0}$	$\delta(\rho - \rho')$
Electron Momentum p_e	$\sim h/2na_0 \ll mc$	$\sim h/\Delta\rho \gg mc$
Magnetic Potential $\mathbf{V}_M$	*Breit* $\frac{e^2}{2\rho}\{\boldsymbol{\alpha}_e \cdot \boldsymbol{\alpha}_p + (\boldsymbol{\alpha}_e \cdot \hat{\mathbf{r}}_e)(\boldsymbol{\alpha}_p \cdot \hat{\mathbf{r}}_p)\}$	*Gaunt* $\frac{e^2}{\rho}\boldsymbol{\alpha}_e \cdot \boldsymbol{\alpha}_p$
Potential Strength $\lvert\langle \mathbf{V}_M \rangle\rvert$	$\sim \alpha^2 \langle e^2/\rho \rangle$	$\sim \langle e^2/\rho \rangle$

Table 3. Properties of Atomic and Resonance States of Positronium

the atomic states. This is a remarkable and unexpected consequence of both the two-body Dirac equation and the Bethe-Salpeter equation. The electron and positron in the resonance states cannot annihilate because of conservation of the Weyl spin: a fermion cannot decompose into any amount of photons which are bosons. Resonance states are also intrinsically dark. There can be no radiative transitions between atomic states and resonance states. Again, bosons (atomic states) cannot emit or absorb photons to become fermions (resonance states). We have also shown that the $S = 0$ resonance states cannot have radiative transitions.

Acknowledgments

The author would like to thank Drs. William Harter, Gordon Drake, Tony Scott, Janine Schertzer, Jonathan Sapirstein, and Peter Milonni for their help and suggestions. Particular credit goes to Dr Gordon Drake for suggesting the separability between the resonance and atomic states based on the work of Sapirstein. In turn, correspondence with Dr. Sapirstein led to the conclusions about this separability contained in this work. Thanks are also due to Dr. Joel Kress for extending the hospitality of Theoretical Division, Los Alamos National Laboratory.

Appendix A. Spherical Bessel Functions

The first few spherical Bessel functions are [25]

$$\begin{aligned} j_0(r) &= \frac{\sin r}{r}, \\ j_1(r) &= \frac{\sin r}{r^2} - \frac{\cos r}{r}, \\ j_2(r) &= \left(\frac{3}{r^3} - \frac{1}{r}\right)\sin r - \frac{3}{r^2}\cos r. \end{aligned} \tag{A.1}$$

We may generate the spherical Bessel functions by forward recursion starting with the first two known functions $j_0(r)$ and $j_1(r)$ by using the relation:

$$j_{l+1}(r) = \frac{(2l+1)}{r} j_l(r) - j_{l-1}(r). \tag{A.2}$$

Note that this recursion works to find j_2 from j_1 and j_0. We wish to show the orthonormality properties of the Bessel functions that satisfy the boundary conditions

$$j_l(k_n r_0) = 0. \tag{A.3}$$

The k_n which satisfy this boundary condition can be found by forward recursion.

Any text on numerical methods will tell you that forward recursion is numerically unstable and can blow up exponentially for small r. These texts then suggest that one use backward recursion to evaluate the $j_l(kr)$. However, one can, indeed, use forward recursion directly to find the zeros of the spherical Bessel functions. The zeros of j_l never occur in the region where the forward recursion relations fail. Indeed, this failure only occurs for small r before the first maximum of $|j_l|$. The zeros are found using Newton's rule, where a guess is first made using the asymptotic formula for large $k_n r_0$,

$$j_l(k_n r_0) \sim \frac{\cos(k_n r_0 - \frac{1}{2}(l+1)\pi)}{k_n r_0}. \tag{A.4}$$

The zeros of $j_l(k_n r_0)$ should occur near

$$k_n r_0 \sim \frac{1}{2} l\pi + n\pi \text{ for } n = 1, 2, \ldots . \tag{A.5}$$

Note that from (A.4) we find the asymptotic limit

$$[k_n r_0 j_{l\pm1}(k_n r_0)]^2 \sim 1. \tag{A.6}$$

We wish to show that the Bessel functions $j_{l'}(k_n r)$ form an orthonormal set such that

$$N_{\ell n}^2 \int_0^{r_0} r^2 j_{l'}(k_m r) j_{l'}(k_n r) dr = \delta_{mn} \text{ for } l' = l-1,\ l,\ l+1 \tag{A.7}$$

$$N_{\ell n} = \sqrt{\frac{2}{r_0^3\ j_{l\pm1}^2(k_n r_0)}},$$

where the k_n obey the boundary condition $j_l(k_n r) = 0$. Note that the normalizations are independent of $l' = l-1,\ l,\ l+1$.

First, we determine the normalization $N_{\ell' n}$ of $j_{l'}(k_n r)$ for a given k_n which meet the boundary conditions (A.3). The normalization condition is

$$N_{\ell' n}^2 \int_0^{r_0} j_{l'}^2(k_n r) r^2 dr = 1 \text{ for } l' = l-1,\ l,\ l+1. \tag{A.8}$$

Evaluating the integral, we find

$$\int_0^{r_0} j_{l'}^2(k_n r) r^2 dr = \frac{r_0^3}{2}[j_{l'}^2(k_n r_0) - j_{l'-1}(k_n r_0) j_{l'+1}(k_n r_0)] \text{ for } l' > 0. \tag{A.9}$$

However, from (A.2) with $j_l(k_n r_0) = 0$ it follows that

$$j_{l-1}(k_n r_0) = -j_{l+1}(k_n r_0),$$

and

$$-j_{l-1}(k_n r_0) j_{l+1}(k_n r_0) = j_{l\pm1}^2(k_n r_0),$$

so that for $l' = l$ we have

$$\int_0^{r_0} j_l^2(k_n r) r^2 dr = \frac{r_0^3}{2} j_{l\pm1}^2(k_n r_0).$$

We also have from (A.9), letting $l' = l+1$ and $l' = l-1$,

$$\int_0^{r_0} j_{l+1}^2(k_n r) r^2 dr = \frac{r_0^3}{2} j_{l+1}^2(k_n r_0),$$
$$\int_0^{r_0} j_{l-1}^2(k_n r) r^2 dr = \frac{r_0^3}{2} j_{l-1}^2(k_n r_0).$$

We conclude that the normalization of $j_{l'}(k_n r_0)$ are independent of l' for $l' = l-1,\ l,\ l+1$ and are given by

$$N_{\ell' n} = \sqrt{\frac{2}{r_0^3\ j_{l\pm1}^2(k_n r_0)}} \sim \sqrt{\frac{2}{r_0}} k_n \text{ for } l' = l-1,\ l,\ l+1, \tag{A.10}$$

where either sign $\pm$ can be used and where the later approximation follows from the asymptotic limit in (A.6).

To prove the orthogonality conditions of (A.7) we use Bessel's spherical equation

$$\frac{1}{r^2}\frac{d}{dr}[r^2 \frac{dj_{l'}(kr)}{dr}] + [k^2 - \frac{l'(l'+1)}{r^2}] j_{l'}(kr) = 0.$$

We let $j_{l'}(k_m r)$ and $j_{l'}(k_n r)$ be two such solutions with $k_n \neq k_m$ and integrate the above equation over $j_{l'}(k_n r) r^2 dr$ and $j_{l'}(k_m r) r^2 dr$, respectively, to find

$$\int_0^{r_0} j_{l'}(k_n r) \frac{d}{dr}[r^2 \frac{dj_{l'}(k_m r)}{dr}] dr + \int_0^{r_0} j_{l'}(k_n r)[k_m^2 - \frac{l'(l'+1)}{r^2}] j_{l'}(k_m r) r^2 dr = 0,$$
$$\int_0^{r_0} j_{l'}(k_m r) \frac{d}{dr}[r^2 \frac{dj_{l'}(k_n r)}{dr}] dr + \int_0^{r_0} j_{l'}(k_m r)[k_n^2 - \frac{l'(l'+1)}{r^2}] j_{l'}(k_n r) r^2 dr = 0.$$

Taking the difference, integrating by parts, and letting

$$\frac{d}{dr} j_{l'}(kr) = k j'_{l'}(kr),$$

we find

$$r_0^2[j_{l'}(k_n r_0) k_m j'_{l'}(k_m r_0) - j_{l'}(k_m r_0) k_n j'_{l'}(k_n r_0)] = [k_m^2 - k_n^2] \int_0^{r_0} j_{l'}(k_m r) j_{l'}(k_n r) r^2 dr. \tag{A.11}$$

For the case $l' = l$ with (A.3) and (A.11) it follows that, if $k_n \neq k_m$,

$$\int_0^{r_0} j_{\ell'}(k_m r) j_{\ell'}(k_n r) r^2 dr = 0, \text{ for } l' = l. \tag{A.12}$$

For the cases $l' = l + 1$ and $l' = l - 1$ we use the derivative relations for $k = k_n$ or $k = k_m$,

$$\begin{aligned} k j'_{l+1}(kr_0) + (l+2) j_{l+1}(kr_0)/r_0 = &\quad k j_l(kr_0) = 0, \\ k j'_{l-1}(kr_0) - (l-1) j_{l-1}(kr_0)/r_0 = &- k j_l(kr_0) = 0, \end{aligned}$$

or

$$\begin{aligned} k j'_{l+1}(kr_0) = &-(l+2) j_{l+1}(kr_0)/r_0, \\ k j'_{l-1}(kr_0) = &\quad (l-1) j_{l-1}(kr_0)/r_0. \end{aligned}$$

Substituting these on the left of (A.11) with $l' = l + 1$ or $l' = l - 1$, respectively, we find again that, if $k_n \neq k_m$,

$$\int_0^{r_0} j_{l'}(k_m r) j_{l'}(k_n r) r^2 dr = 0, \text{ for } l' = l \pm 1. \tag{A.13}$$

Combining results (A.8), (A.10), (A.12) and (A.13) we obtain the result (A.7).

Appendix B. Addition Theorems for Bessel Harmonics

We give here some important addition theorems for the products of single particle functions of free particles $g^{\ell_e\ j_e}_{n_e}(kr_e,\theta_e,\varphi_e)g^{\ell_p\ j_p}_{n_p}(kr_p,\theta_p,\varphi_p)$ for electron spherical coordinates $\mathbf{r}_e=(r_e,\theta_e,\varphi_e)$ and positron spherical coordinates $\mathbf{r}_p=(r_p,\theta_p,\varphi_p)$ where, for a given vector $\mathbf{k}=(k,\theta_k,\varphi_k)$, we have

$$g^{\ell\ j}_n(kr,\theta,\varphi)\equiv j_\ell(kr)[Y^\ell(\theta,\varphi),\chi^{\frac{1}{2}}]^j_n.$$

We wish to expand such products in terms of the relative coordinates $\boldsymbol{\rho}=\mathbf{r}_e-\mathbf{r}_p=(\rho,\theta_\rho,\varphi_\rho)$. Such addition theorems are derived from the clear and concise work of Danos and Maximon [26]. Another more obscure formalism has been given using the representation theory of the three-dimensional translation-rotation group for which these functions form a bases [27].

Danos and Maximon start with the well known expansion formula for plane-waves into spherical waves,

$$e^{i\mathbf{k}\cdot\boldsymbol{\rho}}=4\pi\sum_{L,N_L}i^Lj_L(k\rho)Y^{L*}_{N_L}(\theta_k,\varphi_k)Y^L_{N_L}(\theta_\rho,\varphi_\rho),\tag{B.1}$$

for a given vector $\mathbf{k}$.

Now we let

$$e^{i\mathbf{k}\cdot\boldsymbol{\rho}}=e^{i\mathbf{k}\cdot\mathbf{r}_e}e^{-i\mathbf{k}\cdot\mathbf{r}_p},\tag{B.2}$$

and using (B.1) for the products on the right, we find that

$$\begin{aligned}4\pi\sum_{L,N_L}i^Lj_L(k\rho)Y^{L*}_{N_L}(\theta_k,\varphi_k)Y^L_{N_L}(\theta_\rho,\varphi_\rho)&=4\pi\sum_{l_e,n_e}i^{l_e}j_{l_e}(kr_e)Y^{l_e*}_{n_e}(\theta_k,\varphi_k)Y^{l_e}_{n_e}(\theta_e,\varphi_e)\\&\quad\times4\pi\sum_{l_p,n_p}(-i)^{l_p}j_{l_p}(kr_p)Y^{l_p*}_{n_p}(\theta_k,\varphi_k)Y^{l_p}_{n_p}(\theta_p,\varphi_p).\end{aligned}$$

Integrating both sides above with $Y^L_{N_L}(\theta_k,\varphi_k)$ over solid angle Ω_k, and using

$$\int Y^L_{N_L}(\theta_k,\varphi_k)Y^{l_e*}_{n_e}(\theta_k,\varphi_k)Y^{l_p*}_{n_p}(\theta_k,\varphi_k)d\Omega_k=\left(\frac{[l_e][l_p]}{4\pi[L]}\right)^{\frac{1}{2}}C^{l_e\ \ l_p\ \ L}_{n_e\ n_p\ N_L}C^{l_e\ \ l_p\ \ L}_{0\ \ 0\ \ 0},$$

where $[L]\equiv2L+1$, etc., and also using the Clebsch-Gordon expansion

$$(l_el_p)^L_{N_L}=\sum_{n_e,n_p}C^{l_e\ \ l_p\ \ L}_{n_e\ n_p\ N_L}Y^{l_e}_{n_e}(\theta_e,\varphi_e)Y^{l_p}_{n_p}(\theta_p,\varphi_p),$$

we have

$$j_L(k\rho)Y^L_{N_L}(\theta_\rho,\varphi_\rho)=\sum_{l_e,l_p}t_{l_e,l_p:L}\ \ j_{l_e}(kr_e)j_{l_p}(kr_p)(l_el_p)^L_{N_L},\tag{B.3}$$

where

$$t_{l_e,l_p:L} = i^{(l_e-l_p-L)}\left(\frac{4\pi[l_e][l_p]}{[L]}\right)^{\frac{1}{2}} C^{l_e\ \ l_p\ \ L}_{0\ \ 0\ \ 0}. \tag{B.4}$$

Note that the 'parity' coefficient $C^{l_e\ \ l_p\ \ L}_{0\ \ 0\ \ 0}$ is zero unless $l_e + l_p - L = even$. That is, the parity of the $j_L(k\rho)Y^L_{N_L}(\theta_\rho, \varphi_\rho)$ in (B.3) is $(-1)^L = (-1)^{l_e+l_p}$

Again, following the treatment of Danos and Maximon, we multiply by the coupled spin

$$\Omega^S_{N_S} = (s_e s_p)^S_{N_S} = \sum_{\sigma_e,\sigma_p} C^{\frac{1}{2}\ \frac{1}{2}\ S}_{\sigma_e\ \sigma_p\ N_S}\chi^{\frac{1}{2}}_{\sigma_e}\chi^{\frac{1}{2}}_{\sigma_p},$$

and then couple the total spin S and angular momentum L to give total J (LS-coupling). We have

$$j_L(k\rho)[Y^L_{N_L}(\theta_\rho,\varphi_\rho)(s_e s_p)^S_{N_S}]^J_N = \sum_{l_e,l_p} t_{l_e,l_p:L}\ \ j_{l_e}(kr_e)j_{l_p}(kr_p)[(l_e l_p)^L_{N_L}(s_e s_p)^S_{N_S}]^J_N.$$

We now switch from LS-coupling to jj-coupling using the $9-j$ coefficients so that,

$$[(l_e l_p)^L_{N_L}(s_e s_p)^S_{N_S}]^J_N = \sum_{j_e,j_p}\sqrt{[j_e][j_p][L][S]}\begin{pmatrix} l_e & l_p & L \\ s_e & s_p & S \\ j_e & j_p & J\end{pmatrix}[(l_e s_e)^{j_e}_{n_e}(l_p s_p)^{j_p}_{n_p}]^J_N,$$

where $(ls)^j_n \equiv [Y^\ell, \chi^{\frac{1}{2}}]^j_n$. Finally using the notation

$$[g^{l_e\ \ j_e} g^{l_p\ \ j_p}_{n_p}]^J_N \equiv j_{l_e}(kr_e)j_{l_p}(kr_p)[(l_e s_e)^{j_e}_{n_e}(l_p s_p)^{j_p}_{n_p}]^J_N,$$

we may write,

$$j_L(k\rho)[Y^L_{N_L}(\theta_\rho,\varphi_\rho)\Omega^S_{N_S}]^J_N = \sum_{l_e,l_p} T_{l_e,l_p:LSJ}\ [g^{l_e\ \ j_e} g^{l_p\ \ j_p}_{n_p}]^J_N, \tag{B.5}$$

where

$$T_{l_e,l_p:LSJ} = \sum_{j_e,j_p} t_{l_e,l_p:L}\sqrt{[j_e][j_p][L][S]}\begin{pmatrix} l_e & l_p & L \\ \frac{1}{2} & \frac{1}{2} & S \\ j_e & j_p & J\end{pmatrix}. \tag{B.6}$$

We can simplify Eqs. (B.5)-(B.6) of Danos and Maximon to appear similar to Eqs. (B.3)-(B.4). Using (B.5), we multiply both sides by $i^{L-J}\sqrt{[L]/[J]}C^{\frac{1}{2}\ \ \frac{1}{2}\ S}_{\frac{1}{2}\ -\frac{1}{2}\ 0}C^{L\ 0\ S}_{0\ 0\ 0\ J}$ and sum over all L and $S = 0, 1$ such that

$$\sum_{L,S} i^{L-J}\sqrt{[L]/[J]}C^{\frac{1}{2}\ \frac{1}{2}\ S}_{\frac{1}{2}\ -\frac{1}{2}\ 0}C^{L\ S\ J}_{0\ 0\ 0}\, j_L(k\rho)[Y^L_{N_L}(\theta_\rho,\varphi_\rho)\Omega^S_{N_S}]^J_N \tag{B.7}$$
$$= \sum_{l_e,l_p,L,S} i^{L-J}\sqrt{[L]/[J]}C^{\frac{1}{2}\ \frac{1}{2}\ S}_{\frac{1}{2}\ -\frac{1}{2}\ 0}C^{L\ S\ J}_{0\ 0\ 0}T_{l_e,l_p:LSJ}\ [g^{l_e\ \ j_e}_{n_e}g^{l_p\ \ j_p}_{n_p}]^J_N.$$

We use the identity [28],

$$\sum_{L,S} C^{l_e\ l_p\ L}_{0\ \ 0\ \ 0}C^{\frac{1}{2}\ \frac{1}{2}\ S}_{\frac{1}{2}\ -\frac{1}{2}\ 0}C^{L\ S\ J}_{0\ 0\ 0}\sqrt{[j_e][j_p][L][S]}\begin{pmatrix} l_e & l_p & L \\ \frac{1}{2} & \frac{1}{2} & S \\ j_e & j_p & J\end{pmatrix} = C^{l_e\ \frac{1}{2}\ j_e}_{0\ \ \frac{1}{2}\ \ \frac{1}{2}}C^{l_p\ \ \frac{1}{2}\ \ j_p}_{0\ -\frac{1}{2}\ -\frac{1}{2}}C^{j_e\ \ j_p\ \ J}_{\frac{1}{2}\ -\frac{1}{2}\ 0}, \tag{B.8}$$

with (B.6) on the right side of (B.7) to find

$$\sum_{L,S} i^{L-J}\sqrt{[L]/[J]}C^{\frac{1}{2}\ \frac{1}{2}\ S}_{\frac{1}{2}\ -\frac{1}{2}\ 0}C^{L\ S\ J}_{0\ 0\ 0}\, j_L(k\rho)[Y^L_{N_L}(\theta_\rho,\varphi_\rho)\Omega^S_{N_S}]^J_N \tag{B.9}$$
$$= \sum_{l_e,l_p,j_e,j_p} i^{(l_e-l_p-J)}C^{l_e\ \frac{1}{2}\ j_e}_{0\ \ \frac{1}{2}\ \ \frac{1}{2}}C^{l_p\ \ \frac{1}{2}\ \ j_p}_{0\ -\frac{1}{2}\ -\frac{1}{2}}C^{j_e\ \ j_p\ \ J}_{\frac{1}{2}\ -\frac{1}{2}\ 0}\left(\frac{4\pi[l_e][l_p]}{[J]}\right)^{\frac{1}{2}}[g^{l_e\ \ j_e}_{n_e}g^{l_p\ \ j_p}_{n_p}]^J_N.$$

Summing over l_e and l_p, evaluating the Clebsch-Gordon coefficients, and equating real and imaginary parts, we find

$$ij_J(k\rho)[Y^J(\theta_\rho,\varphi_\rho)\Omega^0]^J_N \tag{B.10}$$
$$= i\sum_{j_e,j_p\ (j_e-j_p-J=even)} q_{j_e,j_p:J}\{[g^{j_e-\frac{1}{2}\ \ j_e}_{n_e}g^{j_p-\frac{1}{2}\ \ j_p}_{n_p}]^J_N - [g^{j_e+\frac{1}{2}\ \ j_e}_{n_e}g^{j_p+\frac{1}{2}\ \ j_p}_{n_p}]^J_N\}$$
$$+ \sum_{j_e,j_p\ (j_e-j_p-J=odd)} q_{j_e,j_p:J}\{[g^{j_e-\frac{1}{2}\ \ j_e}_{n_e}g^{j_p+\frac{1}{2}\ \ j_p}_{n_p}]^J_N + [g^{j_e+\frac{1}{2}\ \ j_e}_{n_e}g^{j_p-\frac{1}{2}\ \ j_p}_{n_p}]^J_N\},$$

and

$$\sqrt{\frac{J}{2J+1}}j_{J-1}(k\rho)[Y^{J-1}(\theta_\rho,\varphi_\rho)\Omega^1]^J_N + \sqrt{\frac{J+1}{2J+1}}j_{J+1}(k\rho)[Y^{J+1}(\theta_\rho,\varphi_\rho)\Omega^1]^J_N \tag{B.11}$$
$$= \sum_{j_e,j_p\ (j_e-j_p-J=even)} q_{j_e,j_p:J}\{[g^{j_e-\frac{1}{2}\ \ j_e}_{n_e}g^{j_p+\frac{1}{2}\ \ j_p}_{n_p}]^J_N + [g^{j_e+\frac{1}{2}\ \ j_e}_{n_e}g^{j_p-\frac{1}{2}\ \ j_p}_{n_p}]^J_N\}$$
$$+ i\sum_{j_e,j_p\ (j_e-j_p-J=odd)} q_{j_e,j_p:J}\{[g^{j_e-\frac{1}{2}\ \ j_e}_{n_e}g^{j_p-\frac{1}{2}\ \ j_p}_{n_p}]^J_N - [g^{j_e+\frac{1}{2}\ \ j_e}_{n_e}g^{j_p+\frac{1}{2}\ \ j_p}_{n_p}]^J_N\},$$

where

$$q_{j_e,j_p:J} = i^{(j_e-j_p-J)}\left(\frac{2\pi[j_e][j_p]}{[J]}\right)^{\frac{1}{2}}C^{j_e\ \ j_p\ \ J}_{\frac{1}{2}\ -\frac{1}{2}\ 0}. \tag{B.12}$$

Note the similarity between Eqs. (B.12) and (B.4). One should also note that these functions are the same ones used in our momentum basis in (44) and (45).

Let us evaluate the expressions (B.10) and (B.11) for the special case of $J = 0$ for which $j_e = j_p \equiv j$ and $L = S$. We have two expressions corresponding to singlet $S = L = 0$ and triplet $S = L = 1$ states. Namely, for the vector $\boldsymbol{\rho}$ we have

$$j_0(k\rho)[Y^0(\theta_\rho,\varphi_\rho)\Omega^0]^0_0 = \sum_j \sqrt{(2\pi[j]}(-1)^{j-\frac{1}{2}}\{[g_{n_e}^{j-\frac{1}{2}\ \ j} g_{n_p}^{j-\frac{1}{2}\ \ j}]^0_0 - [g_{n_e}^{j+\frac{1}{2}\ \ j} g_{n_p}^{j+\frac{1}{2}\ \ j}]^0_0\}, \tag{B.13}$$

and

$$j_1(k\rho)[Y^1(\theta_\rho,\varphi_\rho)\Omega^1]^0_0 = \sum_j \sqrt{(2\pi[j]}(-1)^{j-\frac{1}{2}}\{[g_{n_e}^{j+\frac{1}{2}\ \ j} g_{n_p}^{j-\frac{1}{2}\ \ j}]^0_0 + [g_{n_e}^{j-\frac{1}{2}\ \ j} g_{n_p}^{j+\frac{1}{2}\ \ j}]^0_0\}. \tag{B.14}$$

These special cases have been derived previously [25].

There is also a set of equations involving the triplet bases $j_J(k\rho)[Y^J(\theta_\rho,\varphi_\rho)\Omega^1]^J_N$ with total spin $S = 1$. In this bases we cannot have $J = 0$. Again, using (B.5), we multiply both sides by $i^{L-J}\sqrt{[L]/[J]}C^{\frac{1}{2}\ \frac{1}{2}\ S}_{\frac{1}{2}\ \frac{1}{2}\ 1}C^{L\ S\ J}_{0\ 1\ 1}$ and sum over L with $S = 1$ such that

$$\begin{aligned}&\sum_L i^{L-J}\sqrt{[L]/[J]}C^{\frac{1}{2}\ \frac{1}{2}\ 1}_{\frac{1}{2}\ \frac{1}{2}\ 1}C^{L\ 1\ J}_{0\ 1\ 1} j_L(k\rho)[Y^L_{N_L}(\theta_\rho,\varphi_\rho)\Omega^1_{N_S}]^J_N \\ &= \sum_{l_e,l_p,L} i^{L-J}\sqrt{[L]/[J]}C^{\frac{1}{2}\ \frac{1}{2}\ 1}_{\frac{1}{2}\ \frac{1}{2}\ 1}C^{L\ 1\ J}_{0\ 1\ 1}T_{l_e,l_p:L1J}\ [g_{n_e}^{l_e\ \ j_e} g_{n_p}^{l_p\ \ j_p}]^J_N.\end{aligned} \tag{B.15}$$

We use the identity [28],

$$\sum_L C^{l_e\ l_p\ L}_{0\ \ 0\ \ 0}C^{\frac{1}{2}\ \frac{1}{2}\ 1}_{\frac{1}{2}\ \frac{1}{2}\ 1}C^{L\ 1\ J}_{0\ 1\ 1}\sqrt{[j_e][j_p][L][1]}\begin{pmatrix} l_e & l_p & L \\ \frac{1}{2} & \frac{1}{2} & 1 \\ j_e & j_p & J\end{pmatrix} = C^{l_e\ \frac{1}{2}\ j_e}_{0\ \frac{1}{2}\ \frac{1}{2}}C^{l_p\ \frac{1}{2}\ j_p}_{0\ \frac{1}{2}\ \frac{1}{2}}C^{j_e\ j_p\ J}_{\frac{1}{2}\ \frac{1}{2}\ 1}, \tag{B.16}$$

with (B.6) on the right side of (B.15) to find

$$\begin{aligned}&\sum_L i^{L-J}\sqrt{[L]/[J]}C^{\frac{1}{2}\ \frac{1}{2}\ 1}_{\frac{1}{2}\ \frac{1}{2}\ 1}C^{L\ 1\ J}_{0\ 1\ 1} j_L(k\rho)[Y^L_{N_L}(\theta_\rho,\varphi_\rho)\Omega^1_{N_S}]^J_N \\ &= \sum_{l_e,l_p,j_e,j_p} i^{(l_e-l_p-J)}C^{l_e\ \frac{1}{2}\ j_e}_{0\ \frac{1}{2}\ \frac{1}{2}}C^{l_p\ \frac{1}{2}\ j_p}_{0\ \frac{1}{2}\ \frac{1}{2}}C^{j_e\ j_p\ J}_{\frac{1}{2}\ \frac{1}{2}\ 1}\left(\frac{4\pi[l_e][l_p]}{[J]}\right)^{\frac{1}{2}}[g_{n_e}^{l_e\ \ j_e} g_{n_p}^{l_p\ \ j_p}]^J_N.\end{aligned} \tag{B.17}$$

Summing over l_e and l_p, evaluating the Clebsch-Gordon coefficients, and equating real and imaginary parts, we find

$$
\begin{aligned}
& ij_J(k\rho)[Y^J(\theta_\rho,\varphi_\rho)\Omega^1]^J_N \qquad\qquad (B.18)\\
&= \quad -i \sum_{j_e,j_p\ (j_e-j_p-J=even)} p_{j_e,j_p:J}\{[g_{n_e}^{j_e-\frac{1}{2}\ \ j_e}\, g_{n_p}^{j_p-\frac{1}{2}\ \ j_p}]^J_N + [g_{n_e}^{j_e+\frac{1}{2}\ \ j_e}\, g_{n_p}^{j_p+\frac{1}{2}\ \ j_p}]^J_N\}\\
&\qquad + \sum_{j_e,j_p\ (j_e-j_p-J=odd)} p_{j_e,j_p:J}\{[g_{n_e}^{j_e-\frac{1}{2}\ \ j_e}\, g_{n_p}^{j_p+\frac{1}{2}\ \ j_p}]^J_N - [g_{n_e}^{j_e+\frac{1}{2}\ \ j_e}\, g_{n_p}^{j_p-\frac{1}{2}\ \ j_p}]^J_N\},
\end{aligned}
$$

and

$$
\begin{aligned}
& \sqrt{\frac{J+1}{2J+1}}j_{J-1}(k\rho)[Y^{J-1}(\theta_\rho,\varphi_\rho)\Omega^1]^J_N - \sqrt{\frac{J}{2J+1}}j_{J+1}(k\rho)[Y^{J+1}(\theta_\rho,\varphi_\rho)\Omega^1]^J_N \qquad (B.19)\\
&= -\sum_{j_e,j_p\ (j_e-j_p-J=even)} p_{j_e,j_p:J}\{[g_{n_e}^{j_e-\frac{1}{2}\ \ j_e}\, g_{n_p}^{j_p+\frac{1}{2}\ \ j_p}]^J_N - [g_{n_e}^{j_e+\frac{1}{2}\ \ j_e}\, g_{n_p}^{j_p-\frac{1}{2}\ \ j_p}]^J_N\}\\
&\quad + i \sum_{j_e,j_p\ (j_e-j_p-J=odd)} p_{j_e,j_p:J}\{[g_{n_e}^{j_e-\frac{1}{2}\ \ j_e}\, g_{n_p}^{j_p-\frac{1}{2}\ \ j_p}]^J_N + [g_{n_e}^{j_e+\frac{1}{2}\ \ j_e}\, g_{n_p}^{j_p+\frac{1}{2}\ \ j_p}]^J_N\},
\end{aligned}
$$

where

$$
p_{j_e,j_p:J} = i^{(j_e-j_p-J)}\left(\frac{2\pi[j_e][j_p]}{[J]}\right)^{\frac{1}{2}} C^{j_e\ j_p\ J}_{\frac{1}{2}\ \frac{1}{2}\ 1}. \qquad (B.20)
$$

Note the similarity between Eqs. (B.20) and (B.4). Again, one should note that these functions are the same ones used in our momentum basis in (44) and (45).

References

[1] Childers R W 1982 *Phys. Rev. D* **26** 2902–2915
[2] Brayshaw D D 1987 *Phys. Rev. D* **36** 1465–1478
[3] Morishita J, Kawaguchi M and Morii T 1988 *Phys. Rev. D* **37** 159–178
[4] Malenfant J 1988 *Phys. Rev. D* **38** 3295–3307
[5] Scott T C, Shertzer J and Moore R A 1992 *Phys. Rev. A* **45** 4393–4398
[6] Salpeter E E 1952 *Phys. Rev.* **87** 328–343
[7] Sapirstein J 1989 *AIP Conf. Proc.* **189** 196–205
[8] Sapirstein J, Cheng K T and Chen M H 1999 *Phys. Rev. A* **59** 259–266
[9] Grant I P 2007 *Relativistic Quantum Theory of Atomcs and Molecules: Theory and Computation* (Springer)
[10] Brown G E and Ravenhall D G 1951 *Proc. Roy. Soc. London A* **208** 552–559
[11] Sucher J 1985 *Phys. Rev. Lett.* **55** 1033–1035
[12] Bethe H A and Salpeter E E 1957 *Quantum Mechanics of One- and Two-Electron Atoms* (Academic Press, New York)
[13] Sakurai J J 1967 *Advanced Quantum Mechanics* (Addison-Wesley, New York)
[14] Wolfenstein L and Ravenhall D G 1952 *Phys. Rev.* **88** 279–282
[15] Ferrell R A 1951 *Phys. Rev.* **84** 858
[16] Ishidzu T 1951 *Progr. Theoret. Phys.* **6** 48–60
[17] Ishidzu T 1951 *Progr. Theoret. Phys.* **6** 154–165
[18] Karplus R and Klein A 1952 *Phys. Rev.* **87** 848–858
[19] Fulton T and Martin P C 1954 *Phys. Rev.* **95** 811–822
[20] Salpeter E E and Bethe H A 1951 *Phys. Rev.* **84** 1232–1242
[21] Gell-Mann M and Low F 1951 *Phys. Rev.* **84** 350–354
[22] Sucher J 1957 *Phys. Rev.* **107** 1448–1449
[23] Feynman R P 1949 *Phys. Rev.* **76** 749–759
[24] Alstine P V and Crater H W 1997 *Found. Phys.* **27** 67–79
[25] Abramowitz M and Stegun I A 1972 *Handbook of Mathematical Functions* (Dover Publishing, New York)
[26] Danos M and Maximon L C 1965 *J. Math. Phys.* **6** 766–779
[27] Wigner E P and Talman J D 1968 *Special Functions, A Group Theoretic Approach* (Benjamin Press, New York)
[28] Biedenharn L C and Louck J D 1981 *Angular Momentum in Quantum Physics (Encyclopedia of Mathematics and its Applications 8)* (Addison-Wesley, Reading Mass.) see equation (3.252) on page 104